

**UNCLASSIFIED**

---

**AD 401 148**

*Reproduced  
by the*

**DEFENSE DOCUMENTATION CENTER**

**FOR**

**SCIENTIFIC AND TECHNICAL INFORMATION**

**CAMERON STATION, ALEXANDRIA, VIRGINIA**



---

**UNCLASSIFIED**

NOTICE: When government or other drawings, specifications or other data are used for any purpose other than in connection with a definitely related government procurement operation, the U. S. Government thereby incurs no responsibility, nor any obligation whatsoever; and the fact that the Government may have formulated, furnished, or in any way supplied the said drawings, specifications, or other data is not to be regarded by implication or otherwise as in any manner licensing the holder or any other person or corporation, or conveying any rights or permission to manufacture, use or sell any patented invention that may in any way be related thereto.

63-3-2

Technical Report No. AF-102

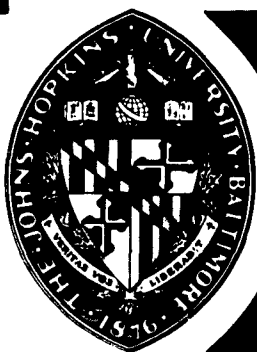
ZERO-CROSSING INTERVALS OF RANDOM PROCESSES

by

A. J. Rainal

401 148

CATALOGED BY ASTIA  
AS AD IN 401148



THE JOHNS HOPKINS UNIVERSITY  
CARLYLE BARTON LABORATORY  
BALTIMORE, MD.

CONTRACT NO. AF 33(657)-11029  
[FORMERLY AF 33(616)-6753]

MARCH 1963

10-1963  
LIBRARY  
ASTIA

Copy No. 10

THE JOHNS HOPKINS UNIVERSITY  
CARLYLE BARTON LABORATORY  
BALTIMORE, MARYLAND

Technical Report No. AF-102

ZERO-CROSSING INTERVALS OF RANDOM PROCESSES

by

A. J. Rainal

Program Element Code: 62405454

Technical Area: 760D

Task: 403601

Project Engineer:

1/Lt. W. F. H. Ring, Extension 33222

Aeronautical Systems Division

Wright-Patterson Air Force Base, Ohio

Contract No. AF 33(657)-11029  
(Formerly No. AF 33(616)-6753)

April, 1963

## TABLE OF CONTENTS

	<u>Page</u>
TABLE OF CONTENTS	
LIST OF ILLUSTRATIONS	
ACKNOWLEDGMENT	
ABSTRACT	
I. INTRODUCTION . . . . .	19
II. THE MEASURING SYSTEM . . . . .	24
A. METHOD OF MEASUREMENT . . .	24
B. SAMPLE SIZE . . . . .	26
III. THE SYNTHESIS SYSTEM . . . . .	30
A. SHAPING THE POWER SPECTRA .	30
B. THE "WHITE" NOISE SOURCE . .	31
C. POWER SPECTRA CONSIDERED . .	39
D. RANDOM POINT-PROCESS TRANSFORMATIONS . . . . .	45
IV. MATHEMATICAL DEDUCTIONS FROM THE PROBABILITY DENSITIES . . . . .	51
V. PROPERTIES OF THE PROBABILITY DENSITIES . . . . .	55
A. EXPECTATIONS . . . . .	55
B. STANDARD DEVIATIONS AND CORRELATION COEFFICIENTS . .	61
VI. PROBABILITIES AND PROBABILITY DENSITIES DEFINED BY THE ZERO POINTS OF GAUSSIAN PROCESSES . . .	68
A. POWER SPECTRAL DENSITY $w_1(f)$ .	68
B. POWER SPECTRAL DENSITY $w_2(f)$ .	74
C. POWER SPECTRAL DENSITY $w_3(f)$ .	75
D. POWER SPECTRAL DENSITY $w_4(f)$ .	84
VII. PROBABILITIES AND PROBABILITY DENSITIES DEFINED BY THE ZERO POINTS OF A SINE WAVE PLUS A GAUSSIAN PROCESS .	91

	<u>Page</u>
VIII. PROBABILITIES AND PROBABILITY DENSITIES DEFINED BY THE STATIONARY POINTS OF A SINE WAVE PLUS A GAUSSIAN PROCESS	110
IX. STATISTICAL DEPENDENCE OF ZERO- CROSSING INTERVALS . . . . .	128
X. APPLICATIONS . . . . .	134
A. THE MOST RANDOM DISTRIBUTION OF SUCCESSIVE ZERO-CROSSING INTERVALS . . . . .	134
B. TECHNIQUE FOR ESTIMATING THE ASYMPTOTIC EXPONENTIAL BEHAVIOR OF $P_0(\tau)$ . . . . .	138
XI. CONCLUSIONS . . . . .	140
XII APPENDIX . . . . .	142
REFERENCES . . . . .	145
DISTRIBUTION	

## LIST OF ILLUSTRATIONS

- Figure 1      Digital Measurement of Independent Samples of Zero-Crossing Intervals
- Figure 2      Histogram Approximation for  $P_0(u)$
- Figure 3      Synthesis of Gaussian Noise with Prescribed Power Spectra
- Figure 4      Periodic Pulse Sampling of a Noise Voltage  $y(t)$
- Figure 5      The Power Spectral Density for a Periodic Pulse Train Having Statistically Independent Pulse Amplitudes, Pulse Duration  $\tau$ , and Period  $T_0$
- Figure 6      The Linear Filter
- Figure 7      Randomly Weighted Filter Impulse Responses
- Figure 8      The Measured Amplitude Distribution  $p(v)$  Compared with Points Representing a Gaussian Distribution
- Figure 9      The Synthesis of the System Functions  $H_n(j2\pi f)$  for  $n = 0, 1, 2$
- Figure 10     The Synthesis of the System Functions  $H_n(j2\pi f)$  for  $n = 3, 4$
- Figure 11     For the System Function  $H_4(j2\pi f)$ , the Experimental Values of  $\left|\frac{e_0}{e_1}\right|$  are Compared with the Gaussian Function  $\sqrt{W_4(f)}$
- Figure 12     The Linear System
- Figure 13     Transformation of Stationary Points to Zero Points
- Figure 14     The Synthesis of  $D(j2\pi f)$

Figure 15 The Stationary Points of  $x(t)$  and the Zero Points of  $y(t)$  Occur Simultaneously

Figure 16 Block Diagram of the Synthesis and Measuring Systems.

Figure 17 Point Sets Defined by the Zero-Crossing Points and the Stationary Points of a Gaussian Process

Figure 18  $P_0(u_1)$  is the Probability Density Function for Successive Zero-Crossing Intervals of Gaussian Noise having a Power Spectral Density  $W_1(f)$ . Theoretical Approximations are Compared with Experimental Results.

Figure 19  $P_1(u_1)$  is the Probability Density Function for the Sum of Two Successive Zero-Crossing Intervals of Gaussian Noise Having a Power Spectral Density  $W_1(f)$ .  $P_0(u_1)*P_0(u_1)$  is Compared with the Experimental Result to Exhibit the Statistical Dependence of Two Successive Intervals.

Figure 20  $p(n, u_1)$  is the Probability that a Given Interval  $u_1$  contains exactly  $n$  Zero-Crossing Points.  $p(n, u_1)$  and White's  $W_+(n, u_1)$  Probabilities are Compared for the Case of Gaussian Noise Having a Power Spectral Density  $W_1(f)$  when  $n = 0, 1$

Figure 21  $Z(n, u_1)$  is the Conditional Probability that the  $n$ th Zero-Crossing Point from a Given Zero-Crossing Point in  $du_1$  occurs after the Time  $du_1 + u_1$ .  $Z(1, u_1)$  and  $Z(2, u_1)$  are Compared for the Case of Gaussian Noise Having a Power Spectral Density  $W_1(f)$ .



- Figure 22  $P_0(u_2)$  is the Probability Density Function for Successive Zero-Crossing Intervals of Gaussian Noise having a Power Spectral Density  $W_2(f)$ . Theoretical Approximations are Compared with Experimental Results.
- Figure 23  $P_1(u_2)$  is the Probability Density Function for the Sum of Two Successive Zero-Crossing Intervals of Gaussian Noise Having a Power Spectral Density  $W_2(f)$ .  $P_0(u_2)*P_0(u_2)$  is Compared with the Experimental Result to Exhibit the Practical Independence of Two Successive Intervals.
- Figure 24  $p(n, u_2)$  is the Probability that a Given Interval  $u_2$  Contains Exactly  $n$  Zero-Crossing Points.  $p(0, u_2)$  and  $p(1, u_2)$  are Compared for the Case of Gaussian Noise Having a Power Spectral Density  $W_2(f)$
- Figure 25  $Z(n, u_2)$  is the Conditional Probability that the  $n$ th Zero-Crossing Point from a Given Zero-Crossing Point in  $du_2$  Occurs after the Time  $du_2+u_2$ .  $Z(1, u_2)$  and  $Z(2, u_2)$  are compared for the Case of Gaussian Noise Having a Power Spectral Density  $W_2(f)$
- Figure 26  $P_0(u_3)$  is the Probability Density Function for Successive Zero-Crossing Intervals of Gaussian Noise Having a Power Spectral Density  $W_3(f)$ . Theoretical Approximations are Compared with Experimental Results
- Figure 27  $P_1(u_3)$  is the Probability Density Function for the Sum of Two Successive Zero-Crossing Intervals of Gaussian Noise Having a Power Spectral Density  $W_3(f)$ .  $P_0(u_3)*P_0(u_3)$  is Compared With the Experimental Result to Exhibit the Statistical Dependence of Two Successive Intervals

- Figure 28  $p(n, u_3)$  is the Probability that a Given Interval  $u_3$  Contains Exactly  $n$  Zero-Crossing Points.  $p(0, u_3)$  and  $p(1, u_3)$  are Compared for the Case of Gaussian Noise Having a Power Spectral Density  $W_3(f)$
- Figure 29  $Z(n, u_3)$  is the Conditional Probability that the  $n$ th Zero-Crossing Point From a Given Zero-Crossing Point in  $du_3$  Occurs After the Time  $du_3 + u_3$ .  $Z(1, u_3)$  and  $Z(2, u_3)$  are Compared for the Case of Gaussian Noise Having a Power Spectral Density  $W_3(f)$
- Figure 30  $P_0(u_4)$  is the Probability Density Function for Successive Zero-Crossing Intervals of Gaussian Noise Having a Power Spectral Density  $W_4(f)$ . Theoretical Approximations are Compared with Experimental Results
- Figure 31  $P_1(u_4)$  is the Probability Density Function for the Sum of Two Successive Zero-Crossing Intervals of Gaussian Noise Having a Power Spectral Density  $W_4(f)$ .  $Q(u_4) * Q(u_4)$  is Compared with  $U(u_4) - Q(u_4)$  to Exhibit the Statistical Dependence of Two Successive Intervals
- Figure 32  $p(n, u_4)$  is the Probability That a Given Interval  $u_4$  Contains Exactly  $n$  Zero-Crossing Points.  $p(0, u_4)$  and  $p(1, u_4)$  are Compared for the Case of Gaussian Noise Having the Power Spectral Density  $W_4(f)$
- Figure 33  $Z(n, u_4)$  is the Conditional Probability that the  $n$ th Zero-Crossing Point From a Given Zero-Crossing Point in  $du_4$  Occurs After the Time  $du_4 + u_4$ .  $Z(1, u_4)$  and  $Z(2, u_4)$  are Compared for the Case of Gaussian Noise Having a Power Spectral Density  $W_4(f)$

- Figure 34**  $P_0(u_0, a)$  is the Probability Density Function for Successive Zero Crossing Intervals of a Random Process Consisting of Sine Wave of Frequency  $f_0/2$  Plus Gaussian Noise Having the Power Spectral Density  $W_0(f)$ . The Ratio of the Average Sine Wave Power to the Average Noise Power is Denoted by the Parameter  $a$ . Theoretical Approximations are Compared with Experimental Results.
- Figure 35**  $P_1(u_0, a)$  is the Probability Density Function for the Sum of Two Successive Zero-Crossing Intervals of a Random Process Consisting of a Sine Wave of Frequency  $f_0/2$  Plus Gaussian Noise Having the Power Spectral Density  $W_0(f)$ . The Ratio of the Average Sine Wave Power to the Average Noise Power is Denoted by the Parameter  $a$ .
- Figure 36**  $p_a(n, u_0)$  is the Probability that a Given Interval  $u_0$  Contains Exactly  $n$  Zero-Crossing Points of a Random Process Consisting of a Sine Wave of Frequency  $f_0/2$  Plus Gaussian Noise Having the Power Spectral Density  $W_0(f)$ . The Ratio of the Average Sine Wave Power to the Average Noise Power is Denoted by the Parameter  $a$ .
- Figure 37** A Random Process Consisting of a Sine Wave of Frequency  $f_0/2$  Plus Gaussian Noise Having the Power Spectral Density  $W_0(f)$  Defines  $Z_a(n, u_0)$ , the Conditional Probability That the  $n$ th Zero-Crossing Point From a Given Zero-Crossing Point in  $du_0$  Occurs After the time  $du_0 + u_0$ . The Ratio of the Average Sine Wave Power to the Average Noise Power is Denoted by the Parameter  $a$ .

Figure 38  $P_0(u_0, a)$  is the Probability Density Function for Successive Zero-Crossing Intervals of a Random Process Consisting of a Sine Wave of Frequency  $f_0/2$  Plus Gaussian Noise Having the Power Spectral Density  $W_0(f)$ . The Ratio of the Average Sine Wave Power to the Average Noise Power is Denoted by the Parameter  $a$ . Theoretical Approximations are Compared With Experimental Results.

Figure 39  $P_1(u_0, a)$  is the Probability Density Function for the Sum of Two Successive Zero-Crossing Intervals of a Random Process Consisting of a Sine Wave of Frequency  $f_0/2$  Plus Gaussian Noise Having the Power Spectral Density  $W_0(f)$ . The Ratio of the Average Sine Wave Power to the Average Noise Power is Denoted by the Parameter  $a$ .

Figure 40  $p_a(n, u_0)$  is the Probability that a Given Interval  $u_0$  Contains Exactly  $n$  Zero-Crossing Points of a Random Process Consisting of a Sine Wave of Frequency  $f_0/2$  Plus Gaussian Noise Having the Power Spectral Density  $W_0(f)$ . The Ratio of the Average Sine Wave Power to the Average Noise Power is Denoted by the Parameter  $a$ .

Figure 41 A Random Process Consisting of a Sine Wave of Frequency  $f_0/2$  Plus Gaussian Noise Having the Power Spectral Density  $W_0(f)$  Defines  $Z_a(n, u_0)$ , the Conditional Probability that the  $n$ th Zero-Crossing Point From a Given Zero-Crossing Point in  $du_0$  Occurs After the Time  $du_0 + u_0$ . The Ratio of the Average Sine Wave Power to the Average Noise Power is Denoted by the Parameter  $a$ .

**Figure 42**  $P_0(u_0, a)$  is the Probability Density Function for Successive Zero-Crossing Intervals of a Random Process Consisting of a Sine Wave of Frequency  $f_0/2$  Plus Gaussian Noise Having the Power Spectral Density  $W_0(f)$ . The Ratio of the Average Sine Wave Power to the Average Noise Power is Denoted by the Parameter  $a$ . Theoretical Approximations are Compared with Experimental Results.

**Figure 43**  $P_1(u_0, a)$  is the Probability Density Function for the Sum of Two Successive Zero-Crossing Intervals of a Random Process Consisting of a Sine Wave of Frequency  $f_0/2$  Plus Gaussian Noise Having the Power Spectral Density  $W_0(f)$ . The Ratio of the Average Sine Wave Power to the Average Noise Power is Denoted by the Parameter  $a$ .

**Figure 44**  $p_a(n, u_0)$  is the Probability that a Given Interval  $u_0$  Contains Exactly  $n$  Zero-Crossing Points of a Random Process Consisting of a Sine Wave of Frequency  $f_0/2$  Plus Gaussian Noise Having the Power Spectral Density  $W_0(f)$ . The Ratio of the Average Sine Wave Power to the Average Noise Power is Denoted by the Parameter  $a$ .

**Figure 45** A Random Process Consisting of a Sine Wave of Frequency  $f_0/2$  Plus Gaussian Noise Having the Power Spectral Density  $W_0(f)$  Defines  $Z_a(n, u_0)$ , the Conditional Probability That the  $n$ th Zero-Crossing Point from a Given Zero-Crossing Point in  $du_0$  Occurs After the Time  $du_0 + u_0$ . The Ratio of the Average Sine Wave Power to the Average Noise Power is Denoted by the Parameter  $a$ .

- Figure 46  $P_0(u_0, a)$  is the Probability Density Function for Successive Zero-Crossing Intervals of a Random Process Consisting of a Sine Wave of Frequency  $f_0/2$  Plus Gaussian Noise Having the Power Spectral Density  $W_0(f)$ . The Ratio of the Average Sine Wave Power to the Average Noise Power is Denoted by the Parameter  $a$ . Theoretical Approximations are Compared with Experimental Results.
- Figure 47  $P_1(u_0, a)$  is the Probability Density Function for the Sum of Two Successive Zero-Crossing Intervals of a Random Process Consisting of a Sine Wave of Frequency  $f_0/2$  Plus Gaussian Noise Having the Power Spectral Density  $W_0(f)$ . The Ratio of the Average Sine Wave Power to the Average Noise Power is Denoted by the Parameter  $a$ .
- Figure 48  $p_a(n, u_0)$  is the Probability that a Given Interval  $u_0$  Contains Exactly  $n$  Zero-Crossing Points of a Random Process Consisting of a Sine Wave of Frequency  $f_0/2$  Plus Gaussian Noise Having the Power Spectral Density  $W_0(f)$ . The Ratio of the Average Sine Wave Power to the Average Noise Power is Denoted by the Parameter  $a$ .
- Figure 49 A Random Process Consisting of a Sine Wave of Frequency  $f_0/2$  Plus Gaussian Noise Having the Power Spectral Density  $W_0(f)$  Defines  $Z_a(n, u_0)$ , the Conditional Probability that the  $n$ th Zero-Crossing Point from a Given Zero-Crossing Point in  $du_0$  Occurs After the time  $du_0 + u_0$ . The Ratio of the Average Sine Wave Power to the Average Noise Power is Denoted by the Parameter  $a$ .

Figure 50  $M_0(u_0, a)$  is the Probability Density Function for Successive Intervals Defined by Adjacent Stationary Points of a Random Process Consisting of a Sine Wave of Frequency  $f_0/2$  Plus Gaussian Noise Having the Power Spectral Density  $W_0(f)$ . The Ratio of the Average Sine Wave Power to the Average Noise Power is Denoted by the Parameter  $a$ . Theoretical Approximations are Compared with Experimental Results.

Figure 51  $M_1(u_0, a)$  is the Probability Density Function for the Sum of Two Successive Intervals Defined by Adjacent Stationary Points of a Random Process Consisting of a Sine Wave of Frequency  $f_0/2$  Plus Gaussian Noise Having the Power Spectral Density  $W_0(f)$ . The Ratio of the Average Sine Wave Power to the Average Noise Power is Denoted by the Parameter  $a$ .

Figure 52  $m_2(n, u_0)$  is the Probability that a Given Interval  $u_0$  Contains Exactly  $n$  Stationary Points of a Random Process Consisting of a Sine Wave of Frequency  $f_0/2$  Plus Gaussian Noise Having the Power Spectral Density  $W_0(f)$ . The Ratio of the Average Sine Wave Power to the Average Noise Power is Denoted by the Parameter  $a$ .

Figure 53 A Random Process Consisting of a Sine Wave of Frequency  $f_0/2$  Plus Gaussian Noise Having the Power Spectral Density  $W_0(f)$  Defines  $S_a(n, u_0)$ , the Conditional Probability that the  $n$ th Stationary Point from a Given Stationary Point in  $du_0$  occurs after the Time  $du_0 + u_0$ . The Ratio of the Average Sine Wave Power to the Average Noise Power is Denoted by the Parameter  $a$ .

Figure 54  $M_0(u_0, a)$  is the Probability Density Function for Successive Intervals Defined by Adjacent Stationary Points of a Random Process Consisting of a Sine Wave of Frequency  $f_0/2$  Plus Gaussian Noise Having the Power Spectral Density  $W_0(f)$ . The Ratio of The Average Sine Wave Power to the Average Noise Power is Denoted by the Parameter  $a$ . Theoretical Approximations are Compared with Experimental Results.

Figure 55  $M_1(u_0, a)$  is the Probability Density Function for the Sum of Two Successive Intervals Defined by Adjacent Stationary Points of a Random Process Consisting of A Sine Wave of Frequency  $f_0/2$  Plus Gaussian Noise Having the Power Spectral Density  $W_0(f)$ . The Ratio of the Average Sine Wave Power to the Average Noise Power is Denoted by the Parameter  $a$ .

Figure 56  $m_a(n, u_0)$  is the Probability That a Given Interval  $u_0$  Contains Exactly  $n$  Stationary Points of a Random Process Consisting of a Sine Wave of Frequency  $f_0/2$  Plus Gaussian Noise Having the Power Spectral Density  $W_0(f)$ . The Ratio of the Average Sine Wave Power to the Average Noise Power is Denoted by the Parameter  $a$ .

Figure 57 A Random Process Consisting of a Sine Wave of Frequency  $f_0/2$  Plus Gaussian Noise Having the Power Spectral Density  $W_0(f)$  Defines  $S_a(n, u_0)$ , the Conditional Probability that the  $n$ th Stationary Point from a Given Stationary Point in  $du_0$  Occurs after the Time  $du_0 + u_0$ . The Ratio of the Average Sine Wave Power to the Average Noise Power is Denoted by the Parameter  $a$ .



**Figure 58**  $M_0(u_0, a)$  is the Probability Density Function for Successive Intervals Defined by Adjacent Stationary Points of a Random Process Consisting of a Sine Wave of Frequency  $f_0/2$  Plus Gaussian Noise Having the Power Spectral Density  $W_0(f)$ . The Ratio of the Average Sine Wave Power to the Average Noise Power is Denoted by the Parameter  $a$ . Theoretical Approximations are Compared with Experimental Results.

**Figure 59**  $M_1(u_0, a)$  is the Probability Density Function for the Sum of Two Successive Intervals Defined by Adjacent Stationary Points of a Random Process Consisting of a Sine Wave of Frequency  $f_0/2$  Plus Gaussian Noise Having the Power Spectral Density  $W_0(f)$ . The ratio of the Average Sine Wave Power to the Average Noise Power is Denoted by the Parameter  $a$ .

**Figure 60**  $m_a(n, u_0)$  is the Probability that a Given Interval  $u_0$  Contains Exactly  $n$  Stationary Points of a Random Process Consisting of a Sine Wave of Frequency  $f_0/2$  Plus Gaussian Noise Having the Power Spectral Density  $W_0(f)$ . The Ratio of the Average Sine Wave Power to the Average Noise Power is Denoted by The Parameter  $a$ .

**Figure 61** A Random Process Consisting of a Sine Wave of Frequency  $f_0/2$  Plus Gaussian Noise Having the Power Spectral Density  $W_0(f)$  Defines  $S_a(n, u_0)$ , the Conditional Probability that the  $n$ th Stationary Point from a Given Stationary Point in  $du_0$  Occurs after the Time  $du_0 + u_0$ . The Ratio of the Average Sine Wave Power to the Average Noise Power is Denoted by the Parameter  $a$ .

- Figure 62**  $M_0(u_0, a)$  is the Probability Density Function for Successive Intervals Defined by Adjacent Stationary Points of a Random Process Consisting of a Sine Wave of Frequency  $f_0/2$  Plus Gaussian Noise Having the Power Spectral Density  $W_0(f)$ . The Ratio of the Average Sine Wave Power to the Average Noise Power is Denoted by the Parameter  $a$ . Theoretical Approximations are Compared with Experimental Results.
- Figure 63**  $M_1(u_0, a)$  is the Probability Density Function for the Sum of Two Successive Intervals Defined by Adjacent Stationary Points of A Random Process Consisting of a Sine Wave of Frequency  $f_0/2$  Plus Gaussian Noise Having the Power Spectral Density  $W_0(f)$ . The ratio of the Average Sine Wave Power to the Average Noise Power is Denoted by the Parameter  $a$ .
- Figure 64**  $m_a(n, u_0)$  is the Probability that a Given Interval  $u_0$  Contains Exactly  $n$  Stationary Points of a Random Process Consisting of a Sine Wave of Frequency  $f_0/2$  Plus Gaussian Noise Having the Power Spectral Density  $W_0(f)$ . The Ratio of the Average Sine Wave Power to the Average Noise Power is Denoted by the Parameter  $a$ .
- Figure 65** A Random Process Consisting of a Sine Wave of Frequency  $f_0/2$  Plus Gaussian Noise Having the Power Spectral Density  $W_0(f)$  Defines  $S_a(n, u_0)$ , The Conditional Probability that the  $n$ th Stationary Point from a Given Stationary Point in  $du_0$  Occurs After the Time  $du_0 + u_0$ . The Ratio of the Average Sine Wave Power to the Average Noise Power is Denoted by the Parameter  $a$ .

Figure 66 Each Intensity Pattern Represents an Approximation to the Joint Probability Density of the  $i$ th and  $(i+n)$ th Zero-Crossing Intervals of a Gaussian Process Having Power Spectral Density  $W_3(f)$ .

Figure 67 The Truncated Gaussian Probability Density,  $P_0(\tau)$ , Represents the Most Random Distribution of Successive Zero-Crossing Intervals Having a Given Mean and a Given Standard Deviation.

### ACKNOWLEDGMENTS

The author wishes to acknowledge the excellent support he received while carrying out the investigations leading to this report. Professor W. C. Gore and Dr. F. C. Ogg served as referees. Dr. D. Middleton served as a consultant and contributed encouragement as well as advice. Dr. J. M. Kopper reviewed the manuscript. Mr. H. W. Snyder constructed the experimental equipment and helped to gather the experimental data. Miss P. M. Powers and Mr. W. A. Ray programmed the digital computers. Mrs. M. D. Denburg and Miss P. A. Shipley performed some numerical calculations and plotted the curves. Mr. C. M. LaPorte and Mr. A. L. Mancini prepared the figures. Mrs. D. C. Scholl typed the manuscript. The author wishes to express his sincere gratitude to all these people. The author is also indebted to Dr. E. M. Glaser for some initial guidance. This research was supported by the Air Force Systems Command, United States Air Force.

## ABSTRACT

This report describes a digital system for studying the zero-crossing intervals of random processes. Probabilities and probability densities defined by the zero-crossing points of various Gaussian processes are presented. Probabilities and probability densities defined by the zero-crossing points of a random process consisting of a sine wave plus a Gaussian process are also presented. Finally, probabilities and probability densities defined by the stationary points of a random process consisting of a sine wave plus a Gaussian process are presented. At present none of the probabilities or probability densities can be derived explicitly by analytical methods. The standard deviations associated with the probability densities are also presented. In the case of the Gaussian processes the correlation coefficients for two successive intervals are presented. The first moments associated with the probability densities are compared with the exact theoretical values. All the other experimental results are compared with theoretical approximations. The statistical dependence between the  $i$ th zero-crossing interval and the  $(i+n)$ th zero-crossing interval is investigated.

## I. INTRODUCTION

In many branches of science and technology one encounters the basic density  $P_n(\tau)$ , the probability density of the interval  $\tau$  between the  $m$ th and  $(m+n+1)$ th zero-crossing points of a random process. This density occurs for example in the fields of statistical communication theory, oceanography, statistical mechanics, biophysics, and control engineering. When  $n = 0$  the interval  $\tau$  is called a zero-crossing interval. A striking experimental fact is that the successive zero-crossing intervals of an audio process contain a great deal of the intelligibility. For the most common random process, a Gaussian process with arbitrary power spectrum,  $P_n(\tau)$  cannot be derived explicitly by analytical methods. For a Gaussian process having a certain class of power spectra, S. O. Rice (1) derived two functions which can be used to approximate  $P_0(\tau)$  and  $P_1(\tau)$  for small  $\tau$ . More recently J. A. McFadden (2) and M. S. Longuet-Higgins (8) derived approximations for  $P_0(\tau)$  which compare favorably with experimental results for a larger class of Gaussian processes having arbitrary power spectra.

Some other important theoretical work concerned with  $P_n(\tau)$  has been reported by D. Middleton (3), A. Kohlenberg (4), Kuznetsov, Stratonovich, and Tikhonov (5), V. I. Tikhonov and I. N. Amiantov (6), M. S. Longuet-Higgins (7), C. W. Helstrom (9), H. Steinberg, P. M. Schultheiss, C. A. Wogrin, and F. Zweig (10), D. S. Palmer (11), H. Debart (12), D. Slepian (13), W. M. Brown (14), J. S. Bendat

(15), M. Kac (16), I. Miller and J. E. Freund (17), H. Zuhrt (29), S. Ehrenfeld (30) et al., and L. I. Bialyi (31). Fewer analytical results concerning  $P_0(\tau)$ ,  $P_1(\tau)$  exist for such a common non-Gaussian random process as a sine wave signal plus a Gaussian process. In short, one must conclude that mathematical difficulties seriously limit the understanding of this statistical phenomenon. Under such circumstances one is naturally motivated to turn to experiment for further insight.

Most of the experimental work dealing with this problem has been reported by G. M. White (18), Favreau, Low, and Pfeffer (19), C. R. Gates (20), Kjell Blötekjaer (21), and A. I. Velichkin and V. D. Ponomareva (22). In order to explore the problem further an experimental system has been designed at this Laboratory. The system differs considerably from previous experimental systems, and the measurement is digital rather than analog. This approach permits the system to work in conjunction with a digital computer to help analyze the recorded data. Also, the inherent stability of a digital system allows measurements to be made over periods of hours or days if required.

This report presents a description of the experimental system and the following results concerning the zero-crossing intervals of certain Gaussian processes:

- (1)  $P_0(\tau)$ , the probability density function for successive zero-crossing intervals.
- (2)  $P_1(\tau)$ , the probability density function for the sum of two successive zero-crossing intervals.
- (3)  $p(0, \tau)$ , the probability that a given interval  $\tau$  contains exactly zero zero-crossings.
- (4)  $p(1, \tau)$ , the probability that a given interval  $\tau$  contains exactly one zero-crossing.
- (5)  $Z(1, \tau)$ , the conditional probability that the first zero-crossing from a given zero-crossing in  $d\tau$  occurs after the time  $d\tau + \tau$ .
- (6)  $Z(2, \tau)$ , the conditional probability that the second zero-crossing from a given zero-crossing in  $d\tau$  occurs after the time  $d\tau + \tau$ .
- (7) The expectations and standard deviations associated with  $P_0(\tau)$  and  $P_1(\tau)$ .
- (8) The correlation coefficient for two successive zero-crossing intervals.

This report also presents the following results concerning the zero-crossing intervals of a random process consisting of a sine wave signal of frequency  $\frac{f_0}{2}$  plus Gaussian noise such that the signal-to-noise power ratio equals  $a$ :



- (1)  $P_0(\tau, a)$ , the probability density function for successive zero-crossing intervals.
- (2)  $P_1(\tau, a)$ , the probability density function for the sum of two successive zero-crossing intervals.
- (3)  $p_a(0, \tau)$ , the probability that a given interval  $\tau$  contains exactly zero zero-crossings.
- (4)  $p_a(1, \tau)$ , the probability that a given interval  $\tau$  contains exactly one zero-crossing.
- (5)  $Z_a(1, \tau)$ , the conditional probability that the first zero-crossing from a given zero-crossing in  $d\tau$  occurs after the time  $d\tau + \tau$ .
- (6)  $Z_a(2, \tau)$ , the conditional probability that the second zero-crossing from a given zero-crossing in  $d\tau$  occurs after the time  $d\tau + \tau$ .
- (7) The expectations and standard deviations associated with  $P_0(\tau, a)$  and  $P_1(\tau, a)$ .

Finally, this report presents the following results concerning the intervals defined by the mathematical stationary points of a random process consisting of a sine wave signal of frequency  $\frac{f_o}{2}$  plus Gaussian noise such that the signal-to-noise power ratio equals  $a$ :

- (1)  $M_0(\tau, a)$ , the probability density function for successive intervals defined by adjacent stationary points.

- (2)  $M_1(\tau, a)$ , the probability density function for the sum of two successive intervals defined by adjacent stationary points.
- (3)  $m_a(0, \tau)$ , the probability that a given interval  $\tau$  contains exactly zero stationary points.
- (4)  $m_a(1, \tau)$ , the probability that a given interval  $\tau$  contains exactly one stationary point.
- (5)  $S_a(1, \tau)$ , the conditional probability that the first stationary point from a given stationary point in  $d\tau$  occurs after the time  $d\tau + \tau$ .
- (6)  $S_a(2, \tau)$ , the conditional probability that the second stationary point from a given stationary point in  $d\tau$  occurs after the time  $d\tau + \tau$ .
- (7) The expectations and standard deviations associated with  $M_0(\tau, a)$  and  $M_1(\tau, a)$ .

The above probabilities and probability densities were selected for investigation not only because they are of theoretical interest but also because they are of practical interest, since they are observables which are comparatively simple to measure.

The system measures the basic densities  $P_0(\tau)$ ,  $P_1(\tau)$ ,  $P_0(\tau, a)$ ,  $P_1(\tau, a)$ ,  $M_0(\tau, a)$  and  $M_1(\tau, a)$ . The remaining probabilities are deduced by applying the theory of point-processes. The system can measure these densities at levels other than the zero level.

## II. THE MEASURING SYSTEM

### A. METHOD OF MEASUREMENT

Instead of measuring successive zero-crossing intervals the system measures samples of zero-crossing intervals which are sufficiently independent. However, the random processes under investigation are metrically transitive (23) or ergodic, and hence the statistics of these samples are equal with probability unity to the statistics of successive zero-crossing intervals.

The method of measuring independent samples of zero-crossing intervals is illustrated in Figure 1. The method consists of opening and closing an electronic gate at the proper times following each initiate command. The gate controls the number of clock pulses counted by an electronic counter. The resulting count in the electronic counter is then a measure of the sampled zero-crossing interval. The count is printed on tape in order to monitor each sampled time interval and to check the average zero-crossing interval. The count is also punched on paper tape which feeds into an IBM-7090 digital computer. The circuit details have been reported in the literature (24).

Selecting a zero-crossing interval that corresponds in time with the instant of an initiate command tends to favor the long intervals. Since in general successive intervals are statistically

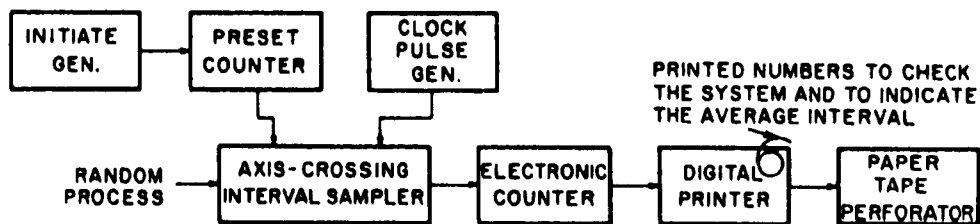
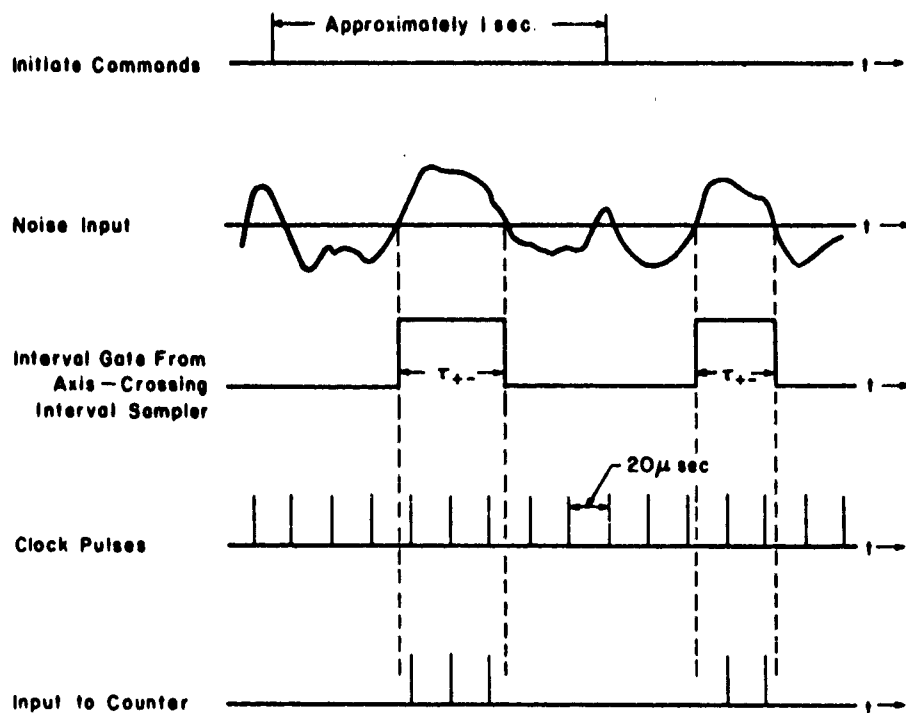


Figure 1 Digital Measurement of Independent Samples of Zero-Crossing Intervals

dependent, this bias may also bias the selection of an interval that occurs after an initiate command. Accordingly, the digital system skips, with equal probability, one or two intervals immediately following the initiate command and then measures the next interval. By skipping these intervals the bias associated with selecting an interval after an initiate command proves to be negligible. The significance of this bias has been discussed recently by McFadden (32). The system has provisions for skipping an arbitrary number of intervals.

#### B. SAMPLE SIZE

Consider a histogram approximation to a probability density  $P_0(u)$  as shown in Figure 2. After measuring  $n$  mutually independent samples of time intervals let the number of time intervals in the range  $u, u + \Delta u$  be denoted by  $S_n$  and let

$$p = \int_u^{u+\Delta u} P_0(u) du \quad . \quad (1)$$

Let the random variable  $X_k$  equal one if the result of the  $k$ th measurement is in the range  $u, u + \Delta u$  and zero otherwise. Also, let all the  $X_k$  have a common probability density with mean  $p$  and variance  $\sigma^2$ . Then

$$S_n = \sum_{k=1}^n X_k \quad (2)$$

and by using the Tchebycheff inequality

$$\Pr\left\{ |S_n - np| \geq t \right\} \leq \frac{nc^2}{t^2} \quad \text{for all } t > 0 \quad (3)$$

where  $\Pr\{E\}$  denotes the probability of the event  $E$ . For  $t = \epsilon n$

$$\Pr\left\{ \left| \frac{S_n}{n} - p \right| \geq \epsilon \right\} \leq \frac{\sigma^2}{n\epsilon^2} \quad (4)$$

Accordingly, as  $n \rightarrow \infty$ ,  $\frac{S_n}{n} \rightarrow p$  with probability 1. This is Bernoulli's (1713) celebrated weak law of large numbers which played a central role in the notion of probability. Cantelli's (1917) celebrated strong law of large numbers not only implies the weak law of large numbers but also asserts that with probability one only finitely many of the events

$$\left| \frac{S_n}{n} - p \right| > \epsilon \quad \text{occur as } n \rightarrow \infty.$$

In short, the weak law asserts convergence in probability; whereas the strong law asserts convergence with probability one.

In experimental work  $n$  is limited by practical considerations.

Hence, one needs a quantitative measure of the manner in which  $\frac{S_n}{n}$  approaches  $p$  with increasing  $n$ . In deriving such a measure notice that we are dealing with repeated independent trials having only two possible outcomes. Accordingly, we will adopt a Bernoulli model and consider each trial as a Bernoulli trial. Using the DeMoivre limit Theorem (1718) and letting  $q = 1-p$  we have that as  $n \rightarrow \infty$ ,

$$\Pr\left\{-x \leq \frac{S_n - np}{\sqrt{npq}} \leq x\right\} = \Pr\left\{-x\sqrt{\frac{pq}{n}} \leq \frac{S_n}{n} - p \leq x\sqrt{\frac{pq}{n}}\right\} \rightarrow \Phi(x) - \Phi(-x) = 2\Phi(x) - 1 \quad (5)$$

where

$$\Phi(x) = \frac{1}{\sqrt{2\pi}} \int_{-\infty}^x e^{-y^2/2} dy$$

Let us require that  $\frac{S_n}{n}$  approach  $p$  to within a given arbitrary amount during 95% of our statistical experience. That is, let our confidence level be 0.95. Then  $x = 1.96$ , and  $\Delta P_o$  as shown in Figure 2 is given by

$$\Delta P_o \Delta u = \left| \frac{S_n}{n} - p \right| \leq 1.96 \sqrt{\frac{pq}{n}} \quad (6)$$

and

$$\Delta P_o \leq \frac{1.96}{\Delta u} \sqrt{\frac{pq}{n}} \quad (7)$$

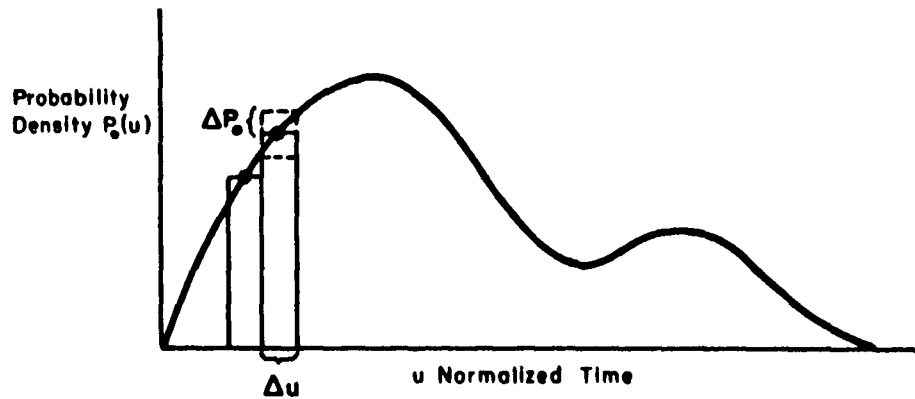


Figure 2 Histogram Approximation for  $P_o(u)$ .

This is the basic result concerning the sample size. It was used to compute the 95% confidence limits presented with the probability density functions. Using this basic result we choose  $n$  to be approximately 40,000.



### III. THE SYNTHESIS SYSTEM

#### A. SHAPING THE POWER SPECTRUM

The method used to synthesize a Gaussian random process with prescribed power spectral density is illustrated in Figure 3. "White" Gaussian noise is applied to a linear network having a system function  $H(j2\pi f)$ . The output of such a network is a Gaussian random process having a power spectral density proportional to  $|H(j2\pi f)|^2$ . Operational amplifiers with appropriate feedback networks were used to synthesize  $H(j2\pi f)$ .

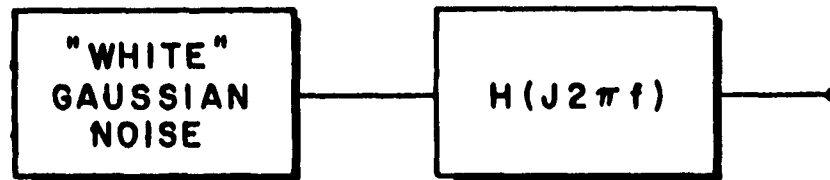


Figure 3      Synthesis of Gaussian Noise with Prescribed Power Spectra.

In order to investigate the zero-crossing intervals of Gaussian processes having certain power spectral densities of interest, the digital system requires a "white" Gaussian noise source having a low frequency cut-off of approximately 1 cps and a high frequency cut-off of at least 8 Kcps. The theory and design of such a noise source has been reported in the literature (25). The theory is described below.

## B. THE "WHITE" NOISE SOURCE

Consider a train of periodic pulses  $u_n(t-nT_0)$  with fixed duration  $\tau$  and with amplitudes determined by the corresponding amplitudes of an ergodic random process. This random pulse train may be the result of periodically sampling the amplitude of a noise voltage  $y(t)$  as is shown in Figure 4. Generalizing Middleton's (3a) result, the power spectral density of the random pulse train is

$$W(f) = \overline{W_u(f)} \left[ \sum_{k=-\infty}^{\infty} K_y(kT_0) e^{i\omega k T_0} + \frac{\bar{y}^2}{T_0} \sum_{m=0}^{\infty} \delta(f - \frac{m}{T_0}) \right] \quad (8)$$

where

$\overline{W_u(f)}$  = average power spectral density of the individual pulses

$K_y(t_1 - t_2) = \overline{(y_1 - \bar{y}_1)(y_2 - \bar{y}_2)}$  = noise autocovariance function

$\bar{y}$  = average value of the pulse amplitudes

$T_0$  = sampling period

$\delta$  = Dirac delta function.

If  $T_0$  is large compared with the noise fluctuation time -- roughly the mean spacing between successive zero-crossings of the noise --, then

$$W(f) = \overline{W_u(f)} \left[ (y^2 - \bar{y}^2) + \frac{\bar{y}^2}{T_0} \sum_{m=0}^{\infty} \delta(f - \frac{m}{T_0}) \right]. \quad (9)$$

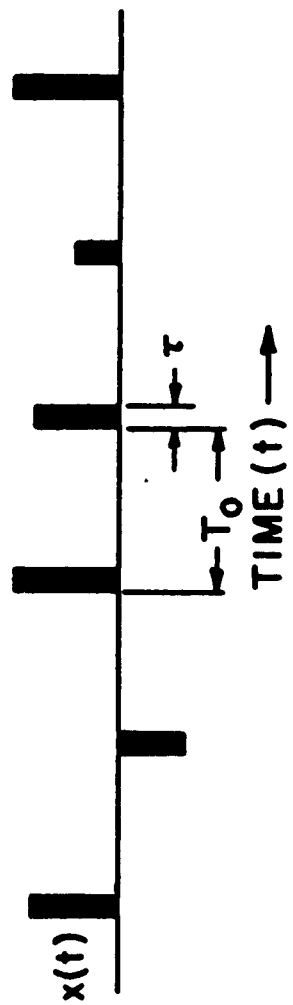
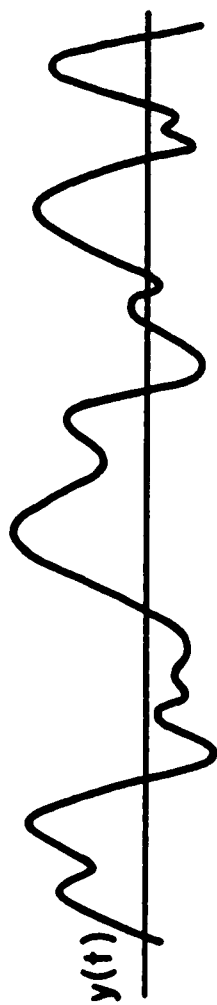


Figure 4 Periodic Pulse Sampling of a Noise Voltage  $y(t)$

The spectrum consists of a continuous part whose distribution is determined solely by the shapes of the individual pulses and whose intensity is proportional to the variance of the pulse amplitudes. In addition there is a discrete spectrum with components at multiples of the sampling rate  $1/T_0$ , whose intensity is proportional to the square of the average pulse amplitude. A typical  $W(f)$  is shown in Figure 5. If  $\bar{y} = 0$ , then spikes in  $W(f)$  vanish. For the white noise source used in the digital system the frequency region from near zero to a little less than  $1/T_0$  cps was extracted by a passive linear low-pass filter.

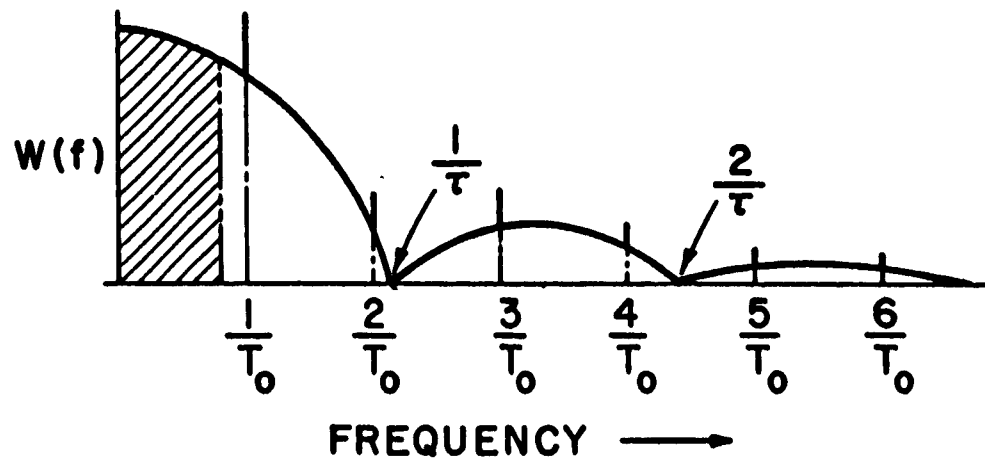


Figure 5 The Power Spectral Density for a Periodic Pulse Train Having Statistically Independent Pulse Amplitudes, Pulse Duration  $\tau$ , and Period  $T_0$ .

Consider the random pulse train  $x(t)$ , see Figure 4, as the input to a linear filter with impulse response  $h(t)$  as is shown in Figure 6. Let  $x(t)$  be represented by a weighted sum of narrow pulses:

$$x(t) = \sum_{n=-\infty}^{\infty} y_n u(t-nT_0) \quad (10)$$

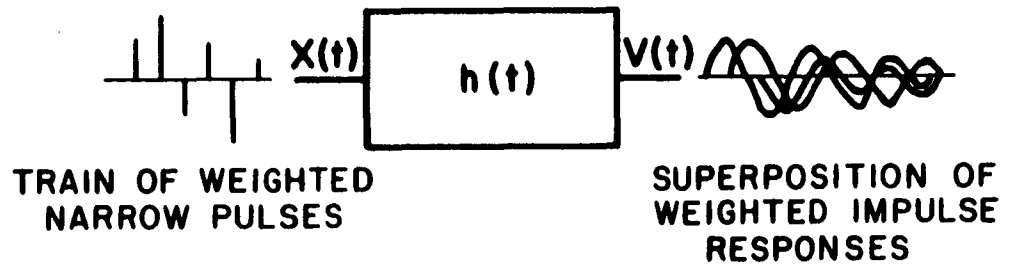


Figure 6 The Linear Filter.

Then, if we assume that the duration of  $u_0(t)$  is short compared with the duration of  $h(t)$ ,  $u_0(t) \doteq \delta(t)$  and the output  $V(t)$  of the filter becomes

$$V(t) = \int_{-\infty}^{\infty} x(\tau) h(t-\tau) d\tau = \sum_{n=-\infty}^{\infty} y_n h(t-nT_0) \quad (11)$$

The filter output  $V(t)$  consists of the weighted sum of impulse responses whose epochs are at integral multiples of  $T_0$ , as shown in Figure 7.

What may be said regarding the amplitude distribution of  $V(t)$ ? In general very little, for this is related to the more

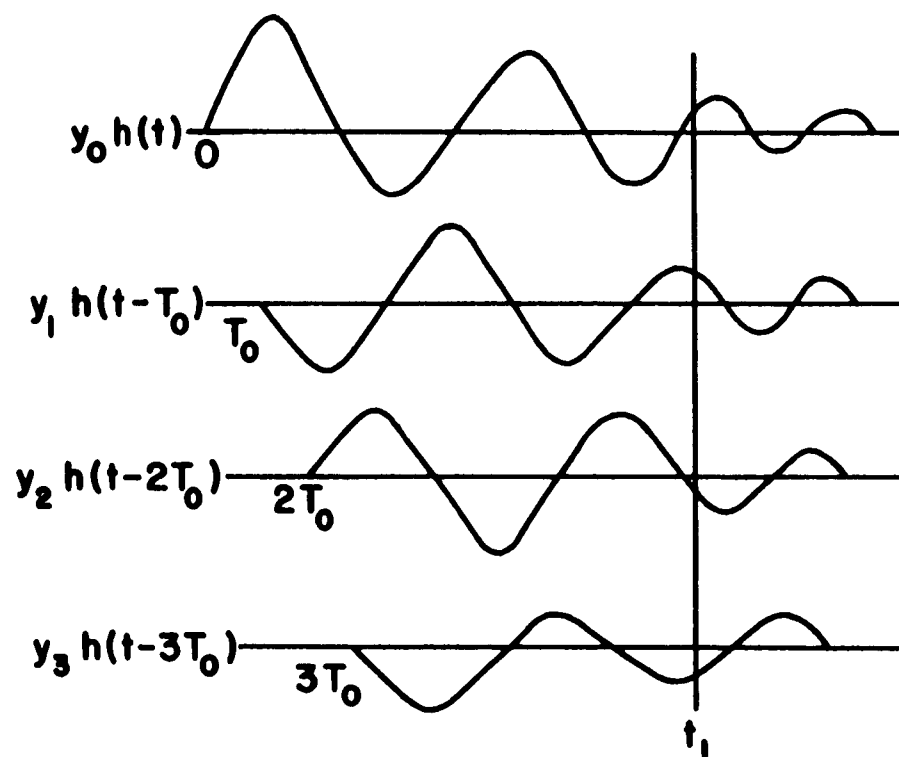


Figure 7 Randomly Weighted Filter Impulse Responses

general problem of determining the output amplitude distribution of a linear system driven by a non-Gaussian random process. However, the form of Equation (11) suggests the application of the central limit theorem of probability. The central limit theorem asserts that under general conditions the sum of a large number of independent random variables approaches a Gaussian distribution. That is to say, if  $n$  independent impulse responses produce non-negligible effects on  $V(t_1)$ , and if  $n$  is sufficiently large, then the ensemble of values  $V(t_1)$  will be Gaussianly distributed. Since the distribution is tending toward a Gaussian distribution, we can perhaps help to minimize  $n$  by providing Gaussianly distributed pulse amplitudes. In any case this is most convenient, for we need only sample the amplitudes of a Gaussian noise voltage whose fluctuation time is approximately one-tenth the sampling period in order to sufficiently approach statistically independent samples. That is, if the sampling rate is 10 Kcps, then we need only sample Gaussian noise having an approximately uniform power spectral density from approximately zero frequency to 100 Kcps.

The amplitude probability density function,  $p(x)$ , for the random pulse train  $x(t)$  whose amplitudes are Gaussianly distributed with zero mean is given by

$$p(x) = \frac{\tau}{T_0} \frac{1}{\sigma\sqrt{2\pi}} e^{-\frac{x^2}{2\sigma^2}} + \left(1 - \frac{\tau}{T_0}\right) \delta(x) \quad (12)$$

Also, the characteristic function  $f(v)$  of  $p(x)$  is given by

$$f(v) = \int_{-\infty}^{\infty} e^{ivx} dP(x) = \frac{\tau}{T_0} \exp \left[ -\frac{v^2 \sigma^2}{2} \right] + \left( 1 - \frac{\tau}{T_0} \right), \quad (13)$$

where  $P(x)$  is the probability distribution function of  $x$ . Notice that if  $\tau = T_0$ , then  $x(t)$  is a boxcar waveform and is Gaussianly distributed. Of course, the output of the linear filter under these conditions will also be Gaussianly distributed.

In order to apply the central limit theorem to the situation under discussion, the impulse response of the linear filter must have a significant width, or memory, extending out to  $nT_0$ . The value of  $n$  required will normally be of the order of ten. For our particular case the value of  $n$  required to regenerate a Gaussian distribution was experimentally determined to be of the order of 3 or 4. Hence, for a sampling rate of 10 Kcps a low-pass filter having a 5 Kcps cut-off frequency will suffice for the linear filter.

Figure 8 shows the measured amplitude distributions compared with points representing a Gaussian distribution for the case of a sampling rate of 10 Kcps and a low-pass filter having a 5 Kcps cut-off frequency.



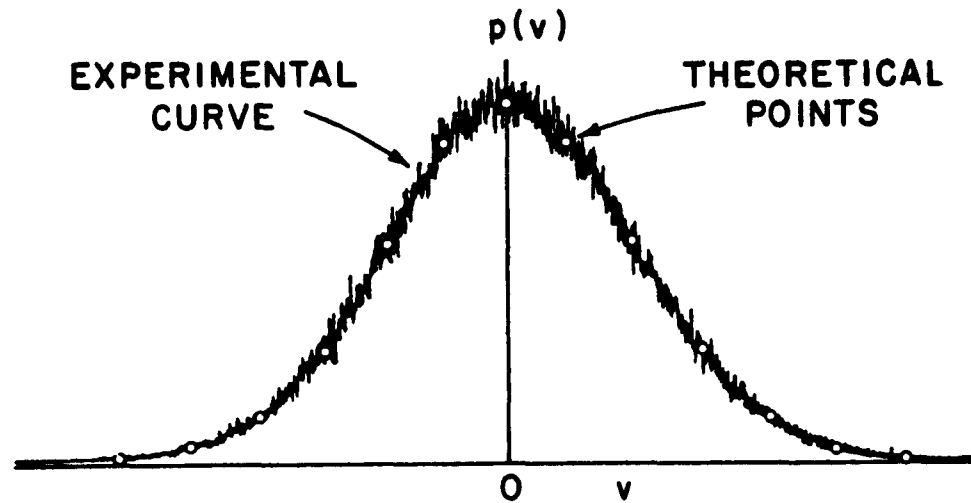


**Figure 8**      The Measured Amplitude Distribution  $p(v)$  Compared with Points Representing a Gaussian Distribution.

### C. THE POWER SPECTRA CONSIDERED

The results presented in this report are concerned with the following power spectral densities:

$$W_0(f) = \frac{1}{1 + \left(\frac{f}{f_0}\right)^2} \quad \text{where } \omega_0 = 2\pi f_0 \quad (14)$$

$$W_1(f) = \frac{1}{\left[1 + \left(\frac{f}{f_1}\right)^2\right]^2} \quad \text{where } \omega_1 = 2\pi f_1 = \frac{1}{\tau_1} \quad (15)$$

$$W_2(f) = \frac{1}{\left[1 + \left(\frac{f}{f_2}\right)^2\right]^3} \quad \text{where } \omega_2 = 2\pi f_2 = \frac{1}{\tau_2} \quad (16)$$

$$W_3(f) = \frac{\left(\frac{f}{f_3}\right)^4}{\left[1 + \left(\frac{f}{f_3}\right)^2\right]^4} \quad \text{where } \omega_3 = 2\pi f_3 = \frac{1}{\tau_3} \quad (17)$$

$$W_4(f) = e^{-\frac{(f-f_4)^2}{2\sigma^2}} \quad \text{where } \omega_4 = 2\pi f_4 \quad (18)$$

$$\text{and "Q factor"} = \frac{f_4}{2\sigma\sqrt{\ln 4}} = 6.1$$

These particular power spectral densities were selected for investigation because they are representative of the spectra that occur

in many branches of science and technology, and because theoretical approximations for the corresponding  $P_0(\tau)$  have been reported (2, 8, 19).

The corresponding system functions  $H_n(j2\pi f)$  were synthesized on an analog computer as indicated in Figures 9 and 10. The system function  $H_4(j2\pi f)$  corresponding to the Gaussian power spectral density  $W_4(f)$  was synthesized by stagger tuning 9 single tuned filters. In this manner the poles of  $H_4(j2\pi f)$  were located at the theoretical (33) pole positions corresponding to a 9th order approximation to the unrealizable Gaussian power spectral density. Figure 11 shows a comparison of the sinusoidal gain of the filter structure as a function of frequency with the theoretical Gaussian function. The comparison is excellent.

The Wiener-Khinchin theorem gives the normalized autocorrelation function for the above power spectra as:

$$\rho_n(\tau) = \frac{\int_0^{\infty} W_n(f) \cos 2\pi f \tau df}{\int_0^{\infty} W_n(f) df} \quad (19)$$

$n = 0, 1, 2, 3, 4$

The results of the integrations yield:

$$\rho_0(\tau) = \sin \frac{\pi}{14} \left\{ e^{-\omega_0 |\tau|} + 2 \sum_{n=1}^3 e^{-\omega_0 |\tau| \cos \frac{n\pi}{7}} \cos \left[ \frac{n\pi}{7} - \omega_0 |\tau| \sin \frac{n\pi}{7} \right] \right\} \quad (20)$$

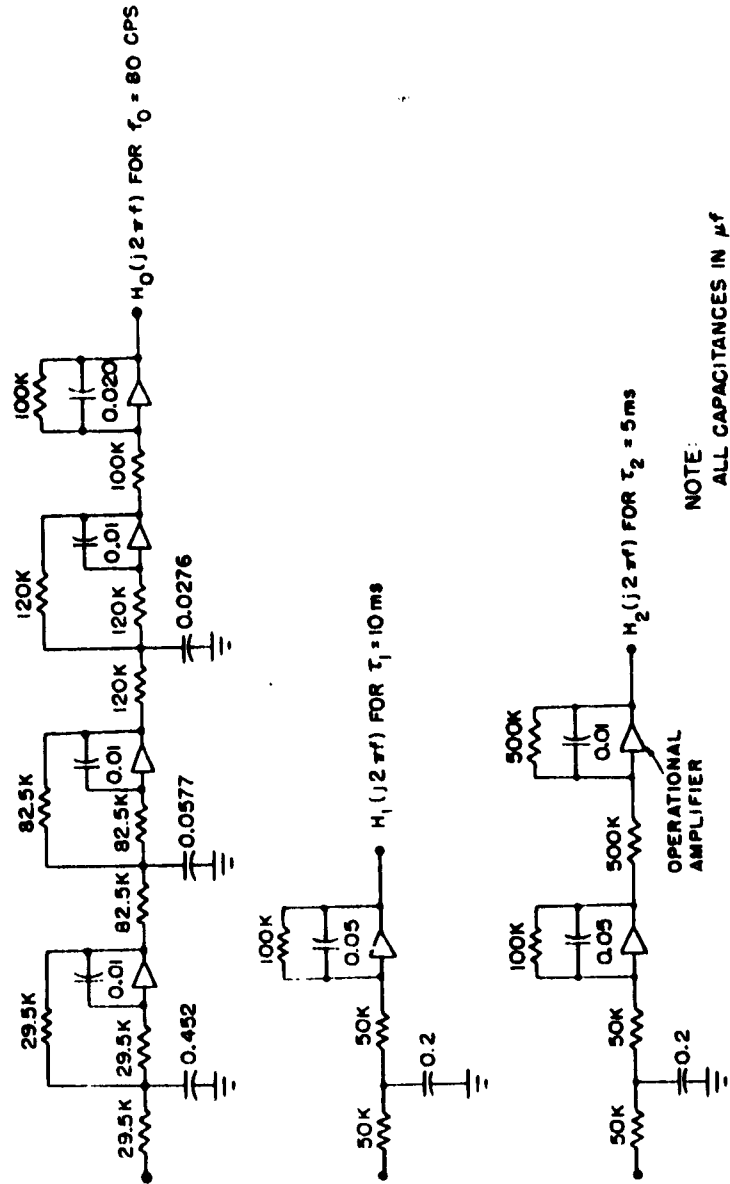


Figure 9 The Synthesis of the System Functions  $H_n(j2\pi f)$  for  $n = 0, 1, 2$ .



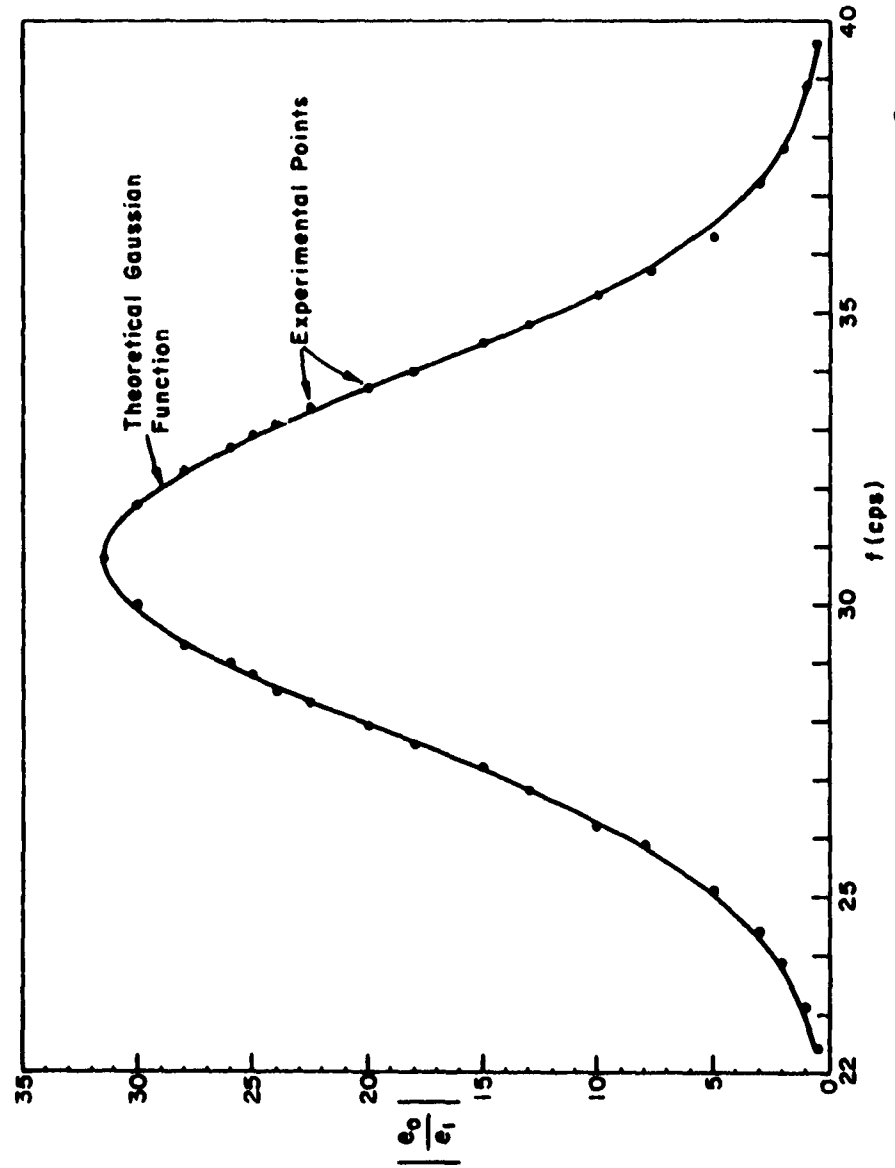


Figure 11 For the System Function  $H_4(j2\pi f)$ , the Experimental Values of  $\left| \frac{e_0}{e_1} \right|$  are Compared with the Gaussian Function  $\sqrt{W_4(f)}$ .

$$\rho_1(\tau) = (1 + \omega_1 |\tau|) e^{-\omega_1 |\tau|} \quad (21)$$

$$\rho_2(\tau) = \left[ 1 + \omega_2 |\tau| + \frac{(\omega_2 \tau)^2}{3} \right] e^{-\omega_2 |\tau|} \quad (22)$$

$$\rho_3(\tau) = \left[ 1 + \omega_3 |\tau| - 2(\omega_3 \tau)^2 + \frac{1}{3} (\omega_3 |\tau|)^3 \right] e^{-\omega_3 |\tau|} \quad (23)$$

$$\rho_4(\tau) = \cos \omega_4 \tau e^{-2(\pi \sigma \tau)^2} \quad (24)$$

The quantity  $\omega_n \tau$  appearing in the normalized autocorrelation functions is defined as normalized time and is denoted by  $u_n$ . All probabilities and probability densities reported in this report are plotted with respect to normalized time  $u_n = \omega_n \tau$ .

The initiate commands discussed in Section II-A above were spaced approximately one second apart. Accordingly, in order to obtain samples of zero-crossing intervals which are sufficiently independent, the time constants and frequencies associated with the power spectral densities were chosen as:

$$\tau_1 = \tau_3 = 10 \text{ m sec} \quad (25)$$

$$\tau_2 = 5 \text{ m sec} \quad (26)$$

$$f_0 = 80 \text{ cps} \quad (27)$$

$$f_4 = 30.8 \text{ cps} \quad (28)$$

Also, for experimental convenience the synthesized power spectral densities had a low frequency cutoff of approximately 1 cps and a high frequency cutoff of 8.5 kc.

#### D. RANDOM POINT-PROCESS TRANSFORMATIONS

Consider the linear system shown in Figure 12.

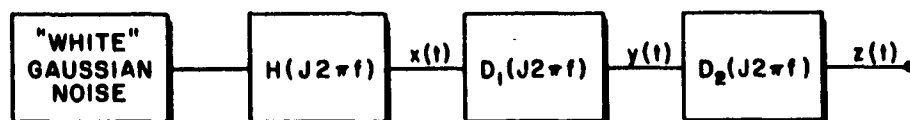


Figure 12 The Linear System.

The power spectral density for the Gaussian random process  $x(t)$  is given by

$$W_x(f) = |H(j2\pi f)|^2 \quad (29)$$

Similarly, the power spectral density for  $y(t)$  is given by

$$W_y(f) = |H(j2\pi f)|^2 |D_1(j2\pi f)|^2 = W_x(f) |D_1(j2\pi f)|^2. \quad (30)$$

If  $D_1(j2\pi f)$  is the system function representing an ideal differentiator then the stationary points of  $x(t)$  and the zero points of  $y(t)$  occur simultaneously.

If  $y(t)$  is a Gaussian process having arbitrary power spectral density  $W_y(f)$ , the average number of zero points per second is given by (27)



$$2 \left[ \frac{\int_0^{\infty} f^2 W_y(f) df}{\int_0^{\infty} W_y(f) df} \right]^{1/2} \quad (31)$$

Hence, the average number of stationary points per second for a Gaussian process  $x(t)$  having power spectral density  $W_x(f)$  must be

$$2 \left[ \frac{\int_0^{\infty} f^2 W_x(f) 4\pi^2 f^2 df}{\int_0^{\infty} W_x(f) 4\pi^2 f^2 df} \right]^{1/2} = 2 \left[ \frac{\int_0^{\infty} f^4 W_x(f) df}{\int_0^{\infty} f^2 W_x(f) df} \right]^{1/2} \quad (32)$$

This last equation agrees with Rice's result (27).

The average number of inflection points per second for a Gaussian process  $x(t)$  having power spectral density  $W_x(f)$  can be determined in a similar manner. Thus, if also  $D_2(j2\pi f) = j2\pi f$ , then the average number of inflection points per second for a Gaussian process  $x(t)$  having power spectral density  $W_x(f)$  must be

$$2 \left[ \frac{\int_0^{\infty} f^2 W_x(f) 16\pi^4 f^4 df}{\int_0^{\infty} W_x(f) 16\pi^4 f^4 df} \right]^{1/2} = 2 \left[ \frac{\int_0^{\infty} f^6 W_x(f) df}{\int_0^{\infty} f^4 W_x(f) df} \right]^{1/2} \quad (33)$$

The same transformation can be extended to higher derivatives.

A method for synthesizing a Gaussian process  $y(t)$  having zero points corresponding in time with the stationary points of a

Gaussian process  $x(t)$  having a Butterworth power spectral density is shown in Figure 13.

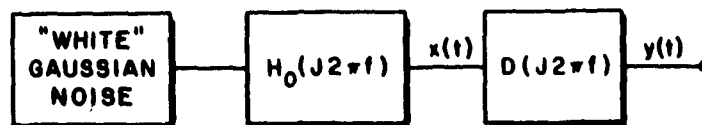


Figure 13 Transformation of Stationary Points to Zero Points.

The circuit having the system function  $D(j2\pi f)$  is shown in Figure 14.

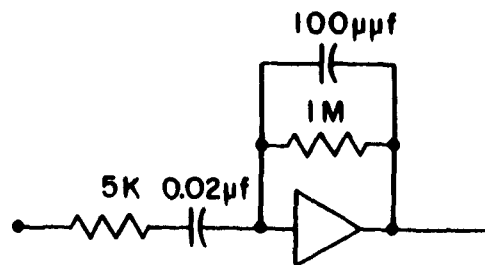


Figure 14 The Synthesis of  $D(j2\pi f)$ .

The system function  $D(j2\pi f)$  is given by

$$D(j2\pi f) = \frac{2j10^{-2}\omega}{[1+j10^{-4}\omega]^2} \quad (34)$$

Accordingly,  $D(j2\pi f)$  has the property of a differentiator since  $|D(j2\pi f)|^2$  behaves like  $f^2$  to well within  $\pm 1$  db in the frequency range of interest (0-500 cps).

Taking  $D(j2\pi f)$  as  $2j10^{-2}\omega$  we find that

$$\sigma_x^2 = \int_0^\infty W_o(f) df ; \quad \sigma_y^2 = [4\pi 10^{-2}]^2 \int_0^\infty f^2 W_o(f) df \quad (35)$$

and

$$\frac{\sigma_y}{\sigma_x} = 4\pi 10^{-2} f_o \left[ \frac{\sin \frac{\pi}{14}}{\sin \frac{3\pi}{14}} \right]^{1/2} = 6.007 \quad (36)$$

This final ratio was verified satisfactorily by using an RMS voltmeter.

Oscilloscope photographs illustrating the transformation of stationary points to zero points by the operator  $D(j2\pi f)$  are shown in Figure 15. The probability densities associated with the intervals defined by the mathematical stationary points of a random process consisting of a sine wave plus a Gaussian process were determined experimentally by using the operator  $D(j2\pi f)$ .

Figure 16 shows a complete block diagram of the measuring and synthesis systems.

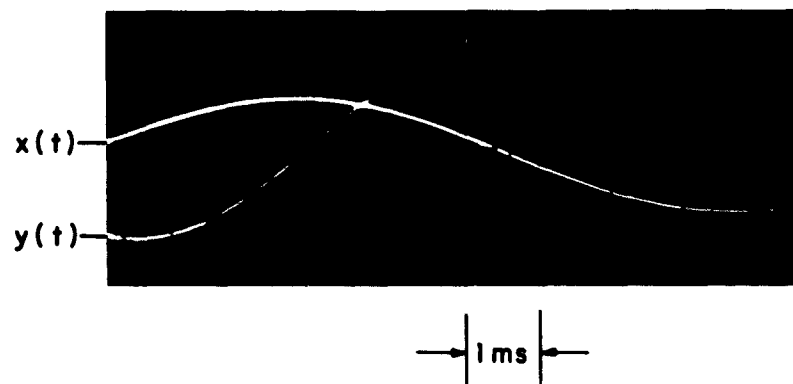
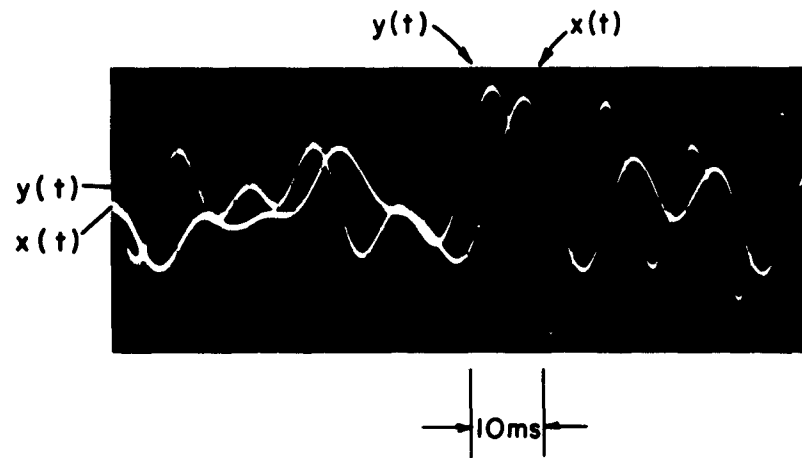


Figure 15: The Stationary Points of  $x(t)$  and the Zero Points of  $y(t)$  Occur Simultaneously.

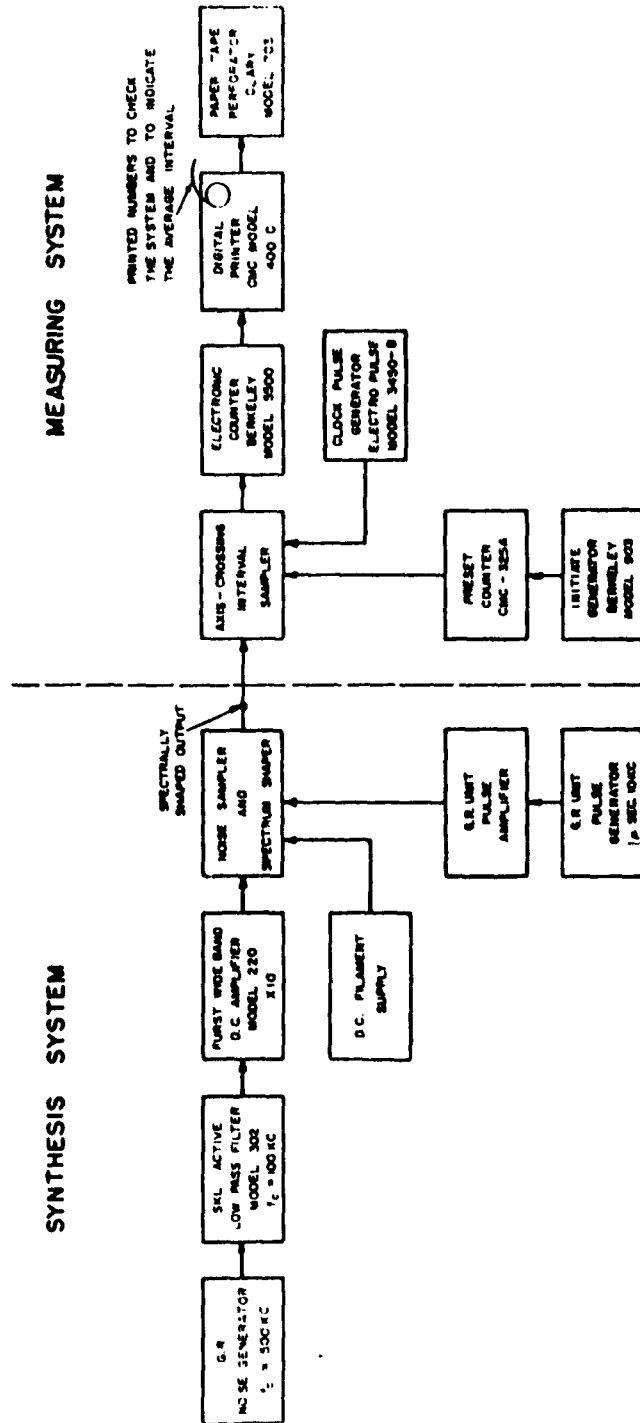


Figure 16 Block Diagram of the Synthesis and Measuring Systems.

#### IV. MATHEMATICAL DEDUCTIONS FROM THE PROBABILITY DENSITIES

A. Kohlenberg (4), P. I. Kuznetsov, P. L. Stratonovich and V. I. Tikhonov (5), J. A. McFadden (2), and perhaps others, have derived some basic identities relating  $p(n, \tau)$ , the probability that a given interval  $(t, t + \tau)$  contains exactly  $n$  points, and  $P_n(\tau)$ , the probability density of the interval between the  $n$ th and  $(n+1)$ th points. These identities apply to general stationary point-processes. Using McFadden's general result (26) we have for a point set defined by the zeros of a random process:

$$p'(n, \tau) = -\beta \int_{\tau}^{\infty} [P_n(l) - 2P_{n-1}(l) + P_{n-2}(l)] dl \quad (37)$$

where

$\beta$  = the expected number of zeros per unit time

$P_n(\tau)$  = the probability density function for the sum of  $n+1$  successive zero-crossing intervals

$p'(n, \tau)$  = the derivative with respect to  $\tau$  of the probability that a given interval  $\tau$  contains exactly  $n$  zeros.

Also, by definition, we have

$$Z(n+1, \tau) = \int_{\tau}^{\infty} P_n(l) dl \quad (38)$$

where

$Z(n+1, \tau)$  = the conditional probability that the  $(n+1)$ th zero-crossing point from a given zero-crossing point in  $d\tau$  occurs after the time  $d\tau + \tau$ .

For  $n = 0$ , and the initial condition  $p(0, 0) = 1$ , Equation (37) yields

$$p(0, \tau) = \beta \left[ \int_0^\tau d\tau_1 \int_0^{\tau_1} P_0(l) dl - \tau \right] + 1 \quad (39)$$

For  $n = 1$  and the initial condition  $p(1, 0) = 0$ , Equation (37) yields

$$p(1, \tau) = \beta \left[ \int_0^\tau d\tau_1 \int_0^{\tau_1} P_1(l) dl - 2 \int_0^\tau d\tau_1 \int_0^{\tau_1} P_0(l) dl + \tau \right] \quad (40)$$

For  $n = 0$  Equation (38) becomes

$$Z(1, \tau) = \int_\tau^\infty P_0(l) dl \quad (41)$$

For  $n = 1$  Equation (38) becomes

$$Z(2, \tau) = \int_\tau^\infty P_1(l) dl \quad (42)$$

Equations (39), (40), (41), and (42) were used to deduce  $p(0, u_n)$ ,  $p(1, u_n)$ ,  $Z(1, u_n)$  and  $Z(2, u_n)$  for  $n = 1, 2, 3$  and  $4$ .

Similar expressions hold for the point set defined by the zero points of a random-process consisting of a sine wave signal of frequency  $\frac{f_0}{2}$  plus Gaussian noise such that the signal-to-noise power ratio equals  $a$ . That is:

$$p_a(0, \tau) = \beta_a \left[ \int_0^\tau d\tau_1 \int_0^{\tau_1} P_0(l, a) dl - \tau \right] + 1 \quad (43)$$

$$p_a(1, \tau) = \beta_a \left[ \int_0^\tau d\tau_1 \int_0^{\tau_1} P_1(l, a) dl - 2 \int_0^\tau d\tau_1 \int_0^{\tau_1} P_0(l, a) dl + \tau \right] \quad (44)$$

$$Z_a(1, \tau) = \int_\tau^\infty P_0(l, a) dl \quad (45)$$

$$Z_a(2, \tau) = \int_\tau^\infty P_1(l, a) dl \quad (46)$$

where

$\beta_a$  = the expected number of zeros per unit time when the signal to noise power ratio equals  $a$ .

Equations (43), (44), (45) and (46) were used to deduce  $p_a(0, u_0)$ ,  $p_a(1, u_0)$ ,  $Z_a(1, u_0)$  and  $Z_a(2, u_0)$  for  $a = 0, .2, 1$  and  $4$ .

Similar expressions also hold for the point set defined by the mathematical stationary points of a random process consisting of a sine wave signal of frequency  $\frac{f_0}{2}$  plus Gaussian noise such that the signal-to-noise power ratio equals  $a$ . That is:

$$m_a(0, \tau) = \gamma_a \left[ \int_0^\tau d\tau_1 \int_0^{\tau_1} M_0(l, a) dl - \tau \right] + 1 \quad (47)$$

$$m_a(1, \tau) = \gamma_a \left[ \int_0^\tau d\tau_1 \int_0^{\tau_1} M_1(l, a) dl - 2 \int_0^\tau d\tau_1 \int_0^{\tau_1} M_0(l, a) dl + \tau \right] \quad (48)$$

$$S_a(1, \tau) = \int_\tau^\infty M_0(l, a) dl \quad (49)$$

$$S_a(2, \tau) = \int_\tau^\infty M_1(l, a) dl \quad (50)$$



where

$\gamma_a$  = the expected number of stationary points per unit time when the signal-to-noise power ratio equals  $a$ .

Equations (47), (48), (49), and (50) were used to deduce  $m_a(0, u_0)$ ,  $m_a(1, u_0)$ ,  $S_a(1, u_0)$  and  $S_a(2, u_0)$  for  $a = 0, .2, 1$  and  $4$ .

## V. PROPERTIES OF THE PROBABILITY DENSITIES

### A. EXPECTATIONS

Consider the point set shown in Figure 17 and defined by the zero-crossing points of a Gaussian process. Let  $X$ ,  $Y$  be two successive zero-crossing intervals and let  $Z = X + Y$ . From symmetry the expectation  $E(X)$  equals the expectation  $E(Y)$ . Hence,  $E(Z) = 2E(X)$ . Accordingly, the expectations,  $E_1(u_n)$ , associated with the  $P_1(u_n)$  densities are related to the expectations,  $E_0(u_n)$ , associated with the  $P_0(u_n)$  densities by:

$$E_1(u_n) = 2E_0(u_n) \quad \text{for } n = 1, 2, 3, 4 \quad (51)$$

The exact theoretical expectations,  $E_0(u_n)$ , associated with the  $P_0(u_n)$  densities, or the average values of successive zero-crossing intervals, are given by (27)

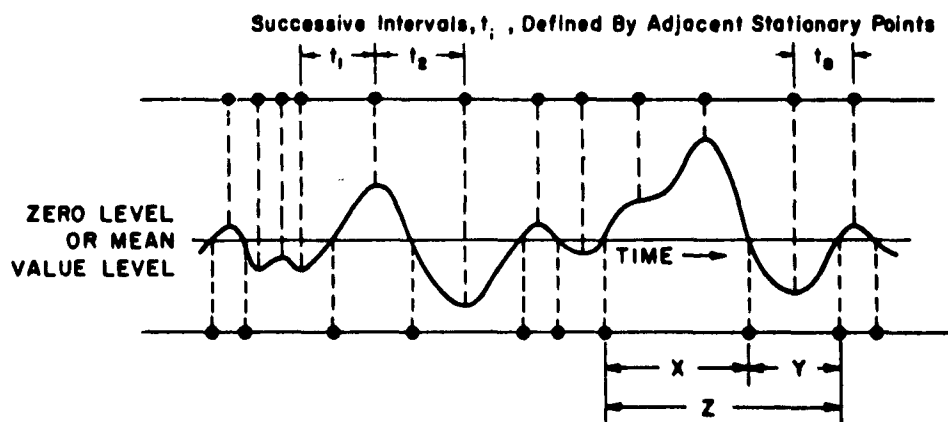


Figure 17 Point Sets Defined by the Zero-Crossing Points and the Stationary Points of a Gaussian Process.

$$E_0(u_n) = \int_0^\infty u_n P_0(u_n) du_n = \frac{1}{2} \omega_n \left[ \frac{\int_0^\infty W_n(f) df}{\int_0^\infty f^2 W_n(f) df} \right]^{1/2} = \pi \left[ -\rho_n''(0) \right]^{-1/2} \quad (52)$$

for  $n = 1, 2, 3, 4$

$\rho_n''(u_n)$  is the second derivative of the normalized autocorrelation function  $\rho_n(u_n)$ . The results for  $n = 1, 2, 3$ , and 4 are:

$$E_0(u_1) = \pi \quad (53)$$

$$E_0(u_2) = 5.4414 \quad (54)$$

$$E_0(u_3) = 1.4050 \quad (55)$$

$$E_0(u_4) = 3.1341 \quad (56)$$

From Equation (51) the theoretical expectations,  $E_1(u_n)$ , associated with the  $P_1(u_n)$  densities are equal to  $2E_0(u_n)$  for  $n = 1, 2, 3, 4$ . The expectations  $E_0(u_n)$  and  $E_1(u_n)$  were also measured. They are compared with the corresponding theoretical values in the tables accompanying Figures 18, 19, 22, 23, 26, 27, 30, and 31. The comparisons are satisfactory in all cases.

Similarly, the expectations,  $E_1(u_0, a)$ , associated with the  $P_1(u_0, a)$  densities are related to the expectations,  $E_0(u_0, a)$ , associated with the  $P_0(u_0, a)$  densities by:

$$E_1(u_0, a) = 2E_0(u_0, a) \quad \text{for all } a \quad (57)$$

The exact theoretical expectations,  $E_0(u_0, a)$ , associated with the  $P_0(u_0, a)$  densities follow from a general result given by Rice (34) and Middleton (3, 3a):

$$E_0(u_0, a) = \int_0^\infty u_0 P_0(u_0, a) du_0 = 2\pi\sqrt{b} \left[ \sum_{n=0}^{\infty} \frac{(-\frac{1}{2})_n}{(n!)^2} (-ba)^n {}_1F_1(\frac{1}{2}; n+1; -a) \right]^{-1}$$

for all a (58)

where

$$(a)_n = (a) (a+1) (a+2) \dots (a+n-1)$$

$$(a)_0 = 1$$

$$a = \frac{S}{N} = \frac{\text{average sine wave power}}{\text{average noise power}}$$

$$b = \frac{\sin \frac{3\pi}{14}}{4 \sin \frac{\pi}{14}}$$

${}_1F_1$  = the confluent hypergeometric function.

The results for  $a = 0, .2, 1$  and  $4$  are:

$$E_0(u_0, 0) = 5.2587 \quad (59)$$

$$E_0(u_0, .2) = 5.4065 \quad (60)$$

$$E_0(u_0, 1) = 5.8286 \quad (61)$$

$$E_0(u_0, 4) = 6.2506 \quad (62)$$

For small values of "a", the random process consisting of a sine wave signal of frequency  $\frac{f_0}{2}$  plus Gaussian noise is approximately Gaussian. Accordingly, one could compute easily the approximate theoretical expectations,  $E_0^*(u_0, a)$ , associated with the  $P_0(u_0, a)$  densities by using an equation analogous to Equation (52). That is:

$$E_0^*(u_0, a) = \pi \left[ -R''(0, a) \right]^{-1/2} = 2\pi\sqrt{b} \left[ \frac{1+a}{1+ab} \right]^{1/2} \quad (63)$$

$R''(u_0, a)$  is the second derivative of the normalized autocorrelation function,  $R(u_0, a)$ , defined by the power spectral density  $W_0(f) + S\delta(f - \frac{f_0}{2})$ .  $R(u_0, a)$  is given by:

$$R(u_o, a) = \frac{\rho_o(u_o) + a \cos \frac{u_o}{2}}{1 + a} \quad (64)$$

Equation (63) agrees with Bendat's result (15).

The results for  $a = 0, .2, 1$  and  $4$  are:

$$E_o^*(u_o, 0) = 5.2587 \quad (65)$$

$$E_o^*(u_o, .2) = 5.3951 \quad (66)$$

$$E_o^*(u_o, 1) = 5.7031 \quad (67)$$

$$E_o^*(u_o, 4) = 6.0306 \quad (68)$$

From Equation (57) the exact theoretical expectations,  $E_1(u_o, a)$ , associated with the  $P_1(u_o, a)$  densities are equal to  $2E_o(u_o, a)$  for all  $a$ . The expectations  $E_o(u_o, a)$  and  $E_1(u_o, a)$  for  $a = 1, .2, 1$ , and  $4$  were also measured. They are compared with the corresponding exact theoretical values in the tables accompanying Figures 34, 35, 38, 39, 42, 43, 46, and 47. The comparisons are satisfactory in all cases.

Finally, the expectations,  $\ell_1(u_o, a)$ , associated with the  $M_1(u_o, a)$  densities are related to the expectations,  $\ell_o(u_o, a)$ , associated with the  $M_o(u_o, a)$  densities by:

$$\ell_1(u_o, a) = 2\ell_o(u_o, a) \text{ for all } a \quad (69)$$

The exact theoretical expectations,  $\ell_o(u_o, a)$ , associated with the  $M_o(u_o, a)$  densities follow by applying the transformation associated with the ideal differentiator operator to the general result given by Rice and Middleton:

$$\ell_o(u_o, a) = \int_0^{\infty} u_o M_o(u_o, a) du_o = 2\pi \sqrt{\frac{c}{b}} \left[ \sum_{n=0}^{\infty} \frac{(-\frac{1}{2})^n}{(n!)^2} (-ca)^n {}_1F_1\left(\frac{1}{2}; n+1; -ba\right) \right]^{-1}$$

for all a (70)

where

$$c = \frac{\sin \frac{5\pi}{14}}{16 \sin \frac{\pi}{14}}$$

The results for a = 0, .2, 1 and 4 are:

$$\ell_o(u_o, 0) = 3.7765 \quad (71)$$

$$\ell_o(u_o, .2) = 3.9429 \quad (72)$$

$$\ell_o(u_o, 1) = 4.5467 \quad (73)$$

$$\ell_o(u_o, 4) = 5.8138 \quad (74)$$

Again, for small values of "a" the random process consisting of a sine wave signal of frequency  $\frac{f_o}{2}$  plus Gaussian noise is approximately Gaussian. Accordingly, one could compute easily the approximate theoretical expectations,  $\ell_o^*(u_o, a)$ , associated with the  $M_o(u_o, a)$  densities by using an equation analogous to Equation (52). That is:

$$\ell_o^*(u_o, a) = \pi \left[ -R_g''(0, a) \right]^{-1/2} = 2\pi \sqrt{\frac{c}{b}} \left[ \frac{1+ab}{1+ac} \right]^{1/2} \quad (75)$$

$R_g''(u_o, a)$  is the second derivative of the normalized autocorrelation function,  $R_g(u_o, a)$ , defined by the power spectral density  $\omega^2 W_o(f) + \omega^2 S\delta(f - \frac{f_o}{2})$ . This latter power spectral density results by applying the transformation associated with the ideal differentiator operator to the power spectral density

$W_0(f) + S\delta(f - \frac{f_0}{2})$ .  $R_s(u_0, a)$  and  $R(u_0, a)$  are related by:

$$R_s(u_0, a) = \frac{R''(u_0, a)}{R''(0, a)} \text{ for all } a \quad (76)$$

The results for  $a = 0, .2, 1$ , and  $4$  are:

$$\ell_0^*(u_0, 0) = 3.7765 \quad (77)$$

$$\ell_0^*(u_0, .2) = 3.9341 \quad (78)$$

$$\ell_0^*(u_0, 1) = 4.3994 \quad (79)$$

$$\ell_0^*(u_0, 4) = 5.1910 \quad (80)$$

From Equation (69) the exact theoretical expectations,  $\ell_1(u_0, a)$ , associated with the  $M_1(u_0, a)$  densities are equal to  $2\ell_0(u_0, a)$  for all  $a$ . The expectations  $\ell_0(u_0, a)$  and  $\ell_1(u_0, a)$  for  $a = 0, .2, 1$ , and  $4$  were also measured. They are compared with the corresponding exact theoretical values and the approximate theoretical values in the tables accompanying figures 50, 51, 54, 55, 58, 59, 62, and 63. The comparisons are satisfactory in all cases.

If one represents the sine wave as the limit of a narrow-band Gaussian process centered at  $\frac{f_0}{2}$  as the bandwidth approaches zero, then it becomes clear that the expectations  $E_0^*(u_0, a)$  and  $\ell_0^*(u_0, a)$  are exact for the case of a random process  $\xi^*(t, a)$  of the form:

$$\xi^*(t, a) = R(t) \sin \left[ \frac{\omega_0 t}{2} + \theta(t) \right] + n(t) \quad (81)$$

In this last equation the random variable  $R_t$  has a Rayleigh probability density function,  $\theta_t$  is uniformly distributed in the interval  $(0, 2\pi)$ , and  $n(t)$  is Gaussian noise having a power spectral density  $W_0(f)$ . In other words  $E_0^*(u_0, a)$  and  $\mathcal{E}_0^*(u_0, a)$  are exact for the Gaussian process,  $\xi^*(t, a)$ , defined by a very narrow-band Gaussian signal centered at  $\frac{f_0}{2}$  plus Gaussian noise having the power spectral density  $W_0(f)$ . Equation (81) should be compared with random process,  $\xi(t, a)$ , defined by a sine wave signal plus Gaussian noise which has the form:

$$\xi(t, a) = A_0 \sin \left[ \frac{\omega_0 t}{2} + \theta(t) \right] + n(t) \text{ where } A_0 \text{ is a constant.} \quad (82)$$

#### B. STANDARD DEVIATIONS AND CORRELATION COEFFICIENTS

Since  $Z = X + Y$ , the variance of  $Z$  is given by:

$$\text{Var}(Z) = \text{Var}(X) + \text{Var}(Y) + 2\text{Cov}(X, Y) \quad (83)$$

where

$$\text{Cov}(X, Y) = E(XY) - E(X) E(Y)$$

The correlation coefficient,  $K(X, Y)$ , of  $X, Y$  is given by

$$K(X, Y) = \frac{\text{Cov}(X, Y)}{\sqrt{\text{Var}(X)\text{Var}(Y)}} \quad (84)$$

From symmetry, we have

$$\text{Var}(X) = \text{Var}(Y) \quad (85)$$



Hence,

$$\text{Var} (Z) = 2 \left[ 1 + K \right] \text{Var} (X) \quad . \quad (86)$$

Let  $K_n$  be the correlation coefficient between two successive zero-crossing intervals of a Gaussian process having the power spectral density  $W_n(f)$ . Then, the variances,  $\sigma_1^2(u_n)$ , associated with the  $P_1(u_n)$  densities are related to the variances,  $\sigma_o^2(u_n)$ , associated with the  $P_o(u_n)$  densities by:

$$\sigma_1^2(u_n) = 2 \left[ 1 + K_n \right] \sigma_o^2(u_n) \text{ for } n = 1, 2, 3, 4 \quad (87)$$

Similarly,

$$\sigma_1^2(u_o, 0) = 2 \left[ 1 + K_o \right] \sigma_o^2(u_o, 0) \quad (88)$$

$$D_1^2(u_o, 0) = 2 \left[ 1 + \chi_o \right] D_o^2(u_o, 0) \quad . \quad (89)$$

In the latter two equations  $\sigma_1^2(u_o, a)$ ,  $\sigma_o^2(u_o, a)$ ,  $D_1^2(u_o, a)$  and  $D_o^2(u_o, a)$  are the variances associated with the respective densities  $P_1(u_o, a)$ ,  $P_o(u_o, a)$ ,  $M_1(u_o, a)$  and  $M_o(u_o, a)$ . Also  $K_o$  and  $\chi_o$  are the correlation coefficients between two successive zero-crossing intervals of the Gaussian processes having the respective power spectral densities  $W_o(f)$  and  $w^2 W_o(f)$ .

McFadden (32) recently derived the following equations valid for a general random process:

$$A = \int_0^{\infty} r(\tau) d\tau = \frac{\sigma_o^2}{E_o(\tau)} \left[ \frac{1}{2} + \sum_{n=1}^{\infty} (-1)^n \rho_n \right] \quad (90)$$

$$B = \int_0^{\infty} \left[ U(\tau) - \frac{1}{E_o(\tau)} \right] d\tau = \frac{\sigma_o^2}{E_o^2(\tau)} \left[ \frac{1}{2} + \sum_{n=1}^{\infty} \rho_n \right] - \frac{1}{2} \quad (91)$$

where

$r(\tau)$  = the normalized autocorrelation function of the infinitely clipped random process

$\sigma_o^2$  = variance of successive zero-crossing intervals

$E_o(\tau) = \frac{1}{\beta}$  = Expectation of successive zero-crossing intervals

$\rho_n$  = correlation coefficient between the  $i$ th and  $(i+n)$ th zero-crossing intervals

$U(\tau)d\tau$  = the conditional probability that a zero occurs between  $t+\tau$  and  $t+\tau+d\tau$  given a zero at time  $t$ .

If one assumes that successive zero-crossing intervals form a Markov chain in the wide sense, then  $\rho_n = \rho_1^n$  and

$$A = \frac{\sigma_o^2}{2E_o(\tau)} \frac{1-\rho_1}{1+\rho_1} > 0 \quad \text{for all } |\rho_1| < 1 \quad (92)$$

$$B = \frac{\sigma_o^2}{2E_o^2(\tau)} \left( \frac{1+\rho_1}{1-\rho_1} \right) - \frac{1}{2} > -\frac{1}{2} \quad (93)$$

Equations (92) and (93) were used by McFadden (2) to compute  $\sigma_o$  and  $\rho_1$  for various Gaussian processes. We used Equations (92) and (93) to compute  $\sigma_o$  and  $\rho_1$  for most of the Gaussian processes

considered in this report. In some cases our results differ somewhat from those reported by McFadden. The standard deviations resulting from the Markov assumption together with the standard deviations computed from Equations (87), (88) and (89) are compared with the experimental standard deviations in the tables accompanying Figures 18, 19, 22, 23, 26, 27, 34, 35, 50, and 51. From the comparisons of the standard deviations in the tables accompanying Figures 26, 27, 50, and 51, we conclude that successive zero-crossing intervals of some Gaussian processes do not form a Markov chain in the wide sense.

Notice that the Markov assumption implies that if  $\rho_1 > 0$  then  $\rho_n > 0$  for all  $n$ . Also, the Markov assumption implies the inequalities given by Equations 92 and 93. These restrictions are not clearly implied by the Gaussian character of the process and depend only on the Markov assumption. Accordingly, one might surmise that the successive zero-crossing intervals of some Gaussian processes do not form a Markov chain in the wide sense.

From Equations (90) and (91) we have that:

$$2 \sum_{n=1}^{\infty} \rho_{2n-1} = \frac{E_o(\tau)}{\sigma_o^2} \left[ E_o(\tau) \left( B + \frac{1}{2} \right) - A \right] . \quad (94)$$

As an approximation, let us assume that  $\sum_{n=2}^{\infty} \rho_{2n-1} = 0$ . (95)

Then,

$$\rho_1 = \frac{E_o(\tau)}{2\sigma_o^2} \left[ E_o(\tau) \left( B + \frac{1}{2} \right) - A \right] . \quad (96)$$

By applying Equation (96) to most of the Gaussian processes considered in this report and by using the experimental variances for successive intervals, the experimental correlation coefficients between two successive intervals were computed. The results are given in the tables accompanying Figures 18, 22, 26, 34, and 50.

If the variances for the sum of two successive intervals are computed from Equations 87, 88, and 89 by using the experimental variances for successive intervals and the experimental correlation coefficients between two successive intervals, the results agree with the measured variances for the sum of two successive intervals to within the experimental error. Hence the experimental values of the correlation coefficients between two successive intervals yield results consistent with experiment. This serves as partial justification for the assumption given by Equation (95).

If one assumes that  $\rho_n = 0$  for  $n \geq 2$ , then Equations (90), (91), and (86), can be used to compute approximate theoretical values of  $\sigma_0$ ,  $\rho_1$  and  $\sigma_1$  for Gaussian processes. For the Gaussian processes considered in this report, these approximate theoretical values compare with our experimental values slightly better than the corresponding theoretical values resulting from the Markov assumption.

For a Gaussian process, Rice (1) derived  $U(\tau)d\tau$ , see Appendix, the conditional probability that a zero occurs between  $t + \tau$  and  $t + \tau + d\tau$  given a zero at  $t$ . Hence,

$$U(\tau) = \sum_{n=0}^{\infty} P_n(\tau) \quad . \quad (97)$$

Also, for a Gaussian process, Rice (1) derived  $Q(\tau)d\tau$ , see Appendix, the conditional probability that a downward zero-crossing occurs between  $t + \tau$  and  $t + \tau + d\tau$  given an upward zero-crossing at  $t$ . Hence

$$Q(\tau) = \sum_{m=0}^{\infty} P_{2m}(\tau) \quad (98)$$

and

$$U(\tau) - Q(\tau) = \sum_{m=0}^{\infty} P_{2m+1}(\tau) \quad . \quad (99)$$

From Figure 31 and Equation (98) we see that the first portion of  $Q(u_4)$  generates  $P_0(u_4)$ . Similarly, from Figure 32 and Equation (99) we see that the first portion of  $U(u_4) - Q(u_4)$  generates  $P_1(u_4)$ . The first normalized portion of the  $Q(u_4)$  function was used to compute approximate theoretical means and variances associated with the  $P_0(u_4)$  density. Similarly, the first normalized portion of the  $U(u_4) - Q(u_4)$  function was used to compute approximate theoretical means and variances associated

with the  $P_1(u_4)$  density. By using these computed variances in Equation (87), the approximate theoretical correlation coefficient between two successive intervals,  $K_4$ , was computed. Because of the unfavorable propagation of errors associated with Equation (87),  $K_4$  should be regarded as a rough estimate. These approximate theoretical results are compared with other results in the table accompanying Figures 30 and 31.

All experimental standard deviations were computed by using the theoretical mean values. In general, these standard deviations would decrease somewhat if one were to use the experimental mean values in the computations.

VI. PROBABILITIES AND PROBABILITY DENSITIES DEFINED  
BY THE ZERO POINTS OF GAUSSIAN PROCESSES

A. POWER SPECTRAL DENSITY  $W_1(f)$

Probabilities and probability densities defined by the zero-crossing points of a Gaussian process having a power spectral density  $W_1(f)$  are presented in Figures 18, 19, 20, and 21. Theoretical approximations derived by S. O. Rice (1) and J. A. McFadden (2) are presented in Figures 18 and 19 for comparison purposes. Figure 18 also presents for comparison an exponential density which was suggested by R. R. Favreau, H. Low, and I. Pfeffer (19) as the exact probability density. From this latter comparison we see that the experimental  $P_0(u_1)$  and the exponential curve deviate significantly in the neighborhoods of  $u_1 = 1$  and  $u_2 = 5$ . Accordingly, we conclude that the exact probability density is not the suggested exponential.

From Equation (98) we have that:

$$Q(\tau) \geq P_0(\tau) \quad \text{for all } \tau \quad . \quad (100)$$

Accordingly, Rice's  $Q(u_1)$  function serves as an upper bound for  $P_0(u_1)$  and is presented in Figure 18. Recently, M. S. Longuet-Higgins (8) deduced bounds for  $P_0(0)$  theoretically as  $0.382 < P_0(0) < Q(0) = 0.406$  and deduced the approximate value  $P_0(0) \doteq 0.385$ . The inequality  $0.382 < P_0(0)$  was used by Longuet-Higgins (8) to disprove rigorously the exponential conjecture of Favreau et al. From Equation (99) we have that:

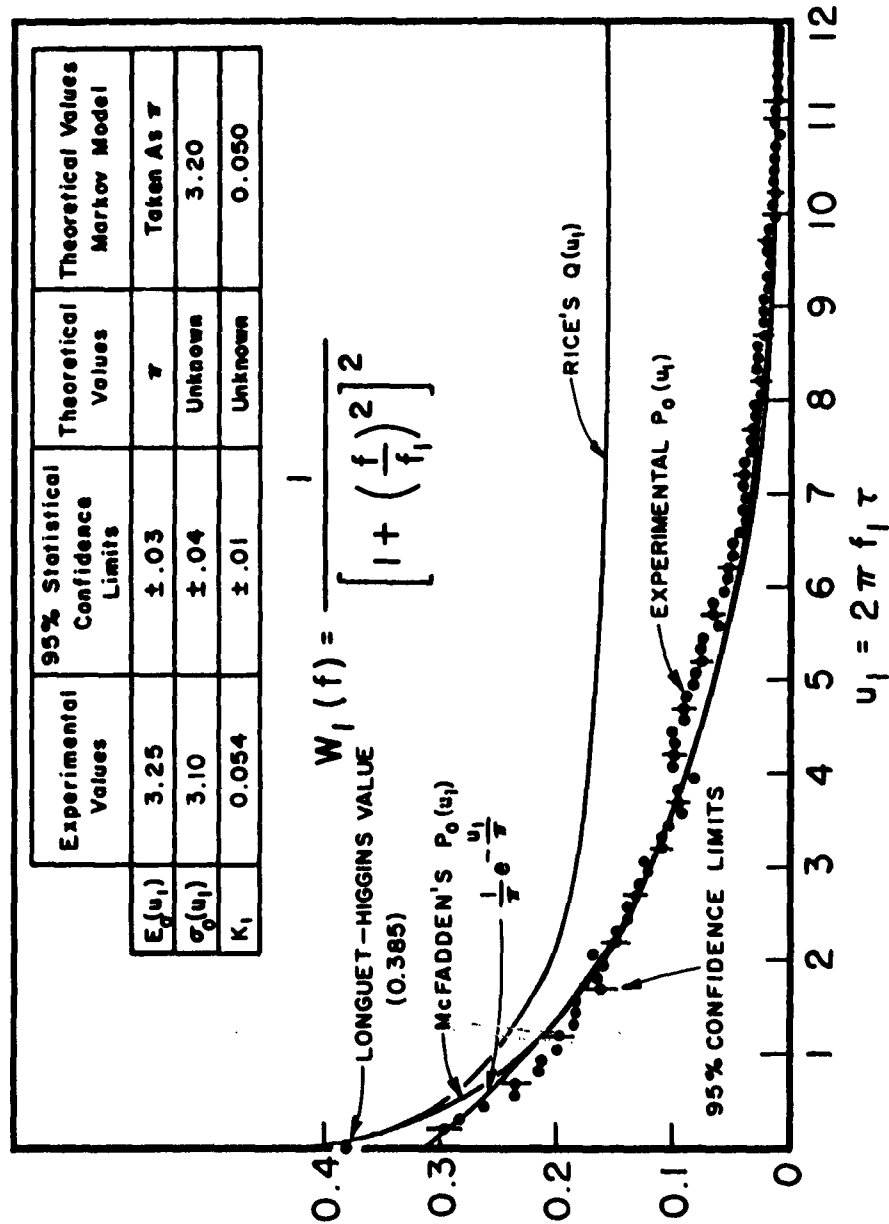


Figure 18 -  $P_0(u_1)$  is the Probability Density Function for Successive Zero-Crossing Intervals of Gaussian Noise Having a Power Spectral Density  $W_1(f)$ . Theoretical Approximations are Compared with Experimental Results.



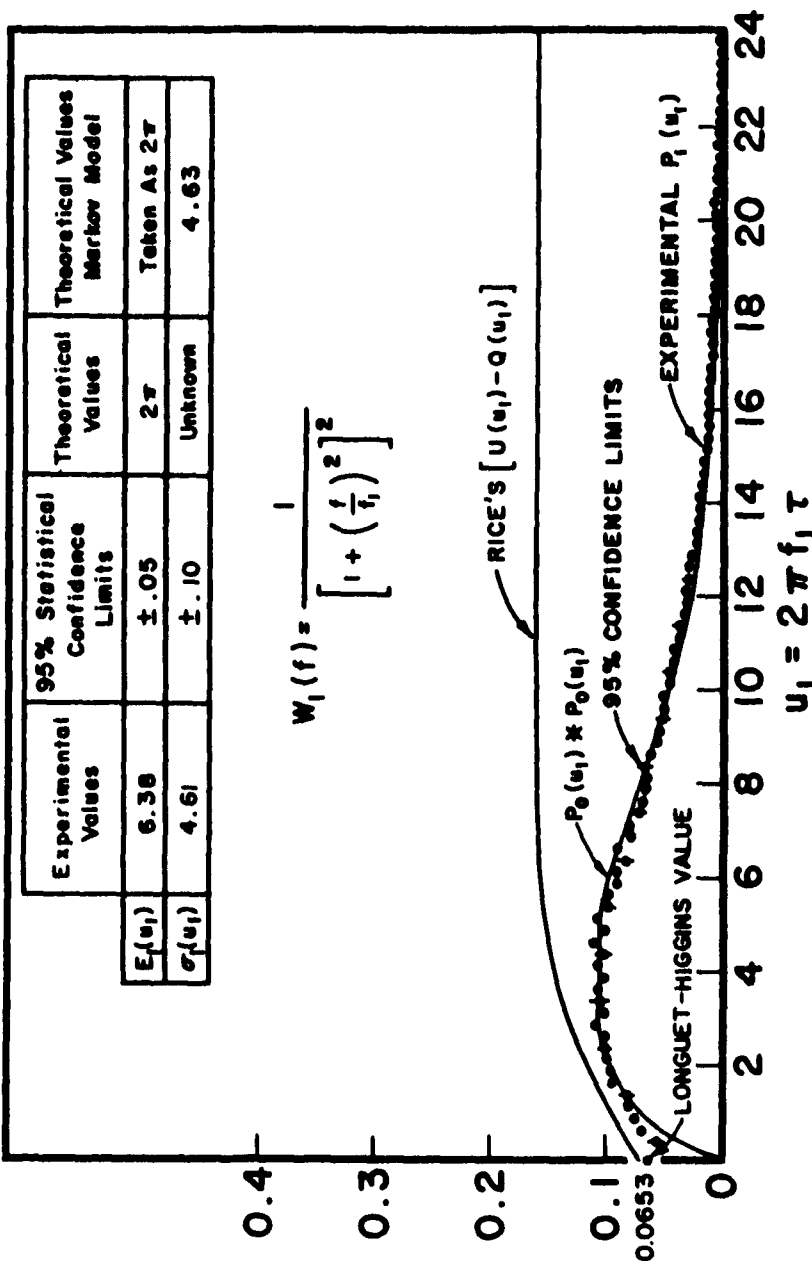


Figure 19  $P_1(u_1)$  is the Probability Density Function for the Sum of Two Successive Zero-Crossing Intervals of Gaussian Noise Having a Power Spectral Density  $W_1(f)$ .  $P_0(u_1) * P_0(u_1)$  is Compared with the Experimental Result to Exhibit the Statistical Dependence of Two Successive Intervals.

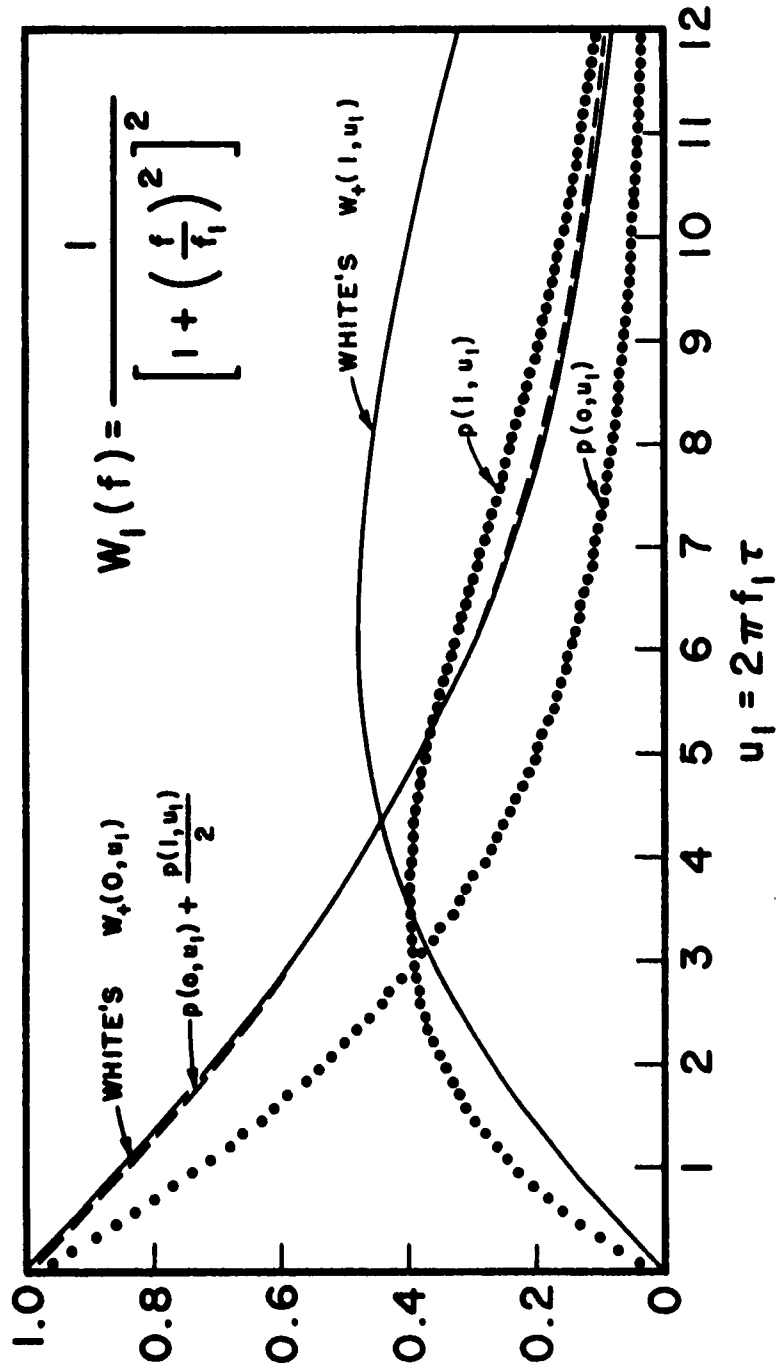


Figure 20  $p(n, u_1)$  is the Probability that a Given Interval  $u_1$  Contains Exactly  $n$  Zero-Crossing Points.  $p(n, u_1)$  and White's  $W_1(n, u_1)$  Probabilities are Compared for the Case of Gaussian Noise Having a Power Spectral Density  $W_1(f)$  when  $n = 0, 1$ .

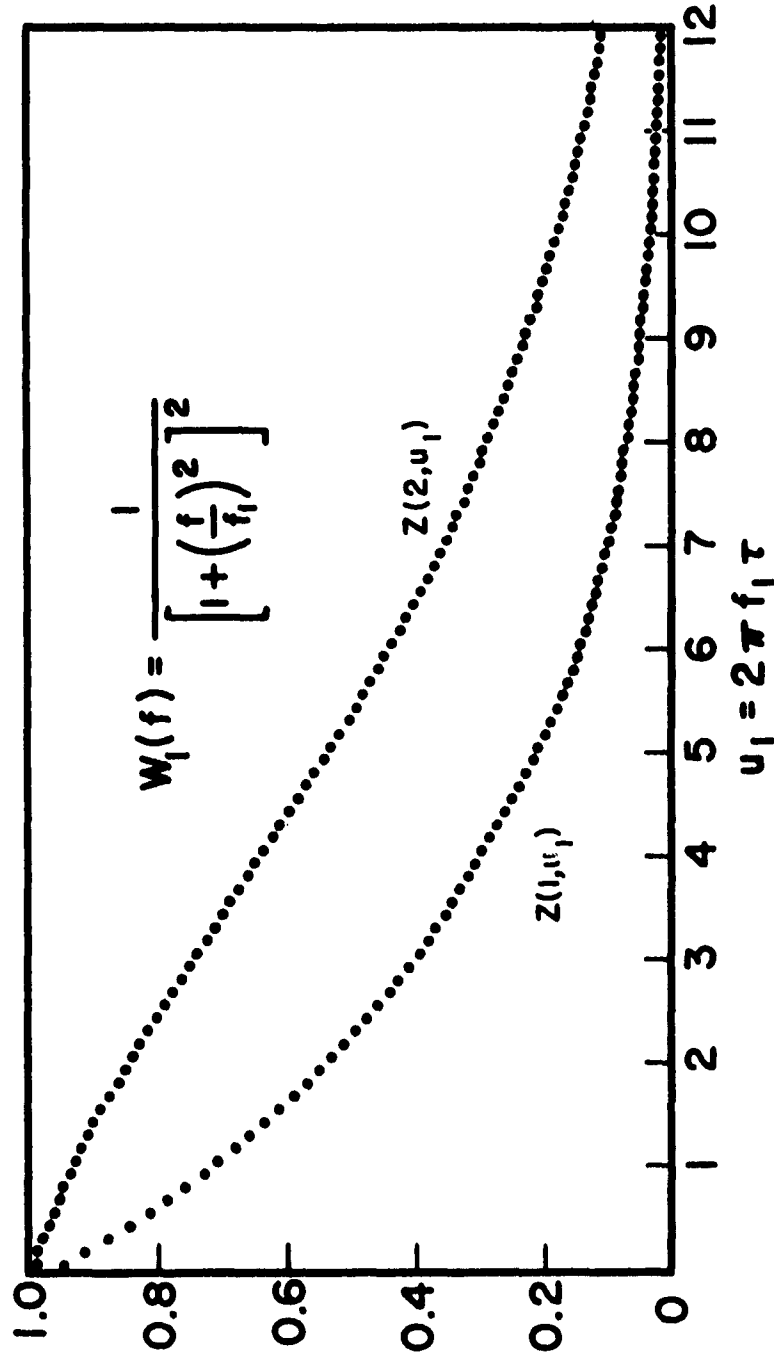


Figure 21  $Z(n, u_1)$  is the Conditional Probability that the  $n$ th Zero-Crossing Point from a Given Zero-Crossing Point in  $du_1$  Occurs after the Time  $du_1 + u_1$ .  $Z(1, u_1)$  and  $Z(2, u_1)$  are Compared for the Case of Gaussian Noise Having a Power Spectral Density  $W_1(f)$ .

$$U(\tau) - Q(\tau) \geq P_1(\tau) \text{ for all } \tau. \quad (101)$$

Accordingly, Rice's  $U(u_1) - Q(u_1)$  function serves as an upper bound for  $P_1(u_1)$  and is presented in Figure 19. Longuet-Higgins (8) deduced bounds for  $P_1(0)$  theoretically as  $0.0645 < P_1(0) < U(0) - Q(0) = 0.0726$  and deduced the approximate value  $P_1(0) \approx 0.0653$ .

G. M. White (18) experimentally determined the following probabilities concerning the zero-crossings of a Gaussian process having a power spectral density  $W_1(f)$ :

- (1)  $W_+(0, u_1)$ , the probability of having no zero-crossings with positive slope in a time interval  $u_1$ .
- (2)  $W_+(1, u_1)$ , the probability of having one zero-crossing with positive slope in a time interval  $u_1$ .

In general

$$W_+(0, \tau) = p(0, \tau) + \frac{1}{2} p(1, \tau) \quad (102)$$

and

$$W_+(1, \tau) = \frac{1}{2} p(1, \tau) + p(2, \tau) + \frac{1}{2} p(3, \tau) \quad (103)$$

or

$$p(2, \tau) \leq W_+(1, \tau) - \frac{p(1, \tau)}{2} \quad (104)$$

Equation (102) states that the interval can contain no upcrossings in two ways: Either it contains no crossings at all, or it contains one. If it contains one, then with conditional probability  $\frac{1}{2}$  it is either upward or downward.

Equation (103) states that the interval can contain exactly one upcrossing in three ways: Either it contains one crossing, or two, or three. If it contains one, then with conditional probability  $\frac{1}{2}$  it is upward or downward. If it contains two, then one of them must be upward. If it contains three, then one or two of them will be upward, each with probability  $\frac{1}{2}$ .

Figure 20 compares  $p(0, u_1) + \frac{1}{2} p(1, u_1)$  with  $W_+(0, u_1)$ . The comparison is excellent. Also, Figure 20 presents both  $W_+(1, u_1)$  and  $p(1, u_1)$ . Accordingly, an upper bound for  $p(2, u_1)$  can be readily computed from inequality (104). This upper bound agrees satisfactorily with the approximate theoretical initial behavior  $p(2, u_1) \sim \frac{0.818}{6\pi} (u_1)^2$  which was deduced by Longuet-Higgins(8).

Figure 19 compares the convolution of  $P_0(u_1)$  with itself,  $P_0(u_1) * P_0(u_1)$ , and  $P_1(u_1)$ . This comparison serves to demonstrate that two successive zero-crossing intervals are statistically dependent. A theorem is proved in Section IX which asserts that for Gaussian processes the sum of  $m + 1$  successive zero-crossing intervals and the sum of the next  $n + 1$  successive zero-crossing intervals are statistically dependent. The theorem applies for all nonnegative integral  $m$  and  $n$ .

#### B. POWER SPECTRAL DENSITY $W_2(f)$

Probabilities and probability densities defined by the zero-crossing points of a Gaussian process having a power spectral

density  $W_2(f)$  are presented in Figures 22, 23, 24, and 25. Theoretical approximations derived by Rice (1) and McFadden (2) are presented in Figure 22 for comparison purposes. Figure 22 also presents an experimental probability density reported by Favreau, et al (19). Rice's  $U(u_2)-Q(u_2)$  function is presented in Figure 23 for comparison purposes. Figure 23 also compares the convolution of  $P_0(u_2)$  with itself,  $P_0(u_2) * P_0(u_2)$ , and  $P_1(u_2)$ . This latter comparison was intended to exhibit the statistical dependence of two successive intervals. In this case the convolution function is nearly equal to  $P_1(u_2)$ . However, as the theorem of Section IX asserts, two successive zero-crossing intervals are still statistically dependent.

The theoretical initial values of  $P_0(u_2)$  and  $P_1(u_2)$  are zero since Rice's  $U(u_2)$  function is initially zero.

### C. POWER SPECTRAL DENSITY $W_3(f)$

Probabilities and probability densities defined by the zero-crossing points of a Gaussian process having a power spectral density  $W_3(f)$  are presented in Figures 26, 27, 28, and 29. Theoretical approximations derived by Rice (1) and McFadden (2) are presented in Figure 26 for comparison purposes. Figure 26 also presents an experimental probability density reported by Favreau, et al. (19).

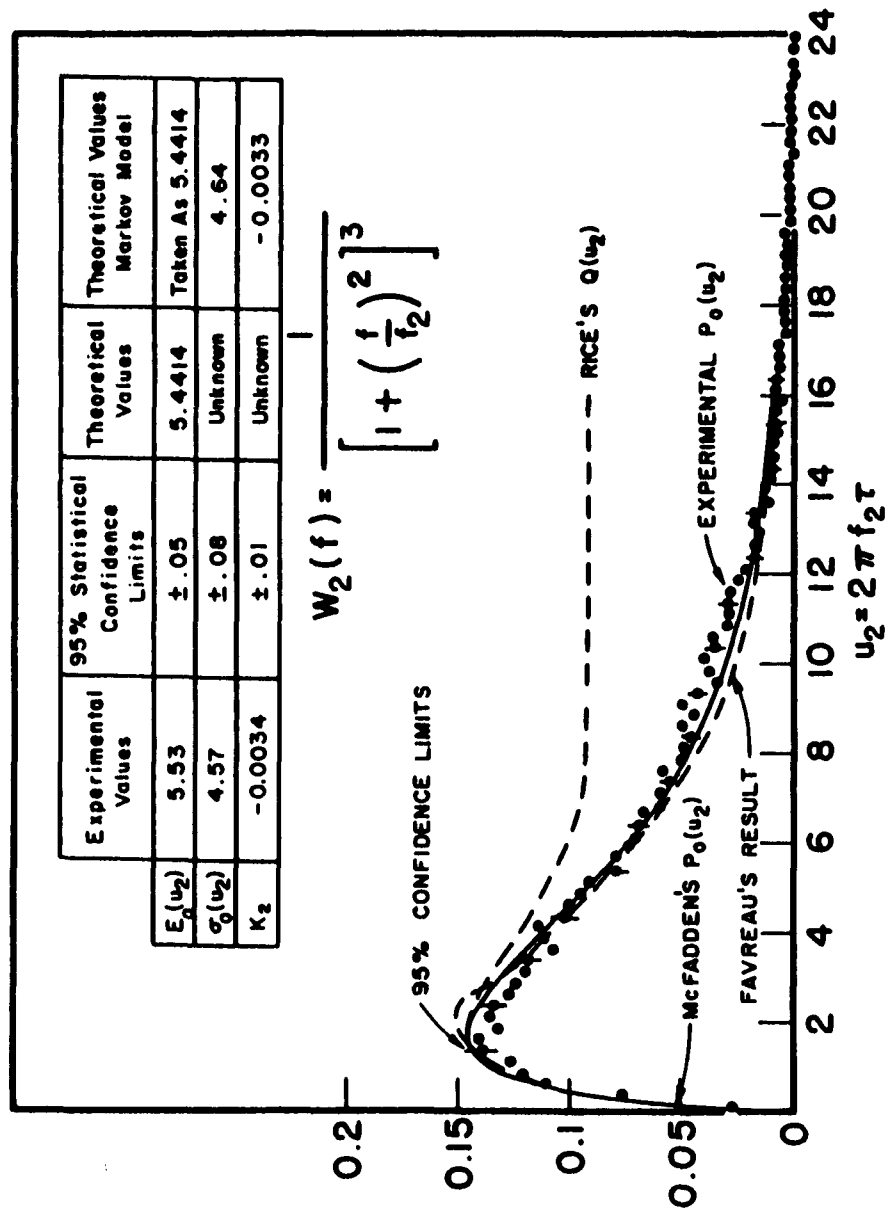


Figure 22  $P_0(u_2)$  is the Probability Density Function for Successive Zero-Crossing Intervals of Gaussian Noise Having a Power Spectral Density  $W_2(f)$ . Theoretical Approximations are Compared with Experimental Results.

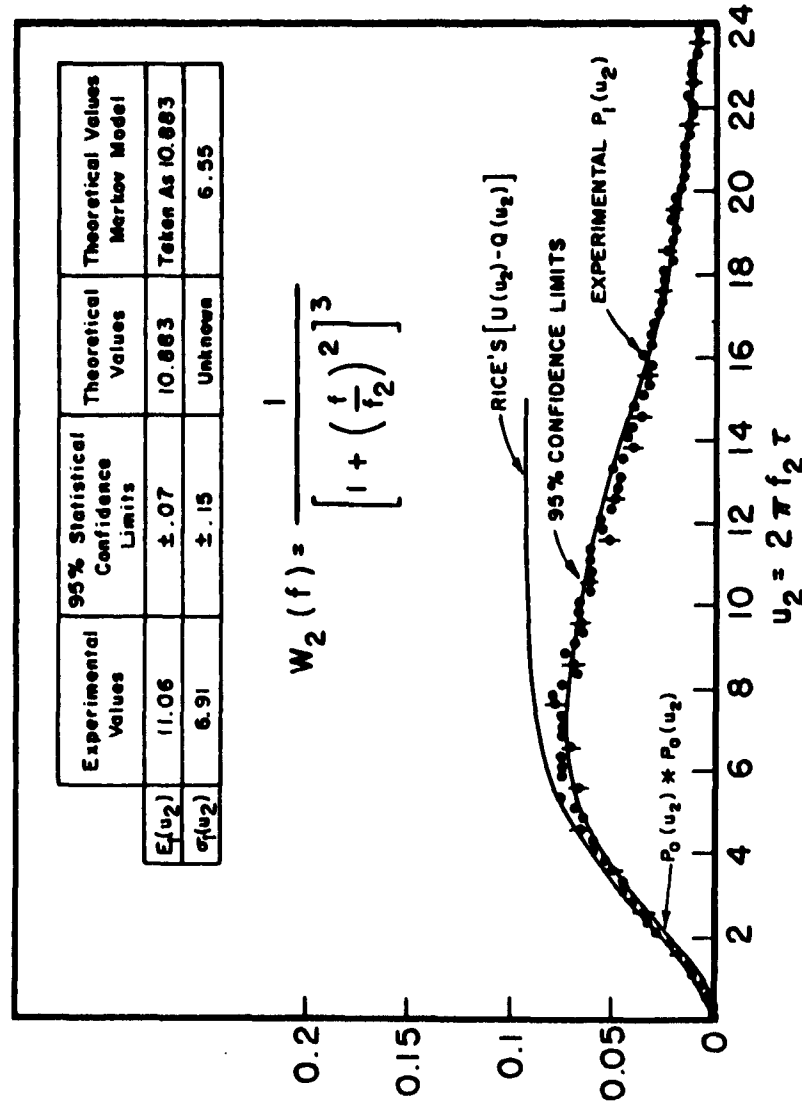


Figure 2.3  $P_1(u_2)$  is the Probability Density Function for the Sum of Two Successive Zero-Crossing Intervals of Gaussian Noise Having a Power Spectral Density  $W_2(f)$ .  $P_0(u_2) * P_0(u_2)$  is Compared with the Experimental Result to Exhibit the Practical Independence of Two Successive Intervals.



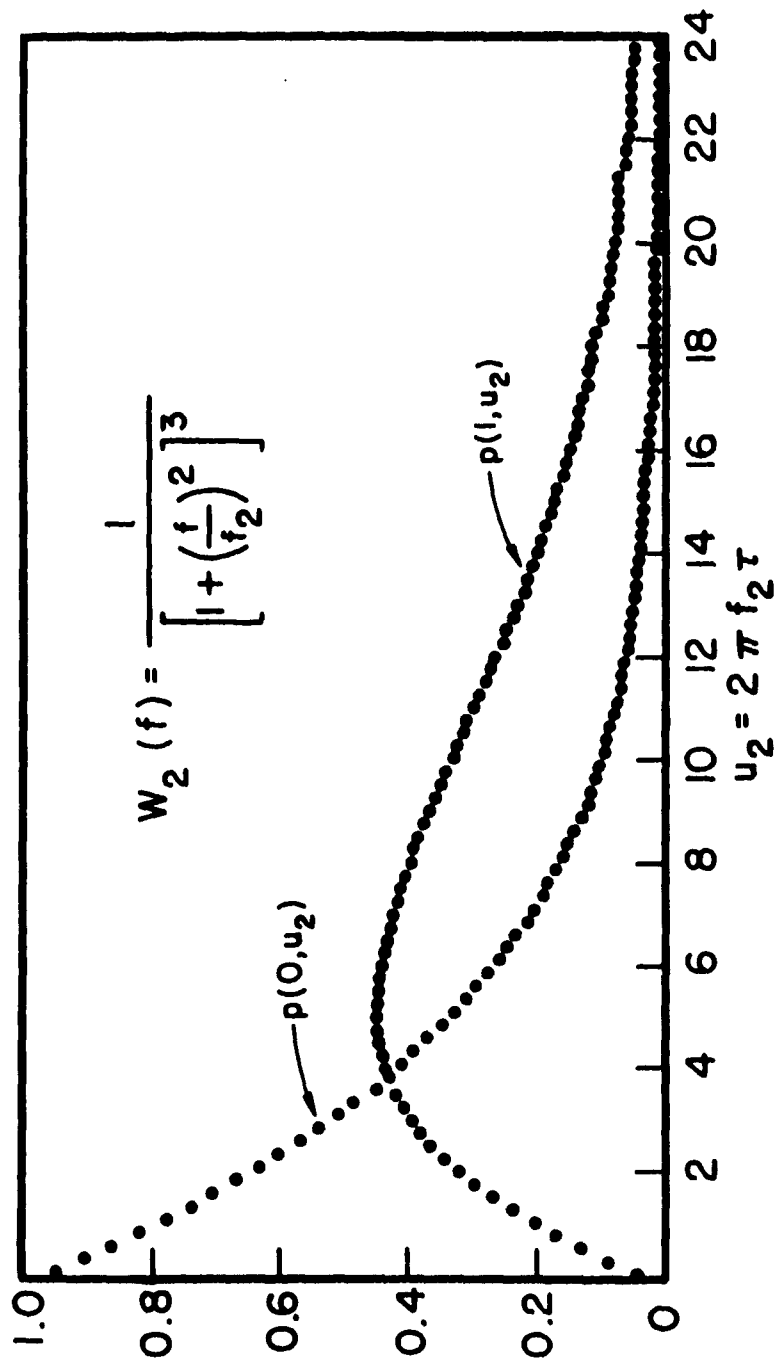


Figure 24  $p(n, u_2)$  is the Probability that a Given Interval  $u_2$  Contains Exactly  $n$  Zero-Crossing Points.  $p(0, u_2)$  and  $p(1, u_2)$  are Compared for the Case of Gaussian Noise Having a Power Spectral Density  $W_2(f)$ .

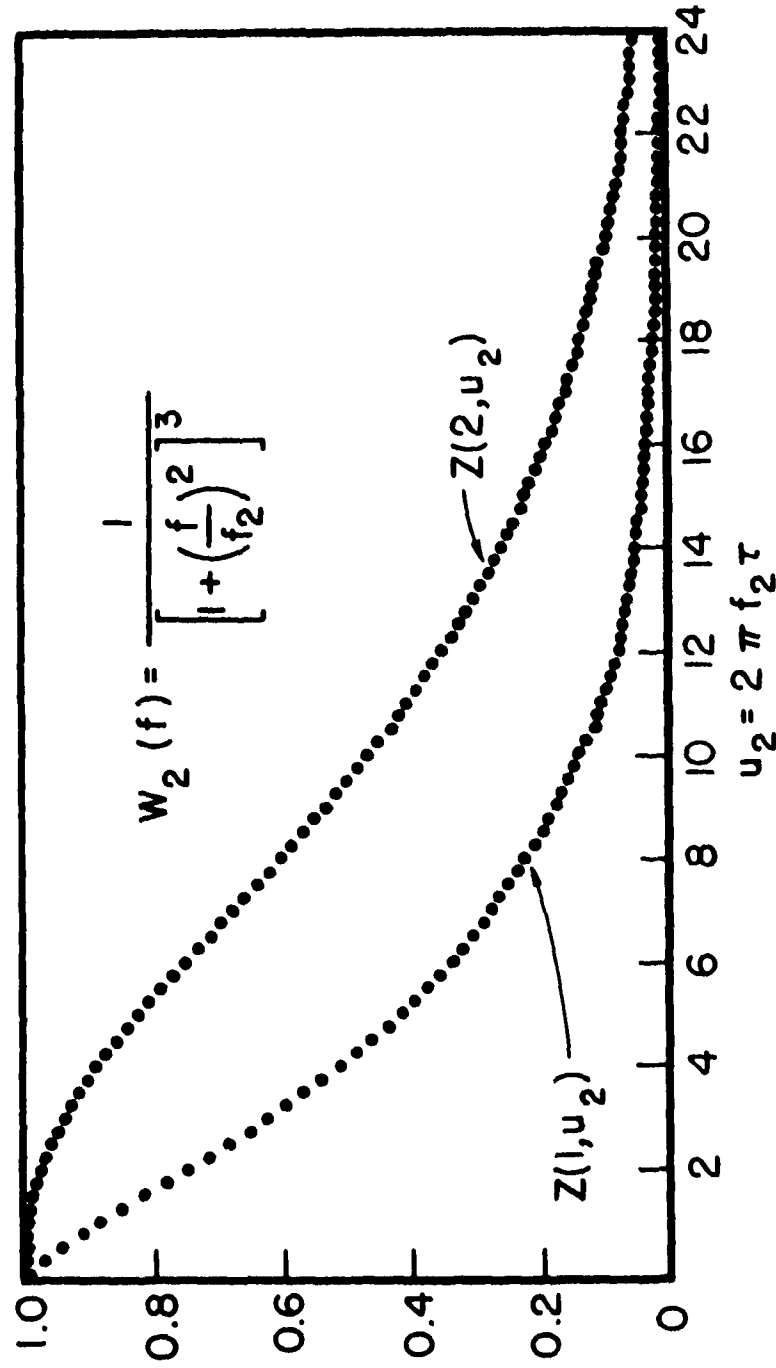


Figure 25  $Z(n, u_2)$  is the Conditional Probability that the  $n$ th Zero-Crossing Point from a Given Zero-Crossing Point in  $du_2$  Occurs After the Time  $du_2 + u_2$ .  $Z(1, u_2)$  and  $Z(2, u_2)$  are Compared for the Case of Gaussian Noise Having a Power Spectral Density  $W_2(f)$ .

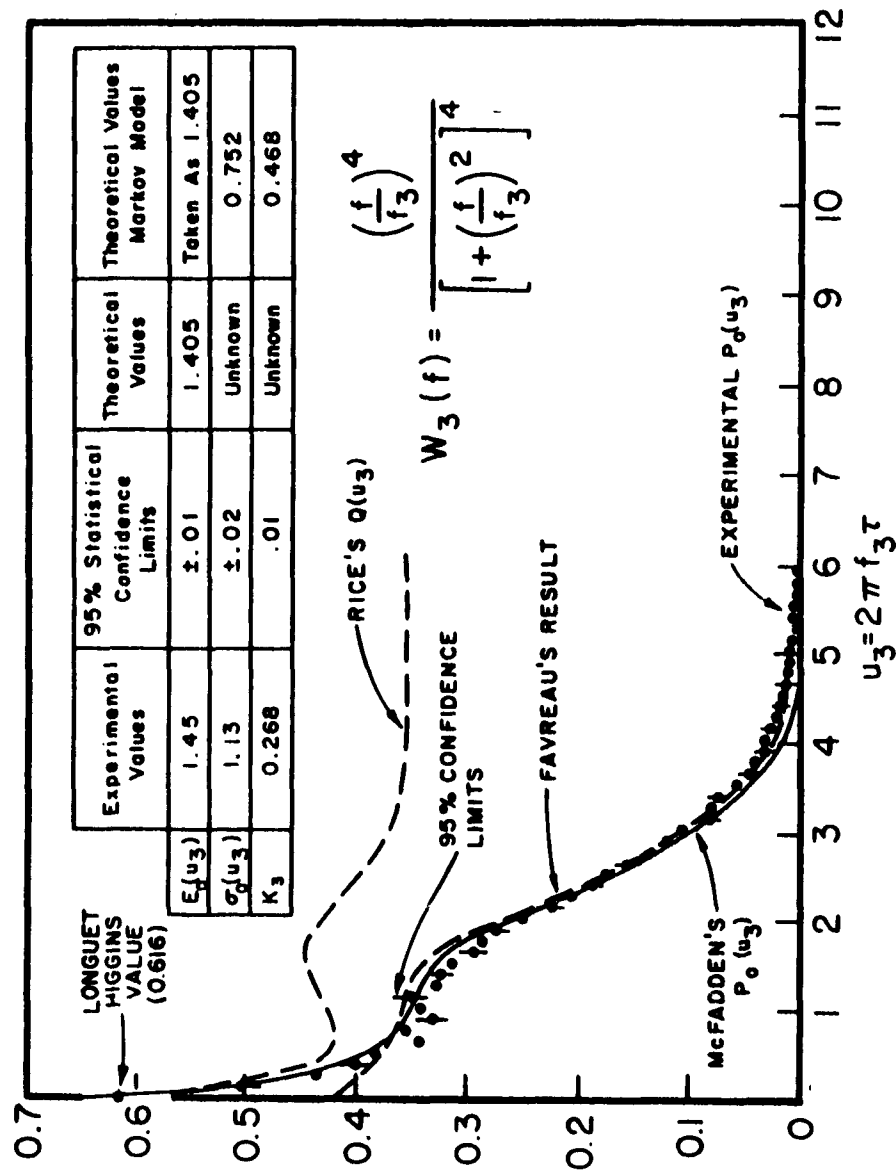


Figure 26  $P(u_3)$  is the Probability Density Function for Successive Zero-Crossing Intervals of Gaussian Noise Having a Power Spectral Density  $W_3(f)$ . Theoretical Approximations are Compared with Experimental Results.

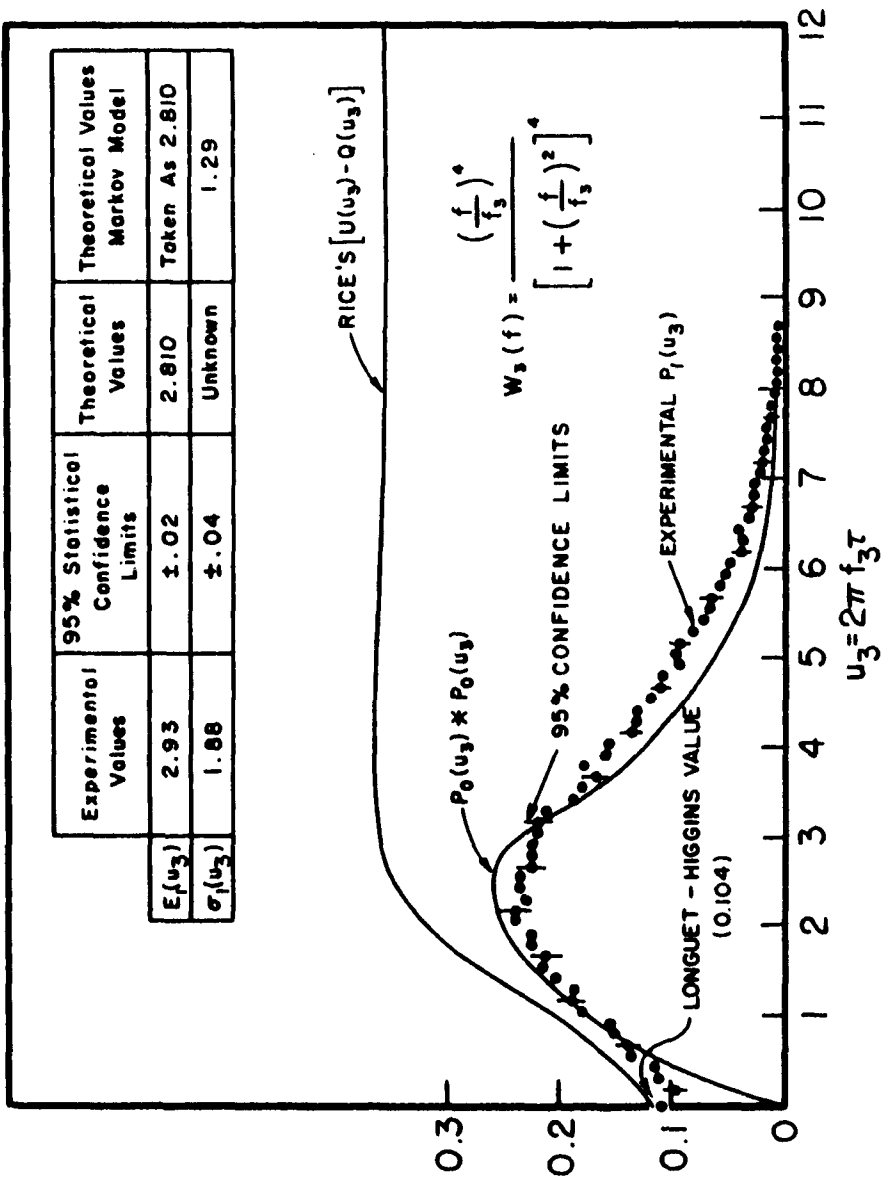


Figure 27  $P_1(u_3)$  is the Probability Density Function for the Sum of Two Successive Zero-Crossing Intervals of Gaussian Noise Having a Power Spectral Density  $W_3(f)$ .  $P_0(u_3) * P_0(u_3)$  is Compared with the Experimental Result to Exhibit the Statistical Dependence of Two Successive Intervals.

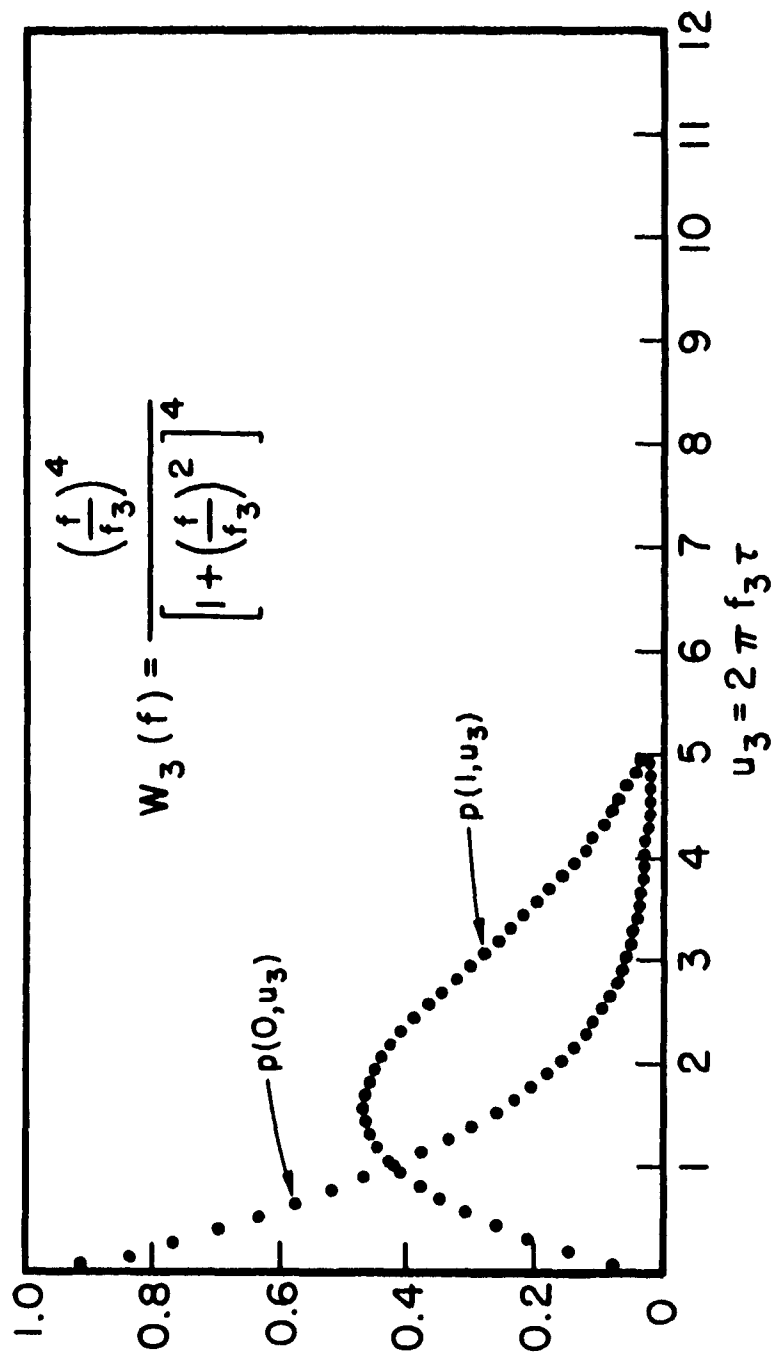


Figure 28  $p(n, u_3)$  is the Probability that a Given Interval  $u_3$  Contains Exactly  $n$  Zero-Crossing Points.  $p(0, u_3)$  and  $p(1, u_3)$  are Compared for the Case of Gaussian Noise Having a Power Spectral Density  $W_3(f)$ .

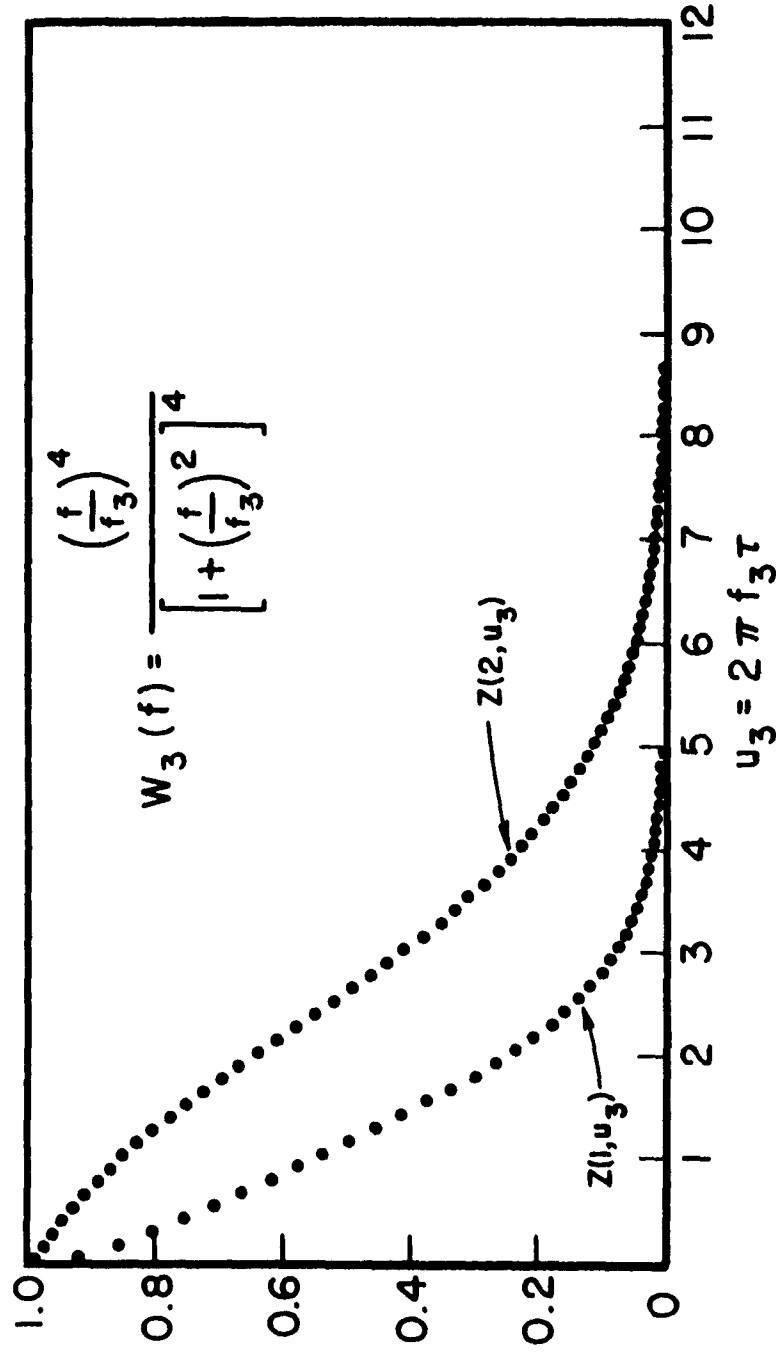


Figure 29  $Z(n, u_3)$  is the Conditional Probability that the  $n$ th Zero-Crossing Point from a Given Zero-Crossing Point in  $u_3$  Occurs After the Time  $u_3 + u_3$ .  $Z(1, u_3)$  and  $Z(2, u_3)$  are Compared for the Case of Gaussian Noise Having a Power Spectral Density  $W_3(f)$ .

Rice's  $Q(u_3)$  function serves as an upper bound for  $P_0(u_3)$  and is presented in Figure 26. Longuet-Higgins (8) deduced bounds for  $P_0(0)$  theoretically as  $0.612 < P_0(0) < Q(0) = 0.650$  and deduced the approximate value  $P_0(0) \doteq 0.616$ . Also, Longuet-Higgins (8) deduced bounds for  $P_1(0)$  theoretically as  $0.103 < P_1(0) < U(0) - Q(0) = 0.116$  and deduced the approximate value  $P_1(0) \doteq 0.104$ .

The experimental probabilities  $p(0, u_n)$  for  $n = 1, 2, 3$  satisfy theorems 1, 3 and Equation (22) of D. Slepian's (13) recent paper regarding bounds for these probabilities.

Rice's  $[U(u_3) - Q(u_3)]$  function is presented in Figure 27 for comparison purposes. Figure 27 also compares the convolution of  $P_0(u_3)$  with itself,  $P_0(u_3) * P_0(u_3)$ , and  $P_1(u_3)$ . This latter comparison serves to demonstrate that two successive zero-crossing intervals are statistically dependent.

The experimental probability densities  $P_0(u_n)$  for  $n = 1, 2, 3$  agree very well with theoretical approximations recently published by Longuet-Higgins (8). The approximate theoretical initial values of Longuet-Higgins were used in the normalization of the experimental densities  $P_0(u_n)$  and  $P_1(u_n)$  for  $n = 1, 3$ .

#### D. POWER SPECTRAL DENSITY $W_4(f)$

Probabilities and probability densities defined by the zero-crossing points of a Gaussian process having a power spectral density  $W_4(f)$  are presented in Figures 30, 31, 32, and 33. Theoretical approximations derived by Rice (4) are presented in Figures 30 and 31 for

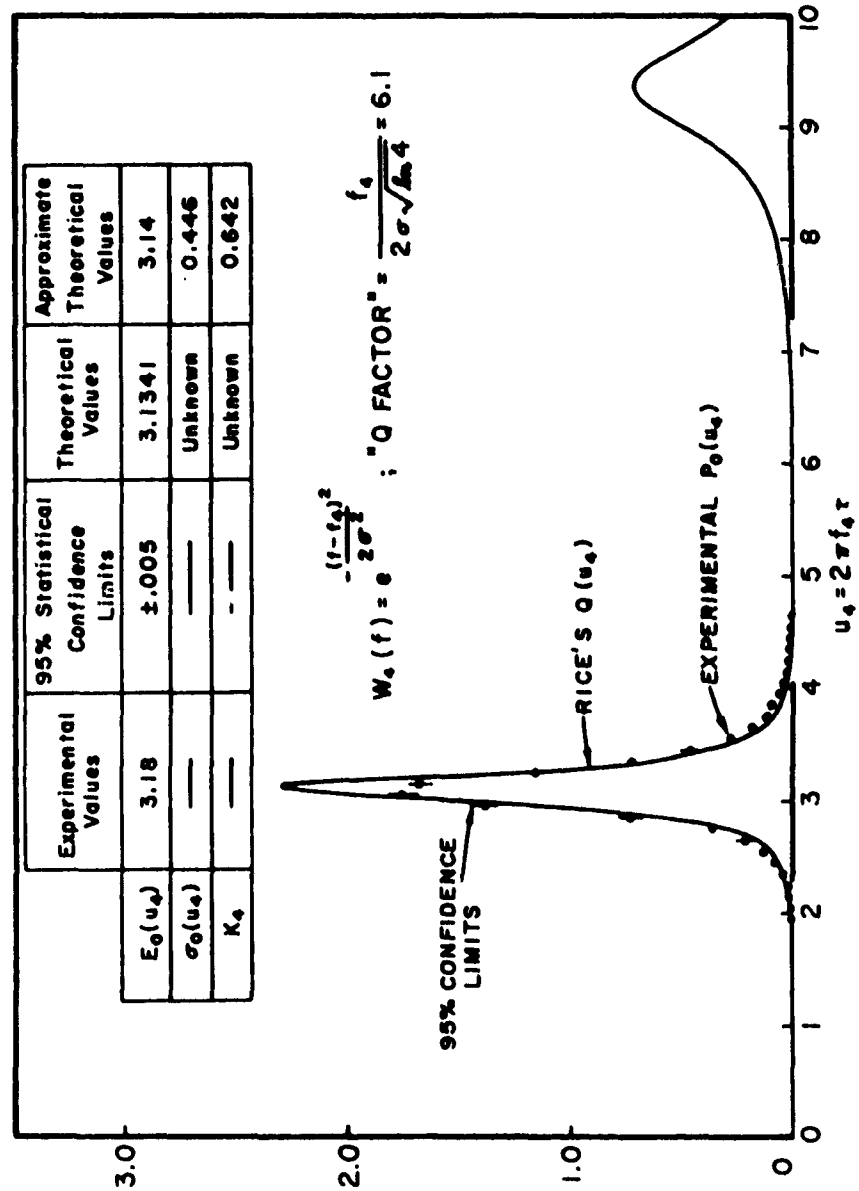


Figure 30  $P(u_4)$  is the Probability Density Function for Successive Zero-Crossing Intervals of Gaussian Noise Having a Power Spectral Density  $W_4(f)$ . Theoretical Approximations are Compared with Experimental Results.



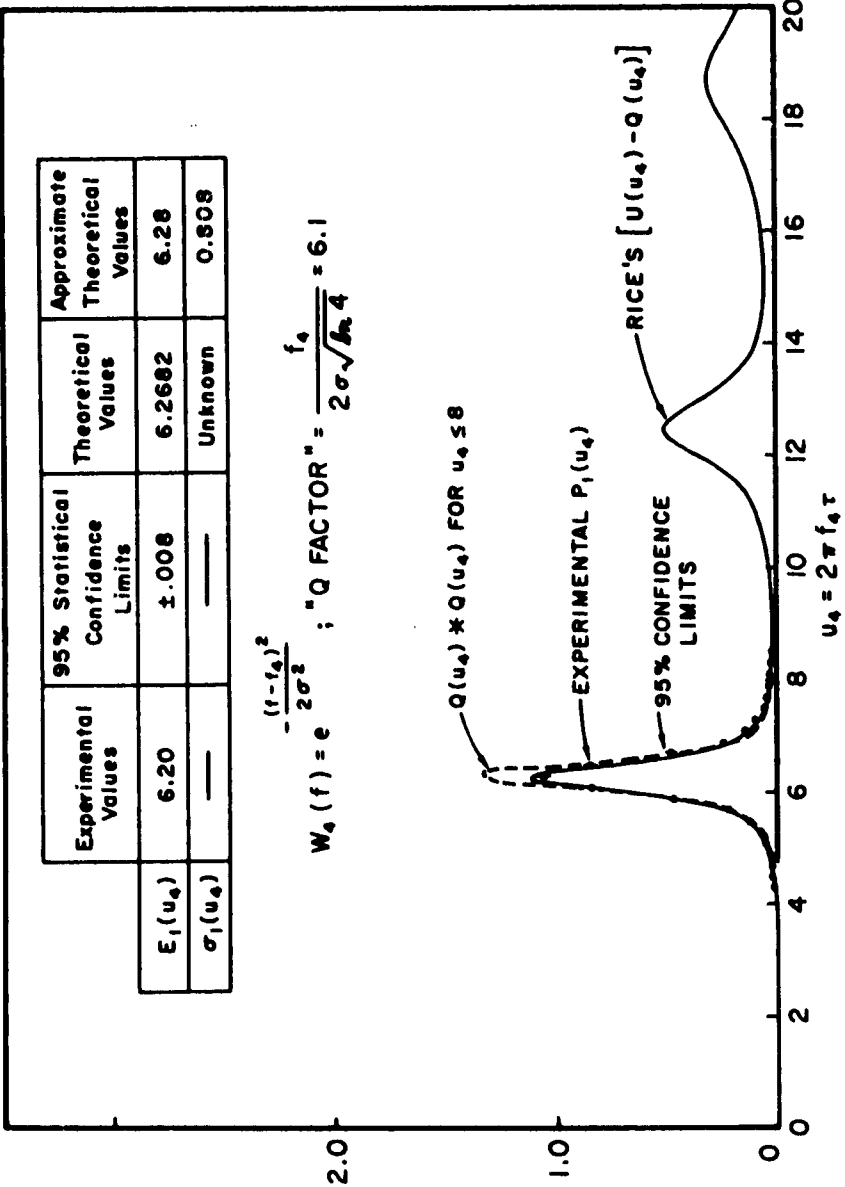


Figure 31  $P_1(u_4)$  is the Probability Density Function for the Sum of Two Successive Zero-Crossing Intervals of Gaussian Noise Having a Power Spectral Density  $W_4(f)$ .  $Q(u_4) * Q(u_4)$  is Compared with  $U(u_4) - Q(u_4)$  to Exhibit the Statistical Dependence of Two Successive Intervals.

comparison purposes. Figure 31 also compares the convolution of the first normalized portion of  $Q(u_4)$  with itself,  $Q(u_4)*Q(u_4)$ , and the first normalized portion of  $U(u_4) - Q(u_4)$ . In accordance with Equations (98) and (99), this comparison serves to demonstrate that two successive zero-crossing intervals are statistically dependent. The theoretical initial values of  $P_0(u_4)$  and  $P_1(u_4)$  are zero since Rice's  $U(u_4)$  function is initially zero.

The results in Figures 32 and 33 were computed by using Equations (39), (40), (41), and (42). The first normalized portions of  $Q(u_4)$  and  $U(u_4) - Q(u_4)$  served as  $P_0(u_4)$  and  $P_1(u_4)$  respectively.

In order to obtain good experimental estimates of  $\sigma_0(u_4)$  and  $\sigma_1(u_4)$ , we see from Figures 30 and 31 that the experimental densities  $P_0(u_4)$  and  $P_1(u_4)$  must be measured with finer resolution. Accordingly, our present experimental estimates of  $\sigma_0(u_4)$  and  $\sigma_1(u_4)$  are not worth reporting.

Notice that a "Q factor" of 6.1 as defined in Equation (18) is approximately the minimum "Q factor" representing a "narrow-band system" as defined in communication theory. Accordingly, the problem of theoretically determining  $P_0(\tau)$  and  $P_1(\tau)$  for narrow-band Gaussian processes is practically solved by using Rice's  $Q(\tau)$  and  $[U(\tau) - Q(\tau)]$  functions as the generating functions of  $P_0(\tau)$  and  $P_1(\tau)$  in accordance with Equations (98) and (99).

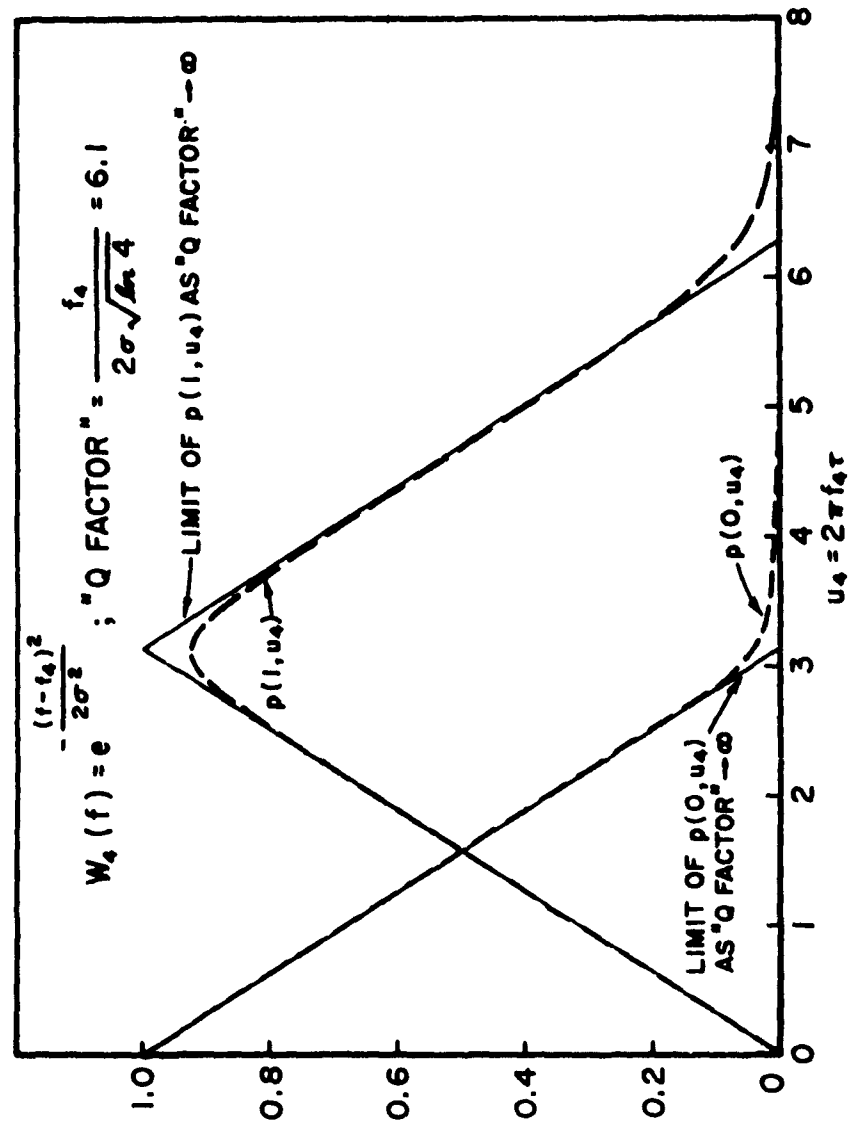


Figure 32  $p(n, u_4)$  is the Probability That a Given Interval  $u_4$  Contains Exactly  $n$  Zero-Crossing Points.  $p(0, u_4)$  and  $p(1, u_4)$  are Compared for the Case of Gaussian Noise Having the Power Spectral Density  $W_4(f)$ .

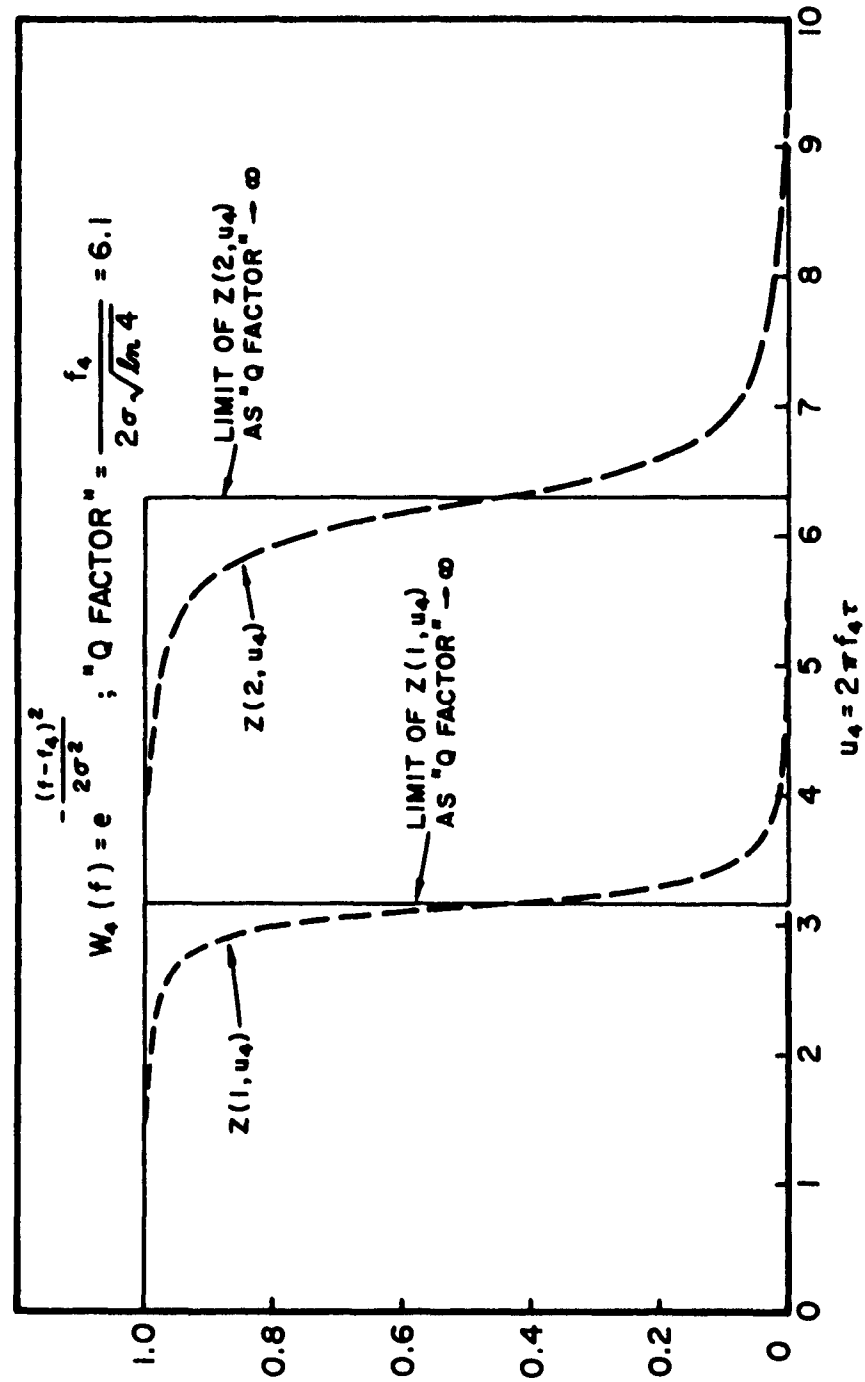


Figure 33  $Z(n, u_4)$  is the Conditional Probability that the nth Zero-Crossing Point From a Given Zero-Crossing Point in  $du_4$  Occurs After the Time  $du_4$ .  $Z(1, u_4)$  and  $Z(2, u_4)$  are Compared for the Case of Gaussian Noise Having a Power Spectral Density  $W_4(f)$ .

A portion of the above work dealing with Gaussian processes has been published recently in the IRE Transactions on Information Theory (35).

VII. PROBABILITIES AND PROBABILITY DENSITIES DEFINED  
BY THE ZERO POINTS OF A SINE WAVE PLUS A  
GAUSSIAN PROCESS

Probabilities and probability densities defined by the zero-crossing points of the random process,  $\xi(u, a)$ , consisting of a sine wave of frequency  $\frac{f_0}{2}$  plus Gaussian noise having a power spectral density  $W_0(f)$  are presented in Figures 34 thru 49. The ratio of the average sine wave power,  $S$ , to the average noise power,  $N$ , is denoted by the parameter  $a$ . For small values of  $a = \frac{S}{N}$ , the random process  $\xi(u, a)$  is approximately Gaussian with normalized autocorrelation function,  $R(u_0, a)$ , given by Equation (64). Accordingly, Rice's probability function  $Q^*(u_0, a) du_0$  approximates the conditional probability that a downward zero-crossing of  $\xi(u, a)$  occurs between  $u + u_0$  and  $u + u_0 + du_0$ , given an upward zero-crossing of  $\xi(u, a)$  at time  $u$ . In accordance with Equation (98),  $Q^*(u_0, a)$  serve as approximations to the initial behavior of  $P_0(u_0, a)$  for small " $a$ " and are presented in Figures 34, 38, 42, and 46. Figure 34 also presents McFadden's theoretical approximation for  $P_0(u_0, 0)$ .  $Q^*(u_0, a) du_0$  is the exact conditional probability that a downward zero-crossing of  $\xi^*(u, a)$  occurs between  $u + u_0$  and  $u + u_0 + du_0$ , given an upward zero-crossing of  $\xi^*(u, a)$  at time  $u$ . The process  $\xi^*(u, a)$  is defined by Equation (81) and the process  $\xi(u, a)$  is defined by Equation (82). When  $a = 0$  the processes  $\xi(u, 0)$  and  $\xi^*(u, 0)$  are identical.

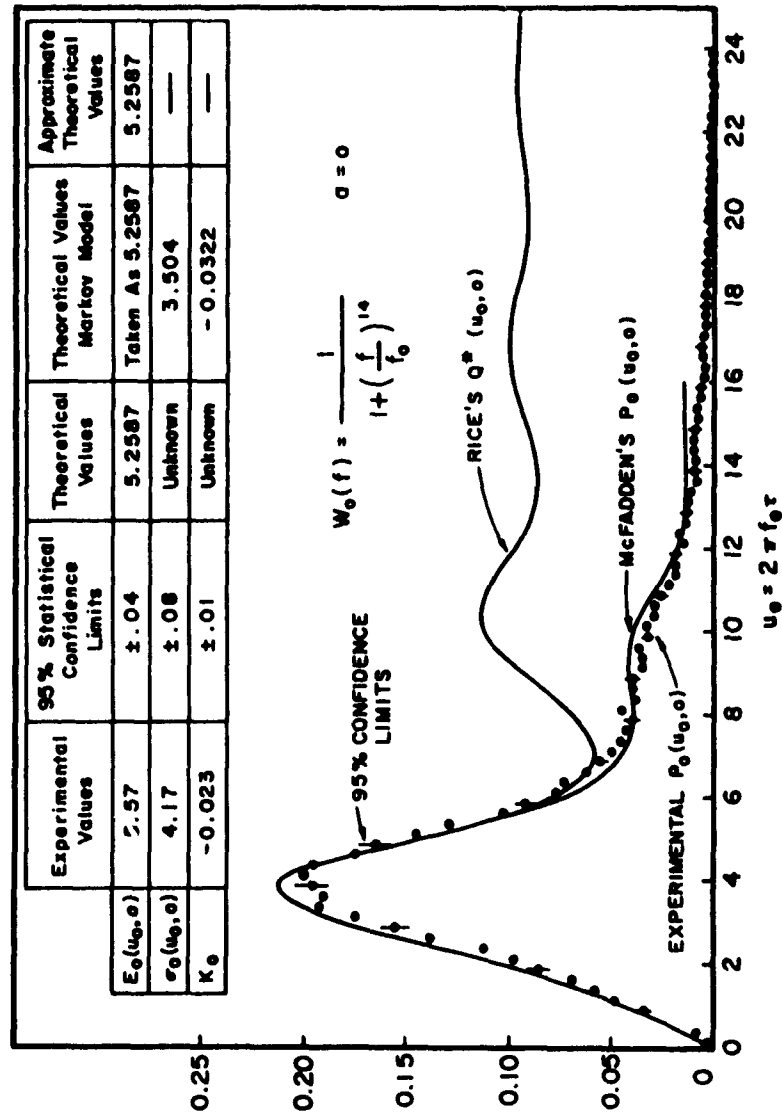


Figure 34  $P_0(u_0, a)$  is the Probability Density Function for Successive Zero-Crossing Intervals of a Random Process Consisting of Sine Wave of Frequency  $f/2$  Plus Gaussian Noise Having the Power Spectral Density  $W_0(f)$ . The Ratio of the Average Sine Wave Power to the Average Noise Power is Denoted by the Parameter  $a$ . Theoretical Approximations are Compared with Experimental Results.

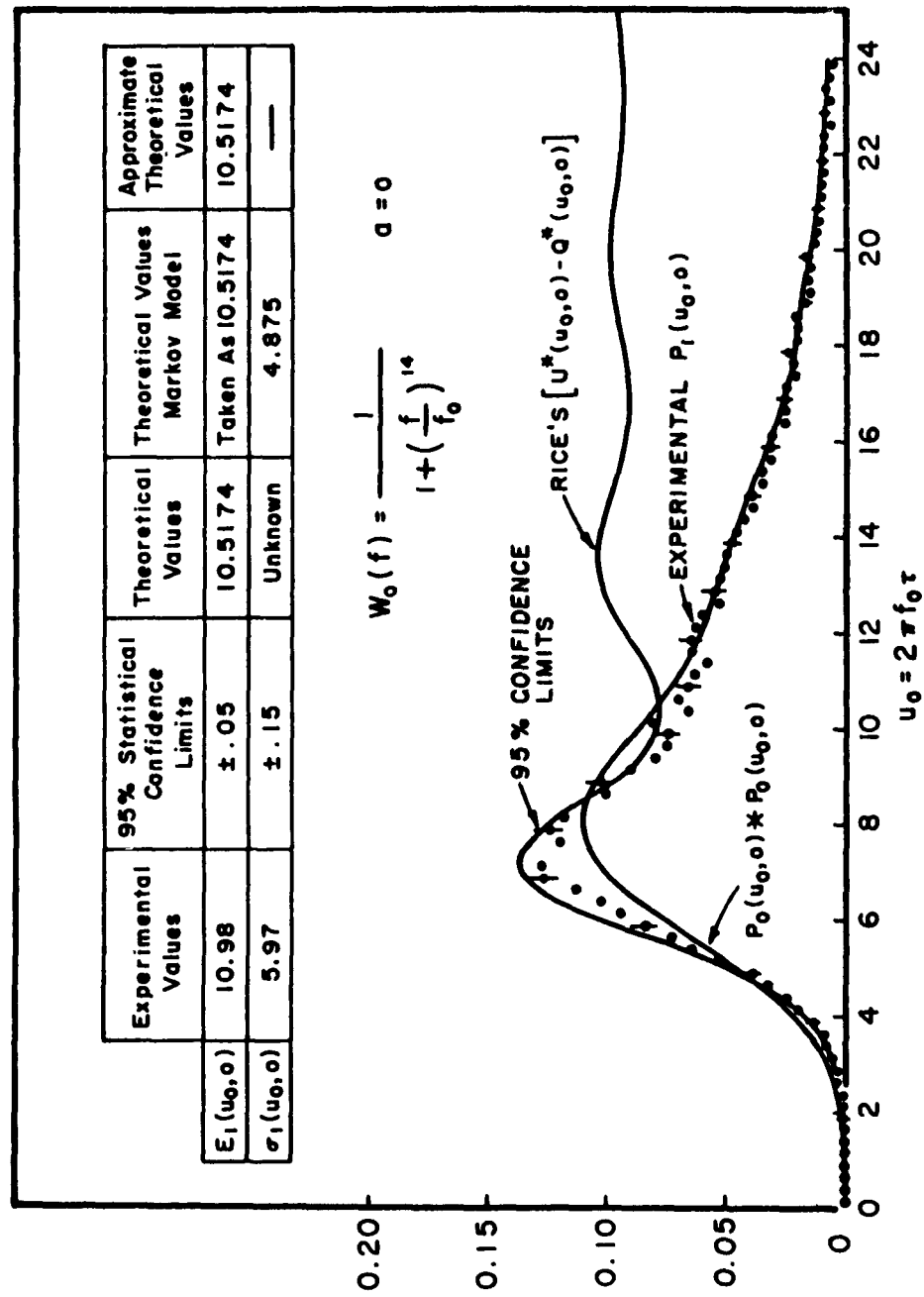


Figure 35  $P_1(u_0, a)$  is the Probability Density Function for the Sum of Two Successive Zero-Crossing Intervals of a Random Process Consisting of a Sine Wave of Frequency  $f/2$  Plus Gaussian Noise Having the Power Spectral Density  $W_0(f)$ . The Ratio of the Average Noise Power is Denoted by the Parameter  $a$ .



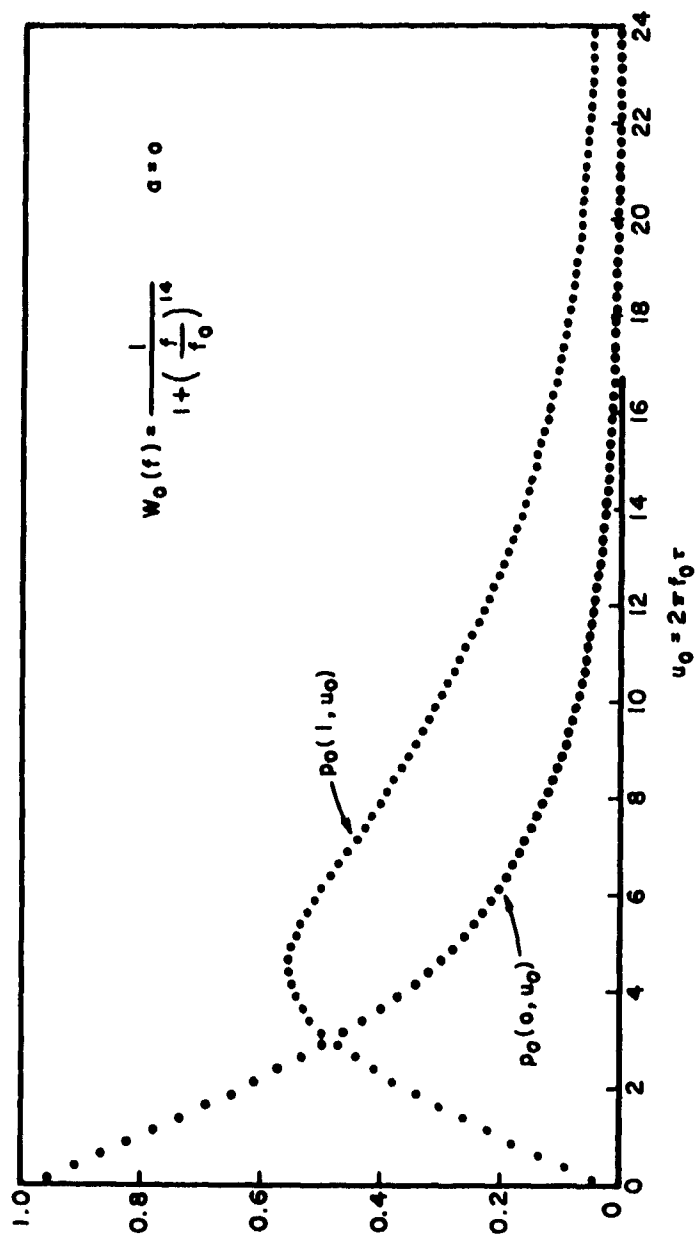


Figure 36

$P_a(n, u_0)$  is the Probability that a Given Interval  $u_0$  Contains Exactly  $n$  Zero-Crossing Points of a Random Process Consisting of a Sine Wave of Frequency  $f_0/2$  Plus Gaussian Noise Having the Power Spectral Density  $W_0(f)$ . The Ratio of the Average Sine Wave Power to the Average Noise Power is Denoted by The Parameter  $a$ .

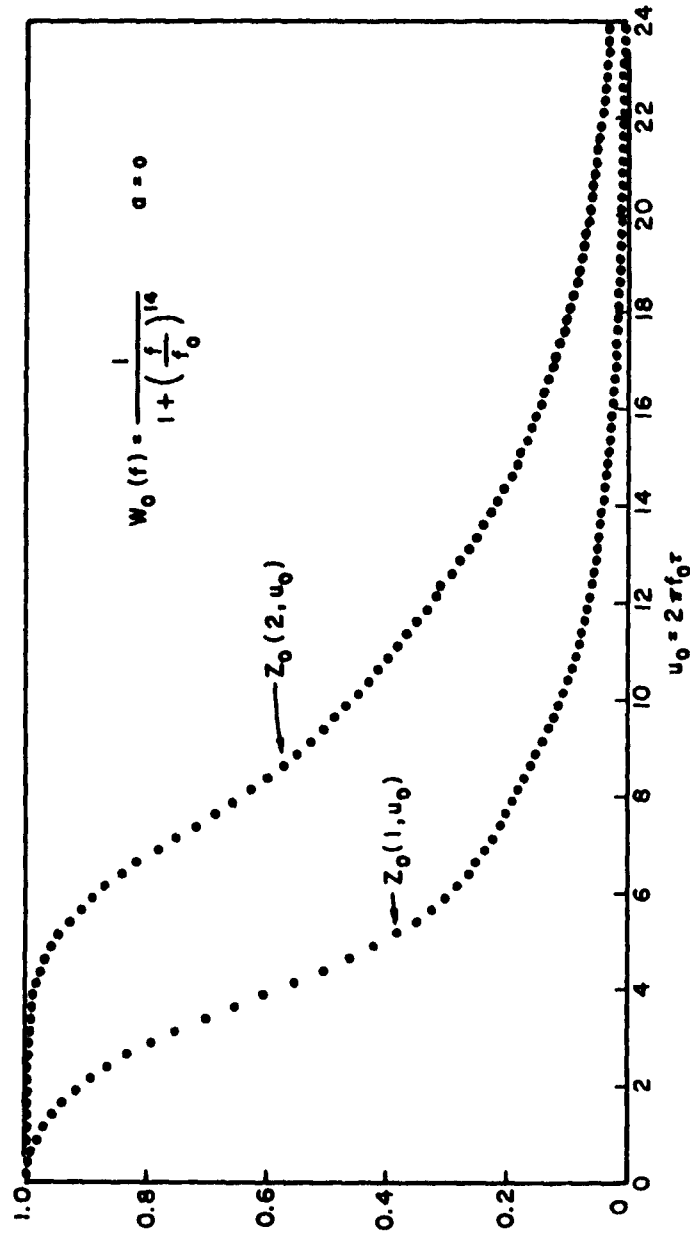


Figure 37 A Random Process Consisting of a Sine Wave of Frequency  $f_0/2$  Plus Gaussian Noise Having the Power Spectral Density  $W(f)$  Defines  $Z_a(n, u_0)$ , the Conditional Probability That the  $n$ th Zero-Crossing Point From a Given Zero-Crossing Point in  $du_0$  Occurs After the Time  $du_0 + u_0$ . The Ratio of the Average Sine Wave Power to the Average Noise Power is Denoted by the Parameter  $a$ .

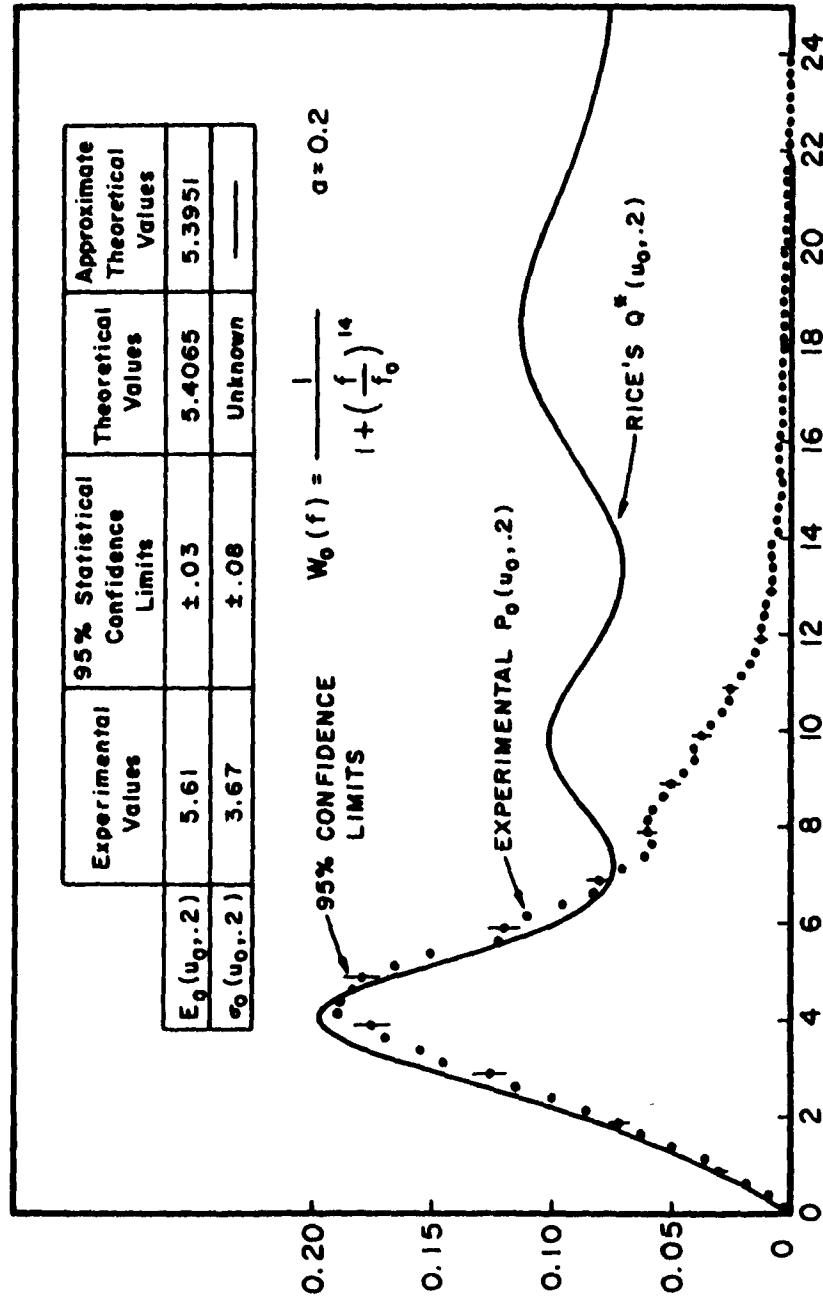


Figure 38  $P_0(u_0, a)$  is the Probability Density Function for Successive Zero-Crossing Intervals of a Random Process Consisting of a Sine Wave of Frequency  $f/2$  Plus Gaussian Noise Having the Power Spectral Density  $W_0(f)$ . The Ratio of the Average Sine Wave Power to the Average Noise Power is Denoted by the Parameter  $a$ . Theoretical Approximations are Compared With Experimental Results.

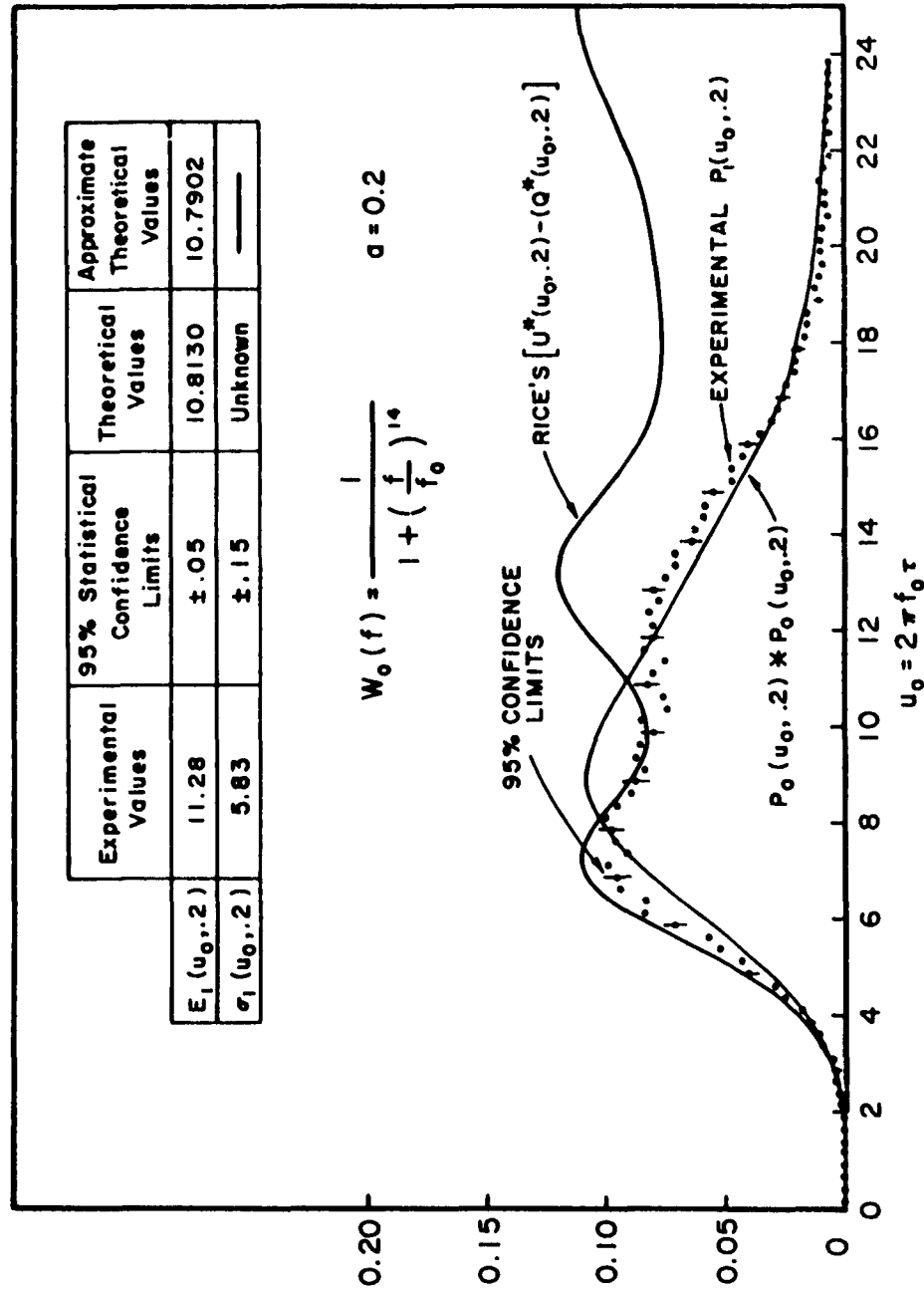


Figure 39  $P_1(u_0, a)$  is the Probability Density Function for the Sum of Two Successive Zero-Crossing Intervals of a Random Process Consisting of a Sine Wave of Frequency Plus Gaussian Noise Having the Power Spectral Density  $W(f)$ . The Ratio to the Average Sine Wave Power to the Average Noise Power is Denoted by the Parameter  $a$ .

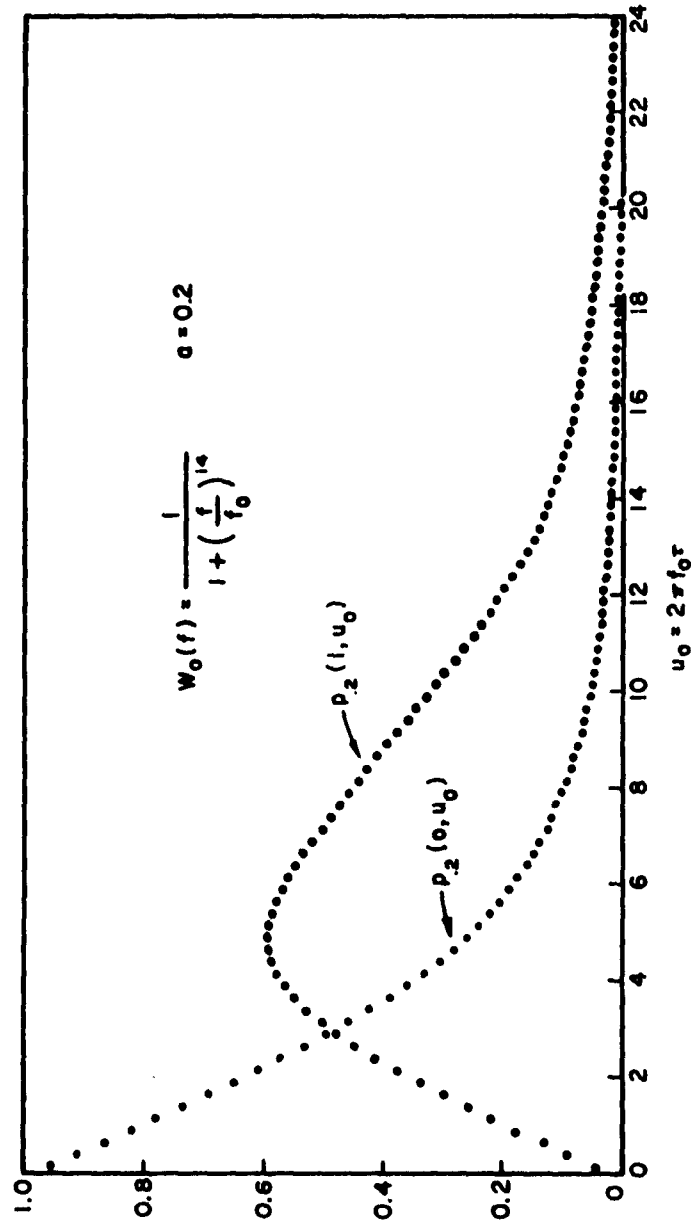


Figure 40  $p_2(n, u_0)$  is the Probability that a Given Interval  $u_0$  Contains Exactly  $n$  Zero-Crossing Points of a Random Process Consisting of a Sine Wave of Frequency  $f_0/2$  Plus Gaussian Noise Having the Power Spectral Density  $W_0(f)$ . The Ratio of the Average Sine Wave Power to the Average Noise Power is Denoted by the Parameter  $a$ .

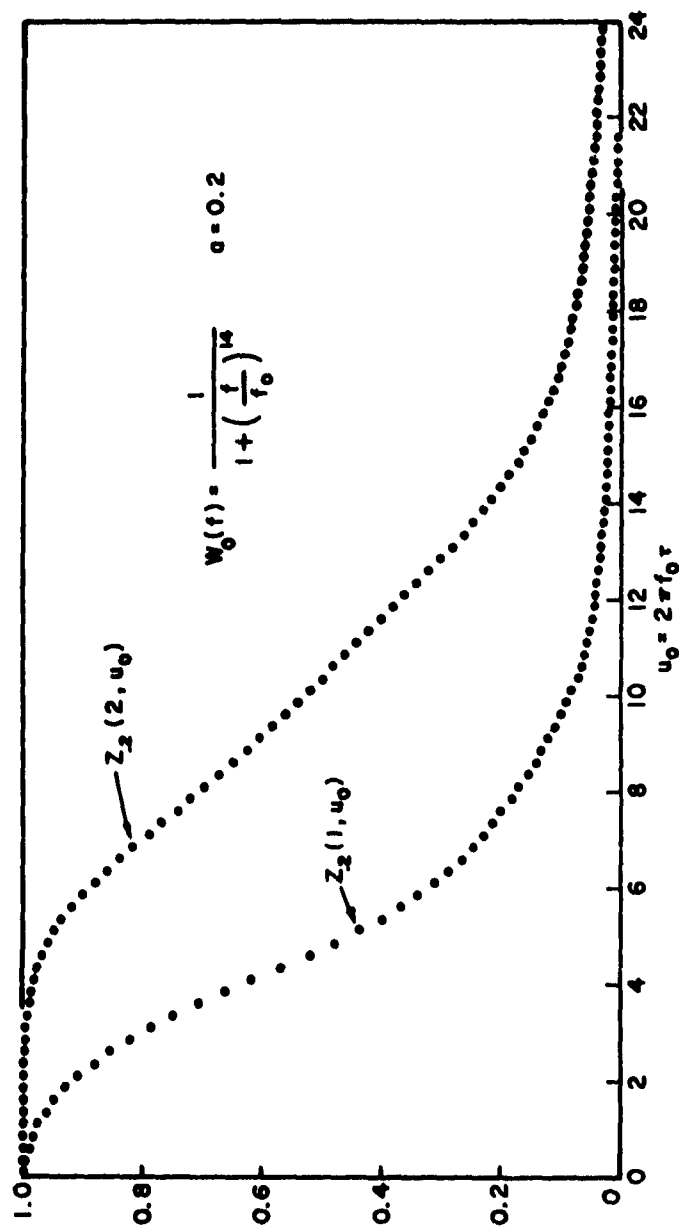


Figure 41 A Random Process Consisting of a Sine Wave of Frequency  $f_0/2$  Plus Gaussian Noise Having the Power Spectral Density  $W(f)$  Defines  $Z(n, u_0)$ , the Conditional Probability that the  $n$ th Zero-Crossing Point in  $du_0^2$  Occurs After the Time  $du_0 + u_0$ . The Ratio of the Average Sine Wave Power to the Average Noise Power is Denoted by the Parameter  $a$ .

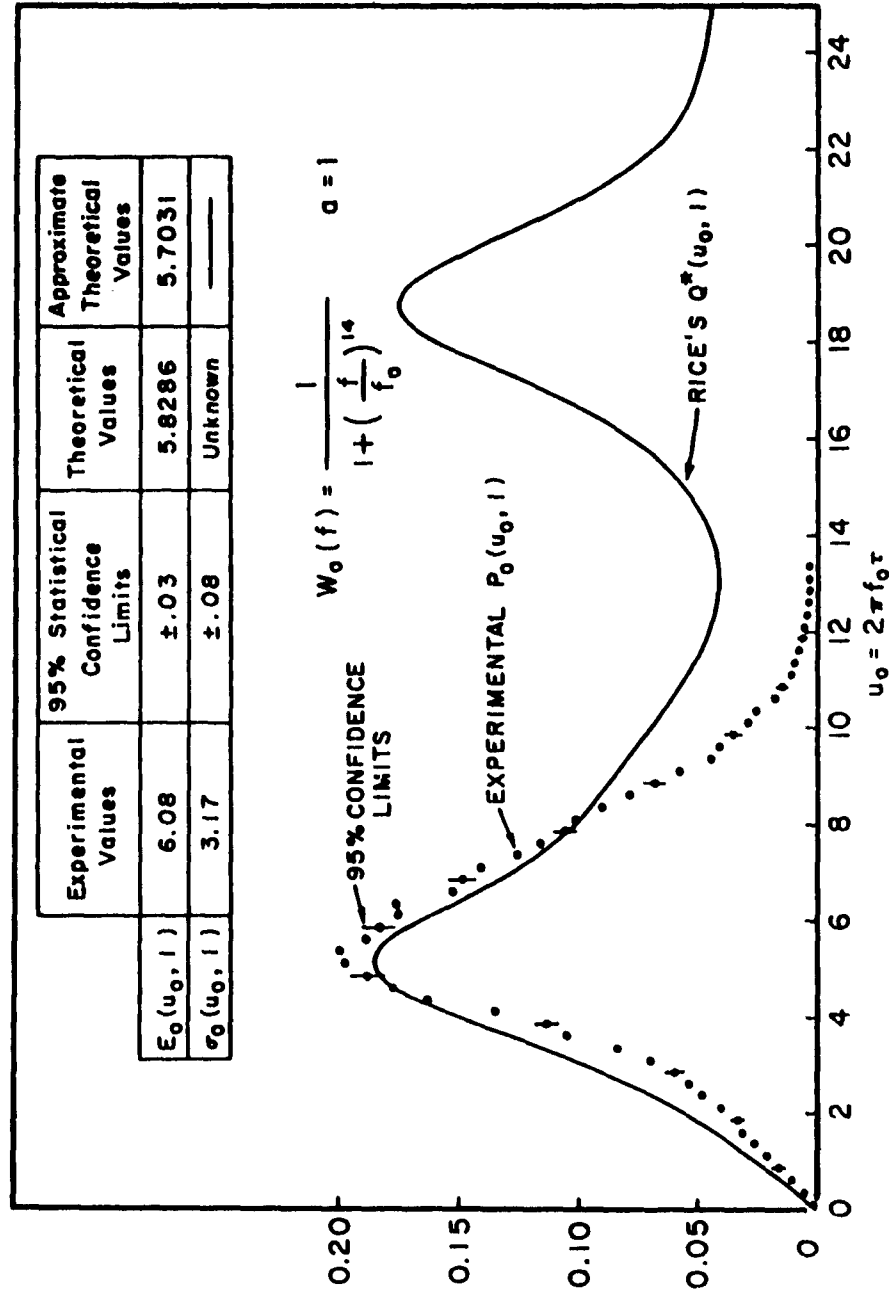


Figure 42  $P(u, a)$  is the Probability Density Function for Successive Zero-Crossing Intervals of a Random Process Consisting of a Sine Wave of Frequency  $f_0/2$  Plus Gaussian Noise Having the Power Spectral Density  $W_0(f)$ . The Ratio of the Average Sine Wave Power to the Average Noise Power is Denoted by the Parameter  $a$ . Theoretical Approximations are Compared with Experimental Results.

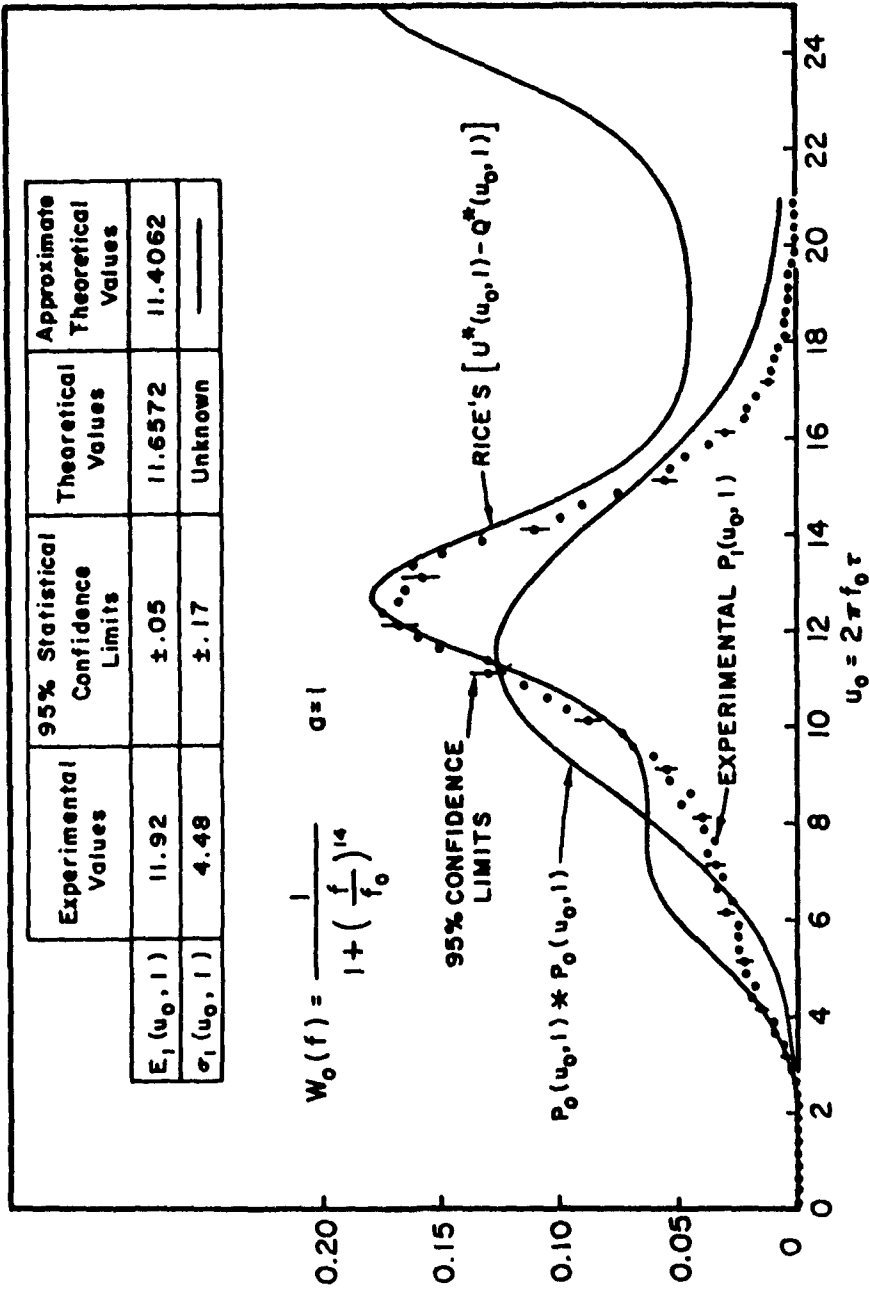


Figure 43  $P_1(u_0, a)$  is the Probability Density Function for the Sum of Two Successive Zero-Crossing Intervals of a Random Process Consisting of a Sine Wave of Frequency  $f_0/2$  Plus Gaussian Noise Having the Power Spectral Density  $W_0(f)$ . The Ratio of the Average Sine Wave Power to The Average Noise Power is Denoted by the Parameter  $a$ .



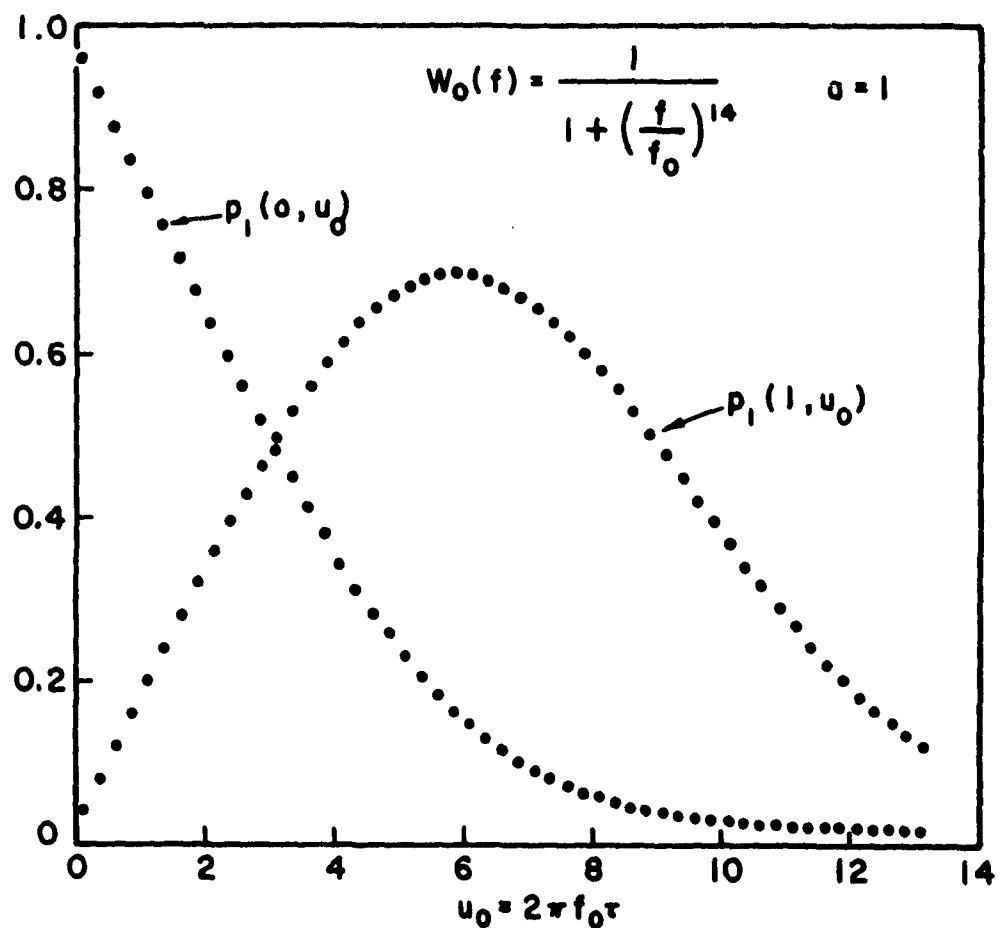


Figure 44  $p_a(n, u_0)$  is the Probability that a Given Interval  $u_0$  Contains Exactly  $n$  Zero-Crossing Points of a Random Process Consisting of a Sine Wave of Frequency  $f_0/2$  Plus Gaussian Noise Having the Power Spectral Density  $W_0(f)$ . The Ratio of the Average Sine Wave Power to the Average Noise Power is Denoted by the Parameter  $a$ .

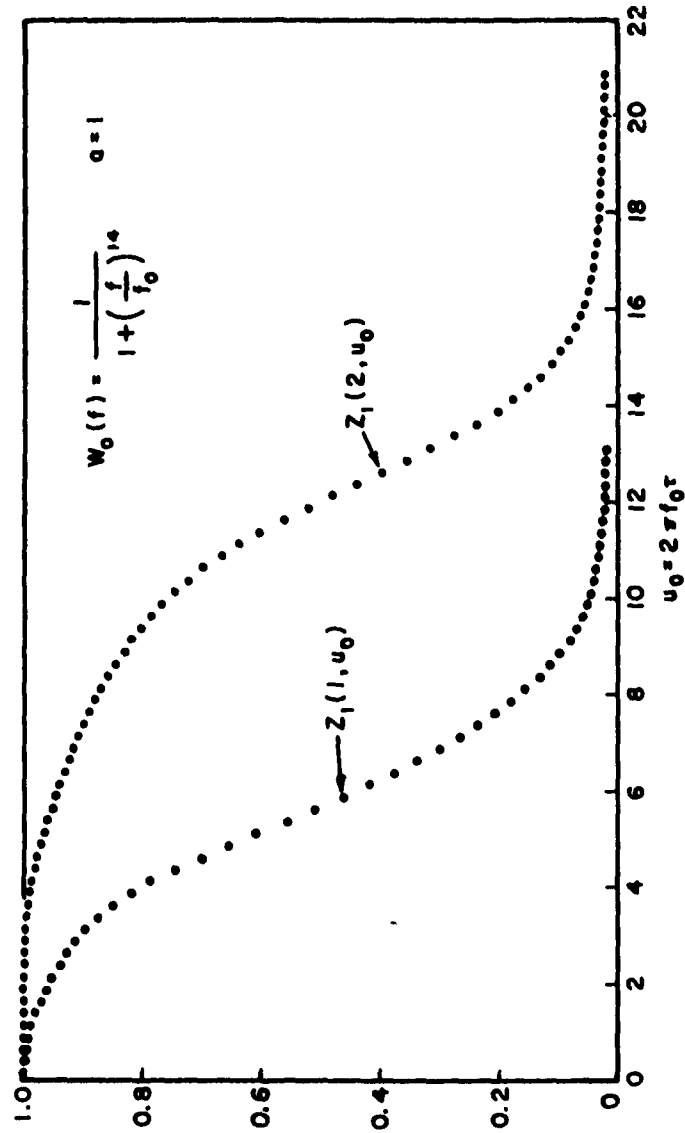


Figure 45 A Random Process Consisting of a Sine Wave of Frequency  $f/2$  Plus Gaussian Noise Having the Power Spectral Density  $W(f)$  Defines  $Z_a(n, u_0)$ , the Conditional Probability That the  $n$ th Zero-Crossing Point from a Given Zero-Crossing Point in  $du$  Occurs after the Time  $du + u_0$ . The Ratio of the Average Sine Wave Power to the Average Noise Power is Denoted by the Parameter  $a$ .

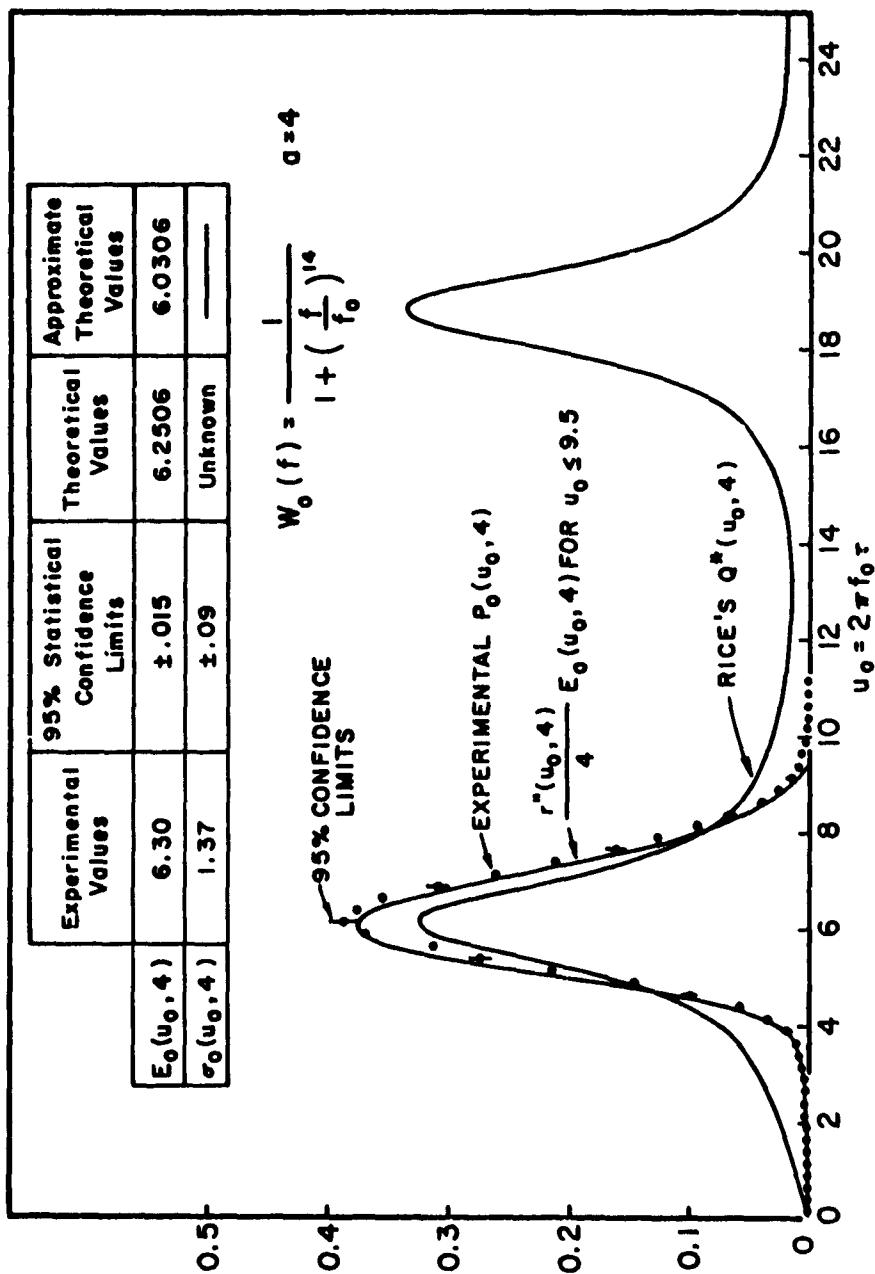


Figure 46  $P(u, a)$  is the Probability Density Function for Successive Zero-Crossing Intervals of a Random Process Consisting of a Sine Wave of Frequency  $f/2$  Plus Gaussian Noise Having the Power Spectral Density  $W_0(f)$ . The Ratio of the Average Sine Wave Power to the Average Noise Power is Denoted by the Parameter  $a$ . Theoretical Approximations are Compared with Experimental Results.

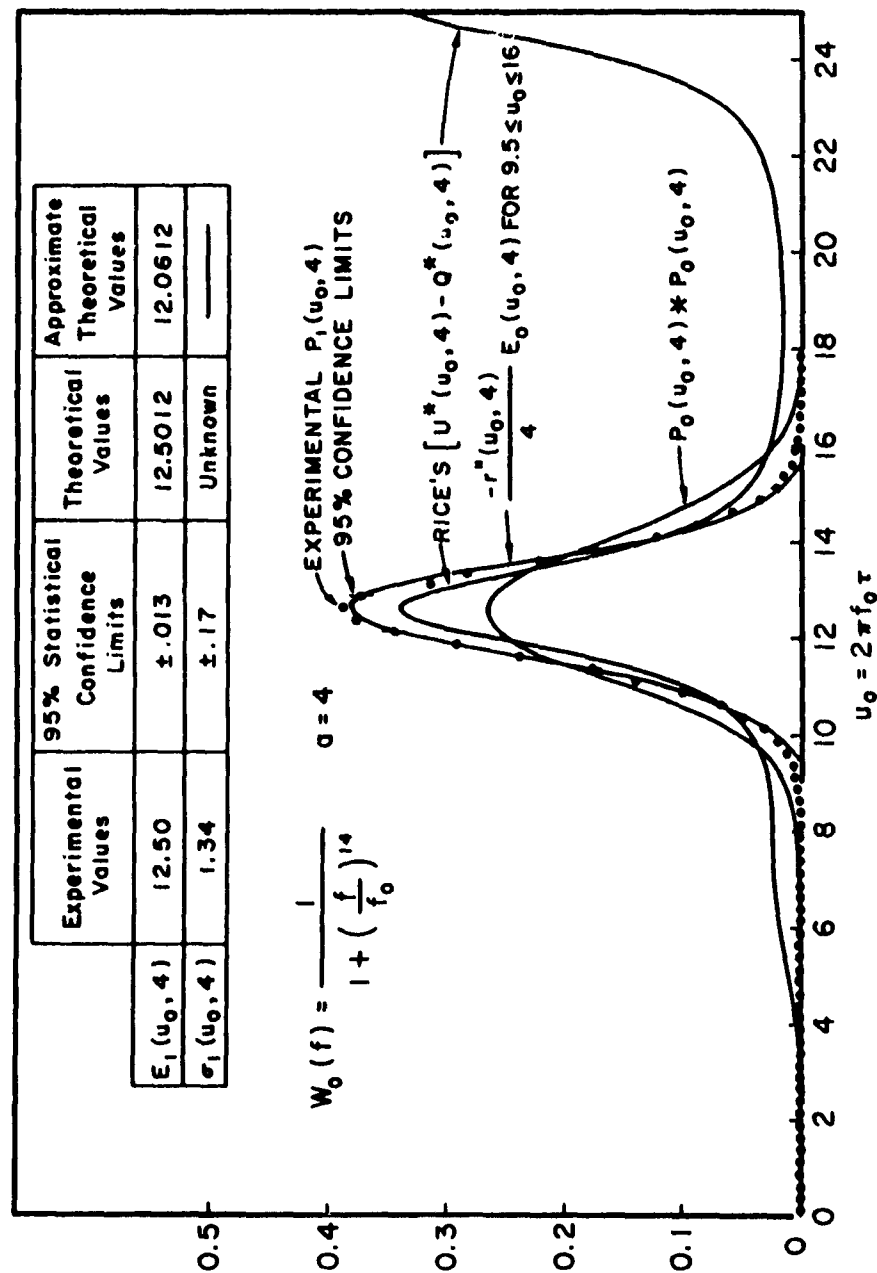


Figure 47  $P_1(u_0, a)$  is the Probability Density Function for the Sum of Two Successive Zero-Crossing Intervals of a Random Process Consisting of a Sine Wave of Frequency  $f_0/2$  Plus Gaussian Noise Having the Power Spectral Density  $W(f)$ . The Ratio of the Average Sine Wave Power to the Average Noise Power is Denoted by the Parameter  $a$ .

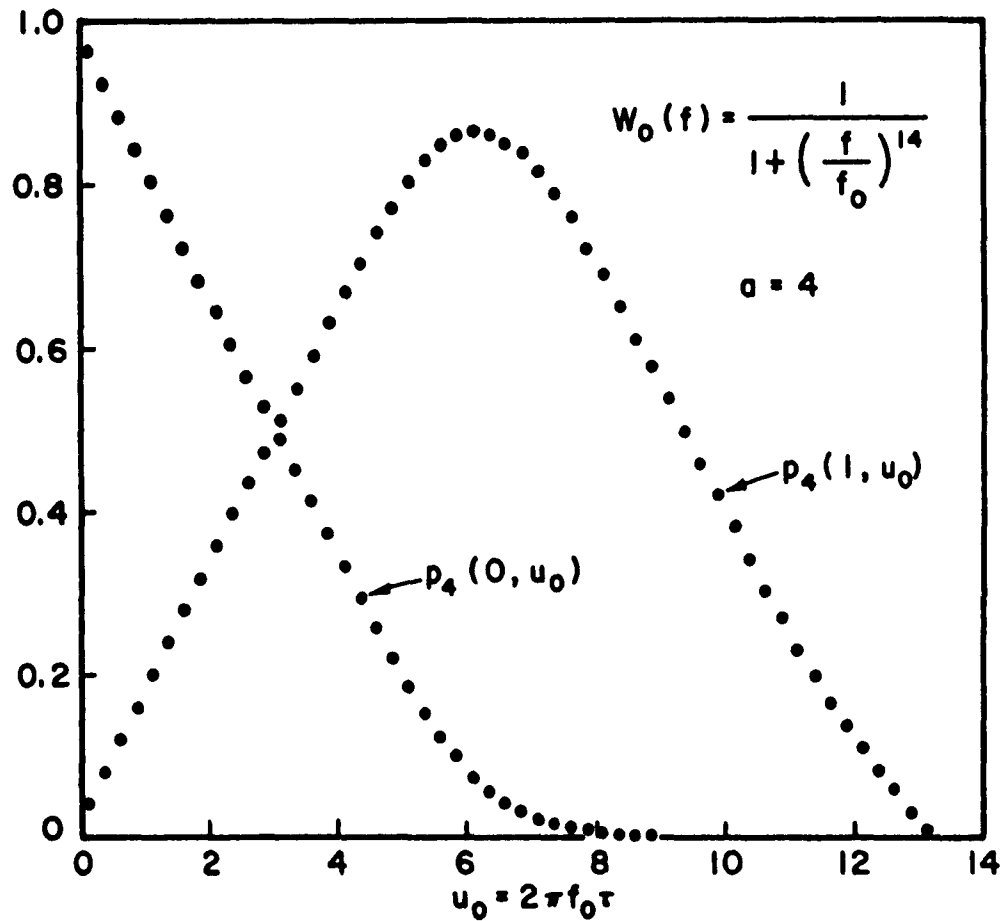


Figure 48  $p_a(n, u_0)$  is the Probability that a Given Interval  $u_0$  Contains Exactly  $n$  Zero-Crossing Points of a Random Process Consisting of a Sine Wave of Frequency  $f_0/2$  Plus Gaussian Noise Having the Power Spectral Density  $W_0(f)$ . The Ratio of the Average Sine Wave Power to the Average Noise Power is Denoted by the Parameter  $a$ .

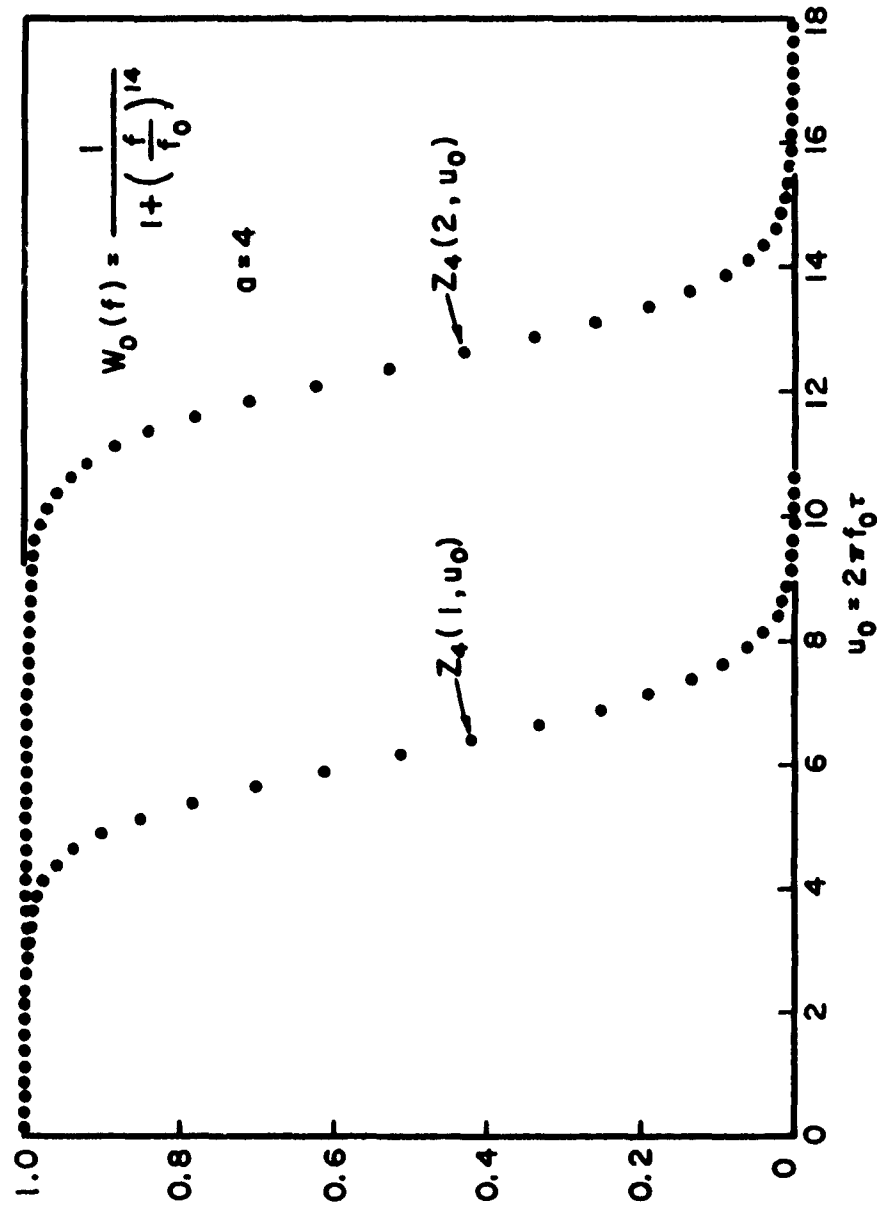


Figure 49 A Random Process Consisting of a Sine Wave of Frequency  $f_0/2$  Plus Gaussian Noise Having the Power Spectral Density  $W_0(f)$  Defines  $Z_n(n, u_0)$ , the Conditional Probability that the  $n$ th Zero-Crossing Point from a Given Zero-Crossing Point in  $du_0$  Occurs After the Time  $du_0 + u_0$ . The Ratio of the Average Sine Wave Power to the Average Noise Power is Denoted by the Parameter  $a$ .

Similarly, for small values of  $a = \frac{S}{N}$ , Rice's probability function  $U^*(u_0, a)du_0$  approximates the conditional probability that a zero of  $\xi(u, a)$  occurs between  $u+u_0$  and  $u+u_0+du_0$  given a zero of  $\xi(u, a)$  at time  $u$ . In accordance with Equation (99),  $U^*(u_0, a) - Q^*(u_0, a)$  serve as approximations to the initial behavior of  $P_1(u_0, a)$  for small " $a$ " and are presented in Figures 35, 39, 43, and 47. Notice that  $U^*(u_0, a)du_0$  is the exact conditional probability that a zero of  $\xi^*(u, a)$  occurs between  $u+u_0$  and  $u+u_0+du_0$  given a zero of  $\xi^*(u, a)$  at time  $u$ .

Figure 35, 39, 43, and 47 also compare the convolution of  $P_0(u_0, a)$  with itself,  $P_0(u_0, a)*P_0(u_0, a)$ , and  $P_1(u_0, a)$  for  $a = 0, .2, 1, 4$ . These latter comparisons serve to demonstrate that successive zero-crossing intervals of  $\xi(u, a)$  are statistically dependent.

For a general random process, McFadden (28) showed that:

$$\frac{r''(\tau)}{4\beta} = \sum_{n=0}^{\infty} (-1)^n P_n(\tau) \quad (105)$$

$r''(\tau)$  is the second derivative of the normalized autocorrelation function of the infinitely clipped random process. The normalized autocorrelation function  $r(u_0, a)$ , see Appendix, for the infinitely clipped process  $\tau(u, a)$  can be computed from a general result given by Davenport (40) and Middleton (3a).

Figure 46 compares the experimental  $P_0(u_0, 4)$  with a first portion of  $\frac{r''(u_0, 4)}{4} E_0(u_0, 4)$  in accordance with Equation (105).

The comparison is excellent. Figure 47 compares the experimental  $P_1(u_0, 4)$  with a second portion of  $\frac{r''(u_0, 4)}{4} E_0(u_0, 4)$  in accordance with Equation (105). Again, the comparison is excellent.



# VIII. PROBABILITIES AND PROBABILITY DENSITIES DEFINED BY THE STATIONARY POINTS OF A SINE WAVE PLUS A GAUSSIAN PROCESS

Probabilities and probability densities defined by the mathematical stationary points of the random process  $\xi(u, a)$ , defined by Equation (82), are presented in Figures 50 thru 65. For small values of  $a = \frac{S}{N}$ , the random process

$$\eta(u, a) = \frac{d\xi(u, a)}{du} \quad (106)$$

is approximately Gaussian with normalized autocorrelation function,  $R_\eta(u_0, a)$ , given by Equation (76). Accordingly, Rice's probability function  $Q_\eta^*(u_0, a) du_0$  approximates the conditional probability that a downward zero-crossing of  $\eta(u, a)$  occurs between  $u + u_0$  and  $u + u_0 + du_0$ , given an upward zero-crossing of  $\eta(u, a)$  at time  $u$ . In accordance with Equation (98),  $Q_\eta^*(u_0, a)$  serve as approximations to the initial behavior of  $M_0(u_0, a)$  for small "a" and are presented in Figures 50, 54, 58, 62. Notice that  $Q_\eta^*(u_0, a) du_0$  is the exact conditional probability that a downward zero-crossing of

$$\eta^*(u, a) = \frac{d\xi^*(u, a)}{du} \quad (107)$$

occurs between  $u + u_0$  and  $u + u_0 + du_0$ , given an upward zero-crossing of  $\eta^*(u, a)$  at time  $u$ .

Similarly, for small values of  $a = \frac{S}{N}$ , Rice's probability function  $U_\eta^*(u_0, a) du_0$  approximates the initial behavior of the

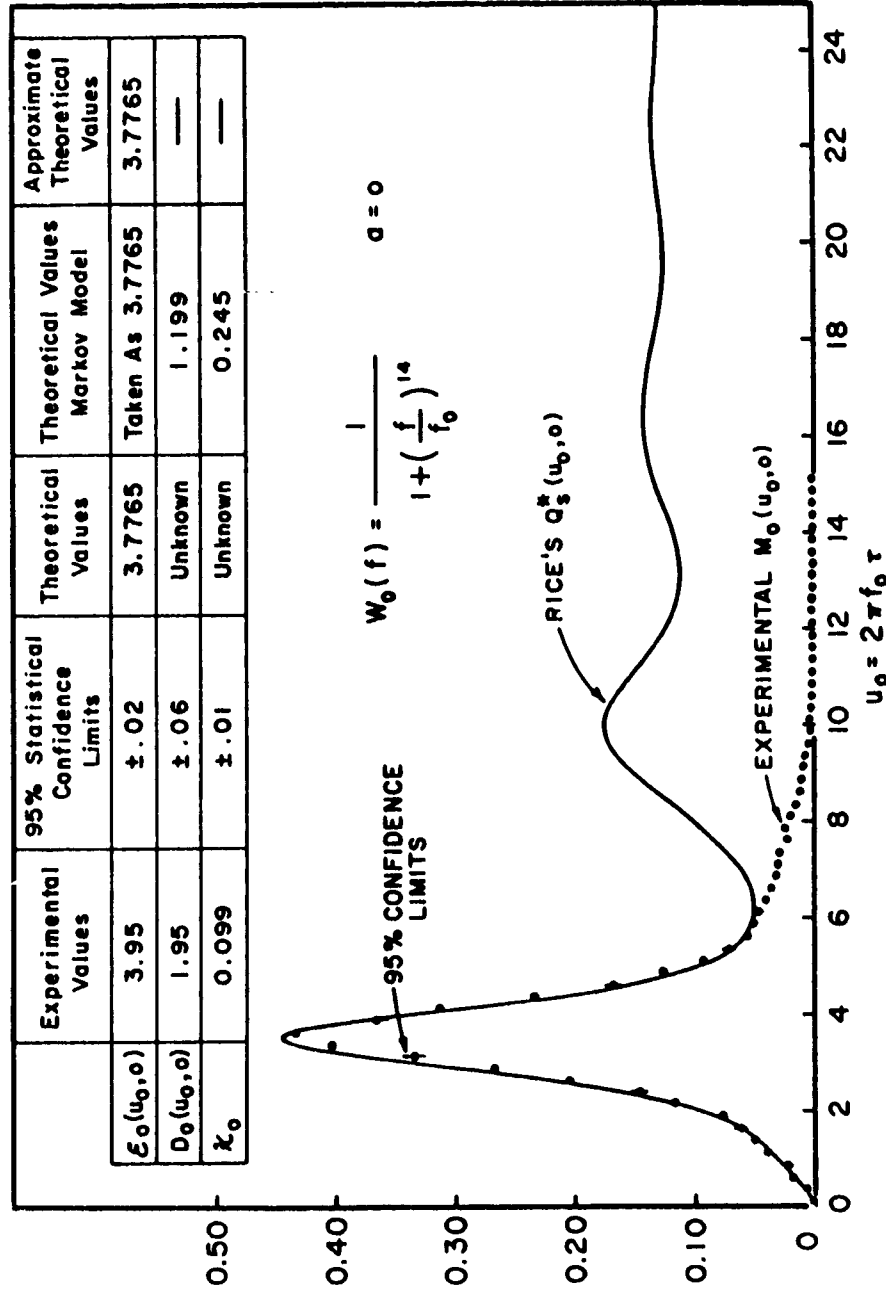


Figure 50  $M_0(u_0, a)$  is the Probability Density Function for Successive Intervals Defined by Adjacent Stationary Points of a Random Process Consisting of a Sine Wave of Frequency  $f_0/2$  Plus Gaussian Noise Having the Power Spectral Density  $W_0(f)$ . The Ratio of the Average Sine Wave Power to the Average Noise Power is Denoted by the Parameter  $a$ . Theoretical Approximations are Compared with Experimental Results.

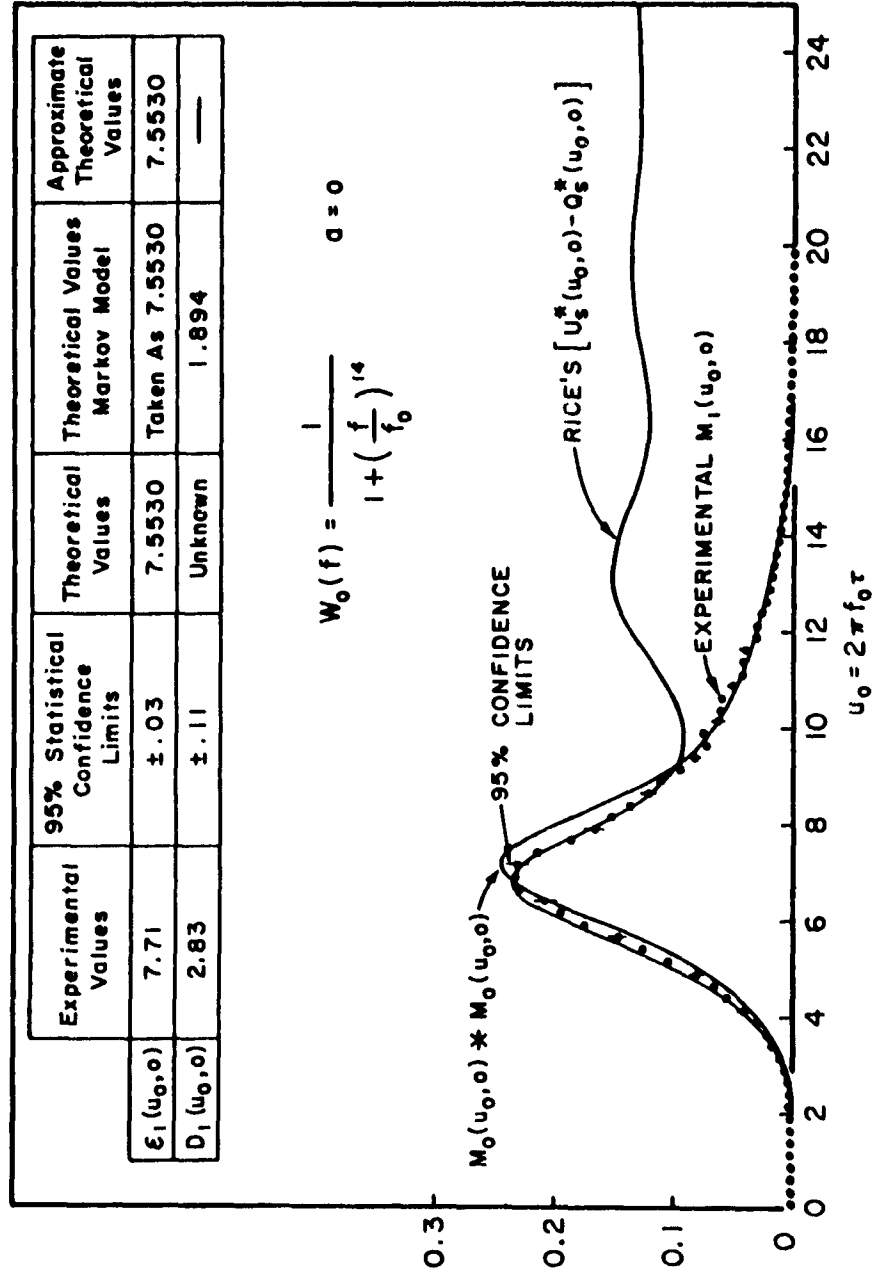


Figure 51  $M_1(u_0, a)$  is the Probability Density Function for the Sum of Two Successive Intervals Defined by Adjacent Stationary Points of a Random Process Consisting of a Sine Wave of Frequency  $f_0/2$  Plus Gaussian Noise Having the Power Spectral Density  $W_0(f)$ . The Ratio of the Average Sine Wave Power to the Average Noise Power is Denoted by the Parameter  $a$ .

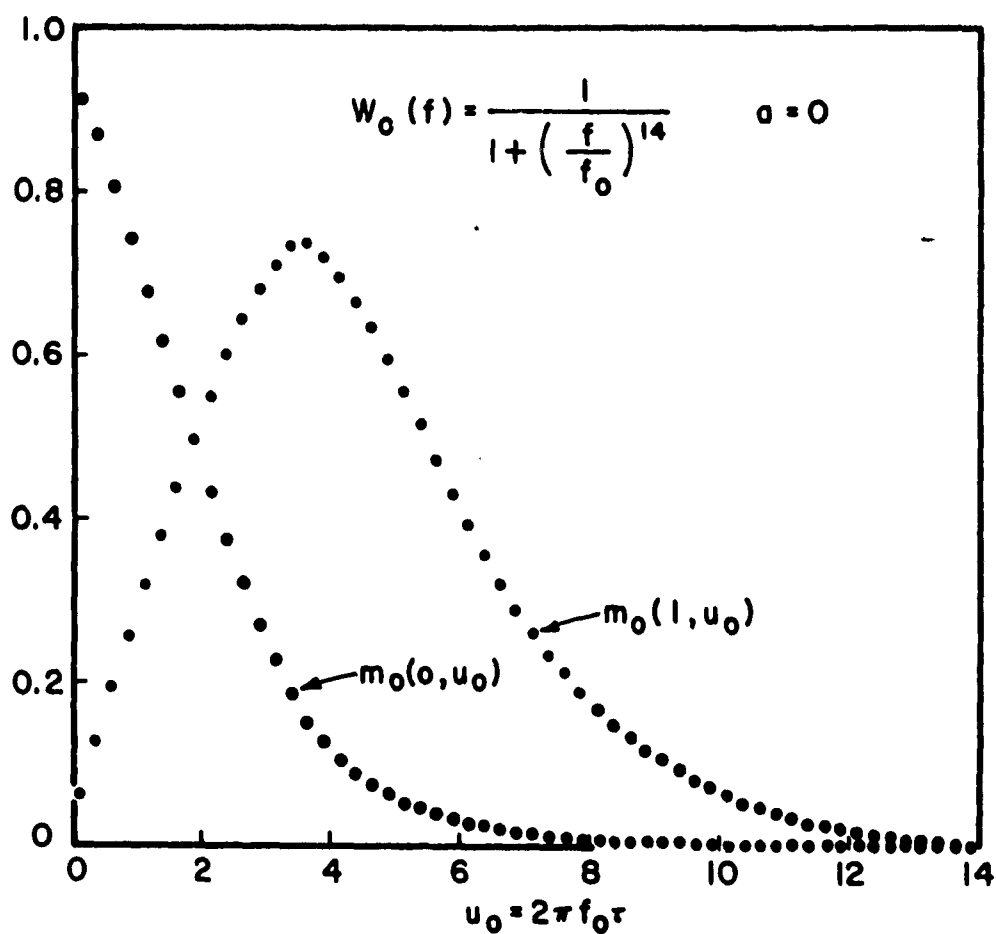


Figure 53  $m_0(n, u_0)$  is the Probability that a Given Interval  $u_0$  Contains Exactly  $n$  Stationary Points of a Random Process Consisting of a Sine Wave of Frequency  $f_0/2$  Plus Gaussian Noise Having the Power Spectral Density  $W_0(f)$ . The Ratio of the Average Sine Wave Power to the Average Noise Power is Denoted by the Parameter  $a$ .

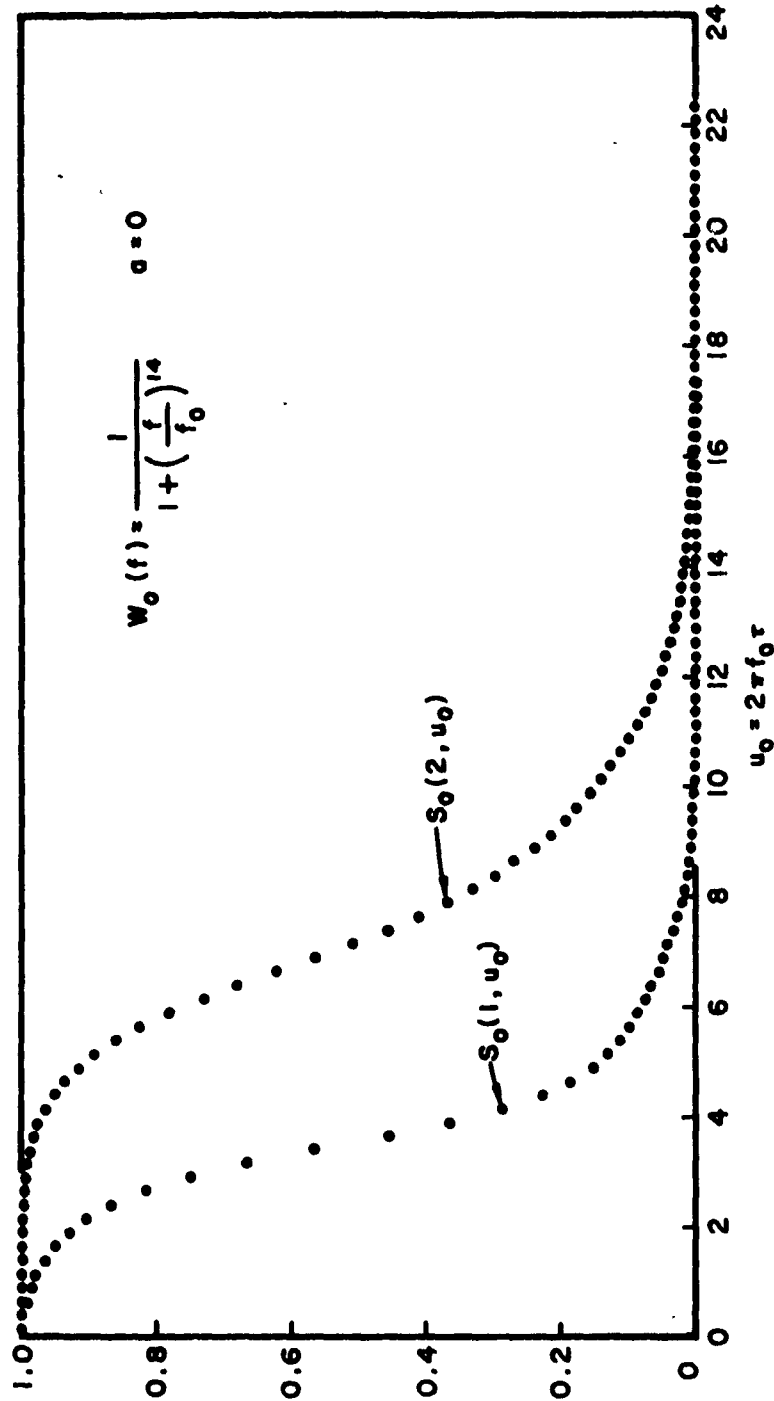


Figure 53 A Random Process Consisting of a Sine Wave of Frequency  $f_0/2$  Plus Gaussian Noise Having the Power Spectral Density  $W_0(f)$  Defines  $S_0(n, u_0)$ , the Conditional Probability that the  $n$ th Stationary Point from a Given Stationary Point in  $du$  Occurs After the Time  $du + u_0$ . The Ratio of the Average Sine Wave Power to the Average Noise Power is Denoted by the Parameter  $a$ .

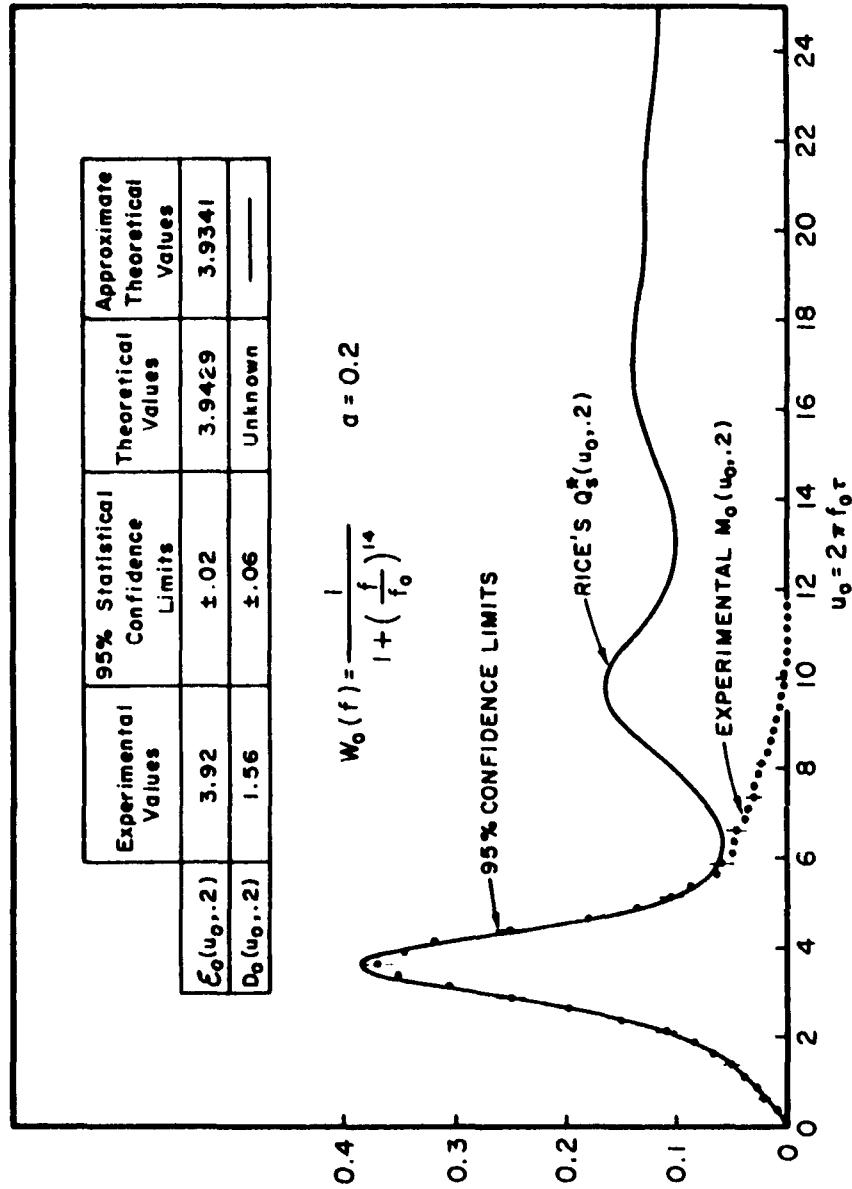


Figure 54  $M(u_0, a)$  is the Probability Density Function for Successive Intervals Defined by Adjacent Stationary Points of a Random Process Consisting of a Sine Wave of Frequency  $f/2$  Plus Gaussian Noise Having the Power Spectral Density  $W(f)$ . The Ratio of The Average Sine Wave Power to the Average Noise Power is Denoted by the Parameter  $a$ . Theoretical Approximations are Compared with Experimental Results.

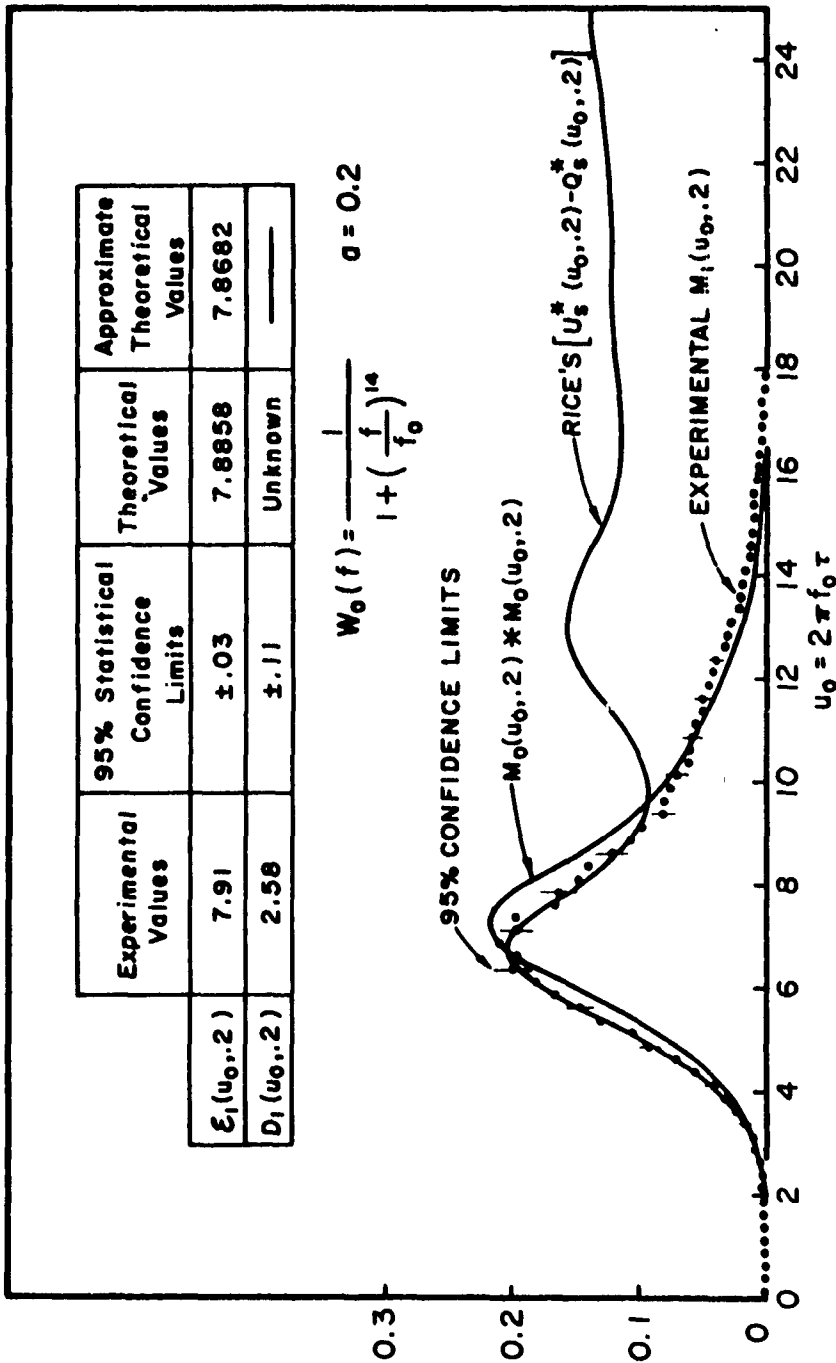


Figure 55  $M_1(u_0, a)$  is the Probability Density Function for the Sum of Two Successive Intervals Defined by Adjacent Stationary Points of a Random Process Consisting of A Sine Wave of Frequency  $f_0/2$  Plus Gaussian Noise Having the Power Spectral Density  $W(f)$ . The Ratio of the Average Sine Wave Power to the Average Noise Power is Denoted by the Parameter  $a$ .

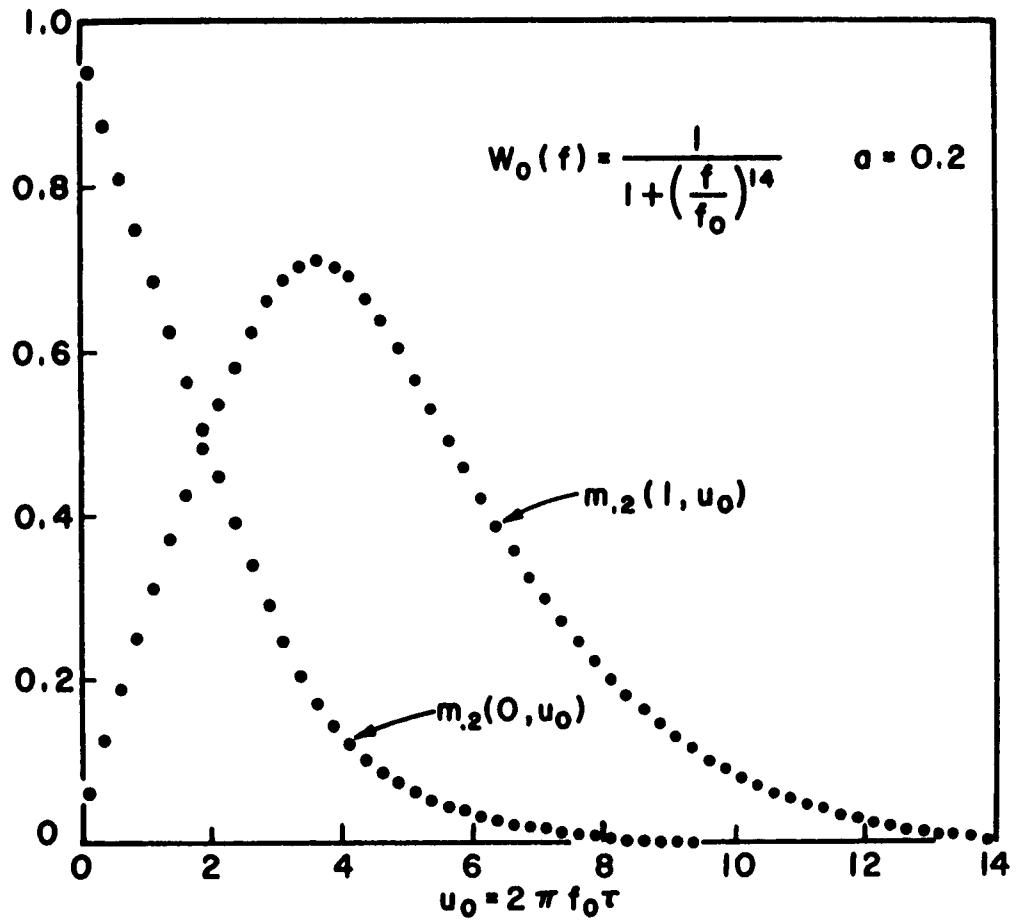


Figure 56  $m_2(n, u_0)$  is the Probability That a Given Interval  $u_0$  Contains Exactly  $n$  Stationary Points of a Random Process Consisting of a Sine Wave of Frequency  $f_0/2$  Plus Gaussian Noise Having the Power Spectral Density  $W_0(f)$ . The Ratio of the Average Sine Wave Power to the Average Noise Power is Denoted by the Parameter  $a$ .



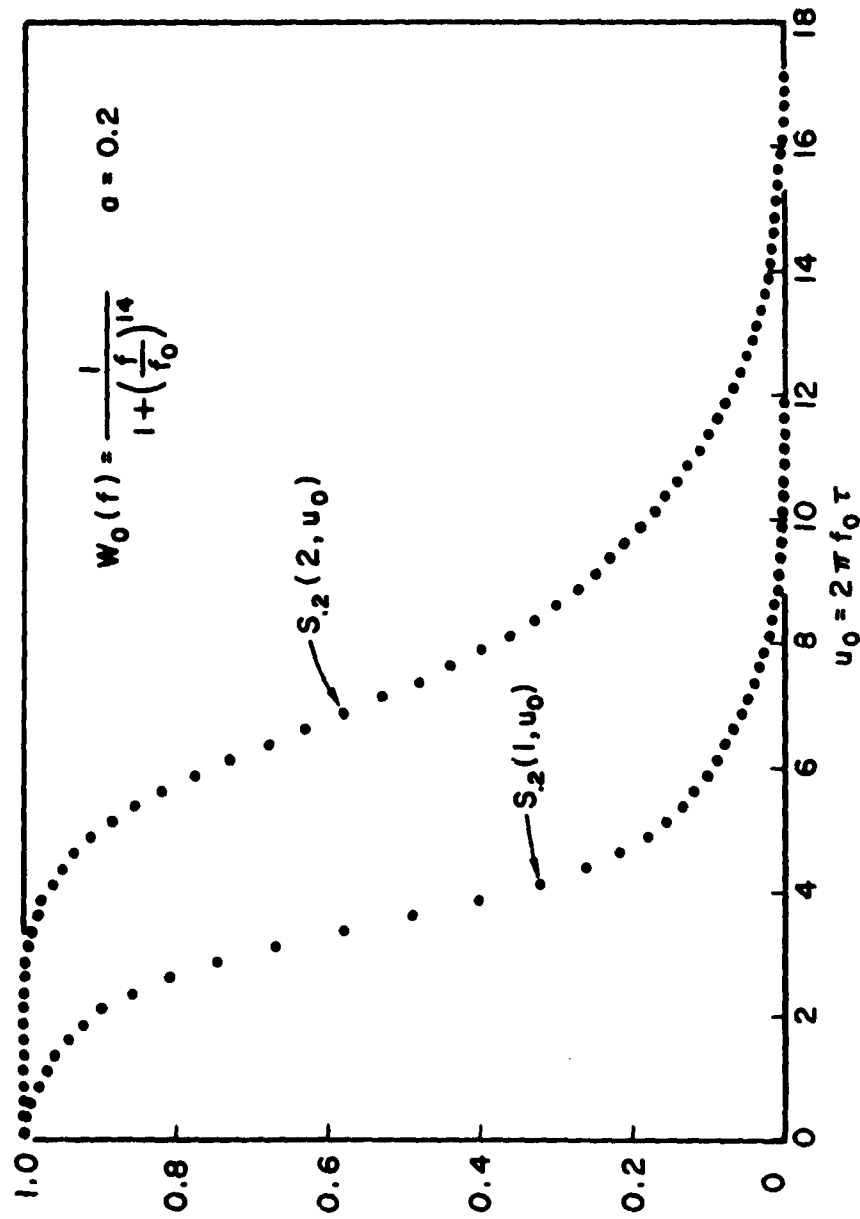


Figure 57 A Random Process Consisting of a Sine Wave of Frequency  $f_0/2$  Plus Gaussian Noise Having the Power Spectral Density  $W_0(f)$  Defines  $S_2(n, u_0)$ , the Conditional Probability that the  $n$ th Stationary Point from a Given Stationary Point in  $du_0$  Occurs after the Time  $du_0 + u_0$ . The Ratio of the Average Sine Wave Power to the Average Noise Power is Denoted by the Parameter  $\alpha$ .

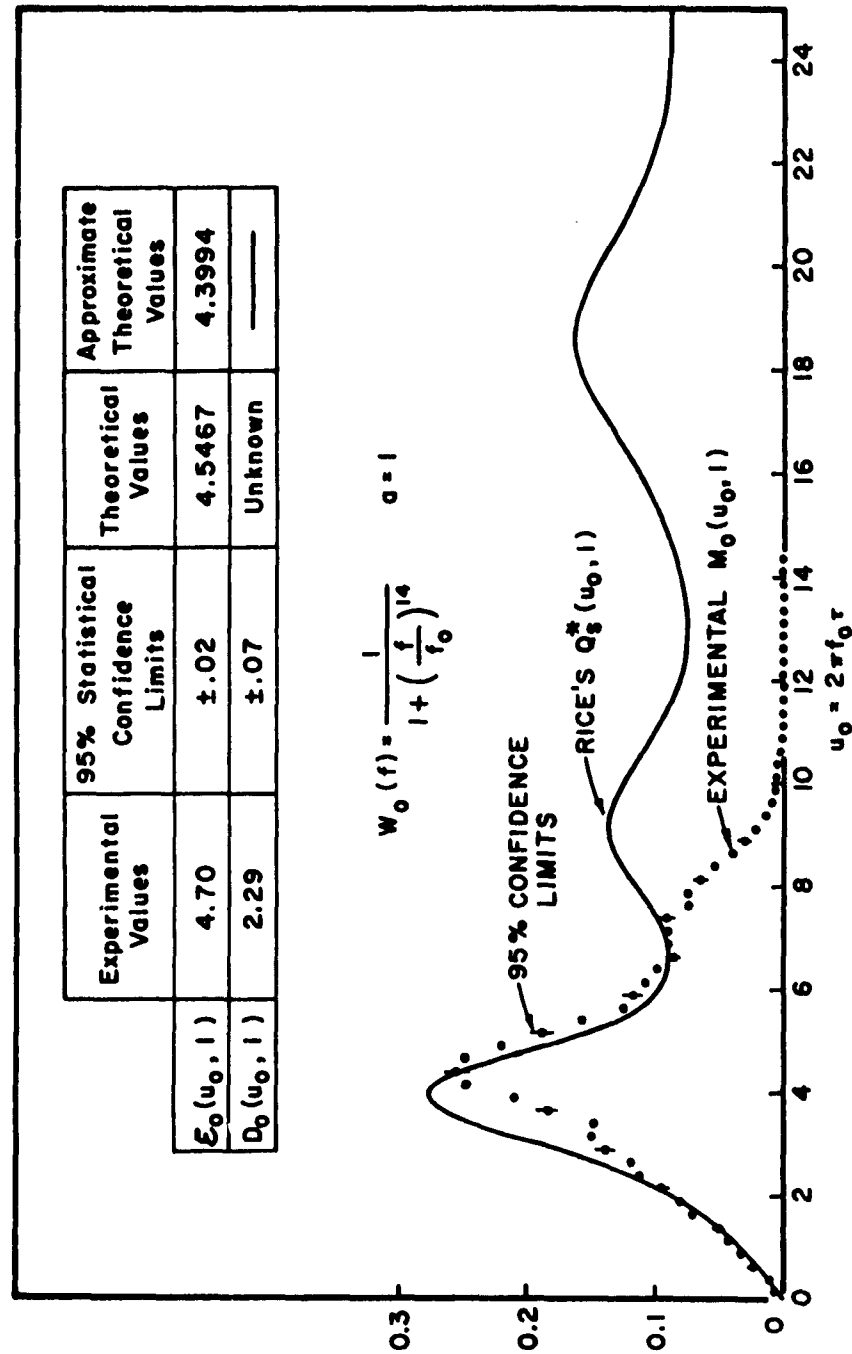


Figure 58  $M_0(u_0, a)$  is the Probability Density Function for Successive Intervals Defined by Adjacent Stationary Points of a Random Process Consisting of a Sine Wave of Frequency  $f_0/2$  Plus Gaussian Noise Having the Power Spectral Density  $W_0(f)$ . The Ratio of the Average Sine Wave Power to the Average Noise Power is Denoted by the Parameter  $a$ . Theoretical Approximations are Compared with Experimental Results.

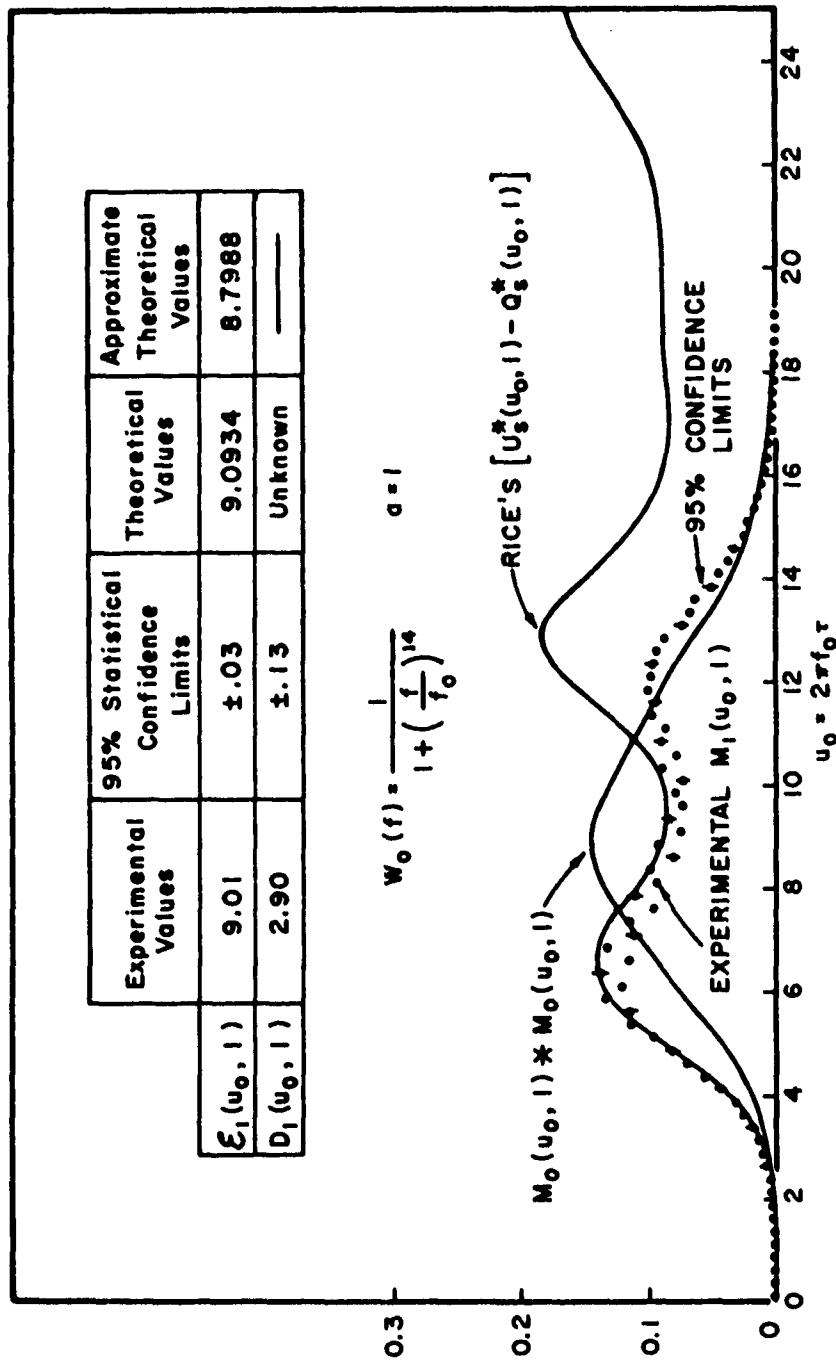


Figure 59  $M_1(u_0, a)$  is the Probability Density Function for the Sum of Two Successive Intervals Defined by Adjacent Stationary Points of a Random Process Consisting of a Sine Wave of Frequency  $f_0/2$  Plus Gaussian Noise Having the Power Spectral Density  $W_0(f)$ . The Ratio of the Average Sine Wave Power to the Average Noise Power is Denoted by the Parameter  $a$ .

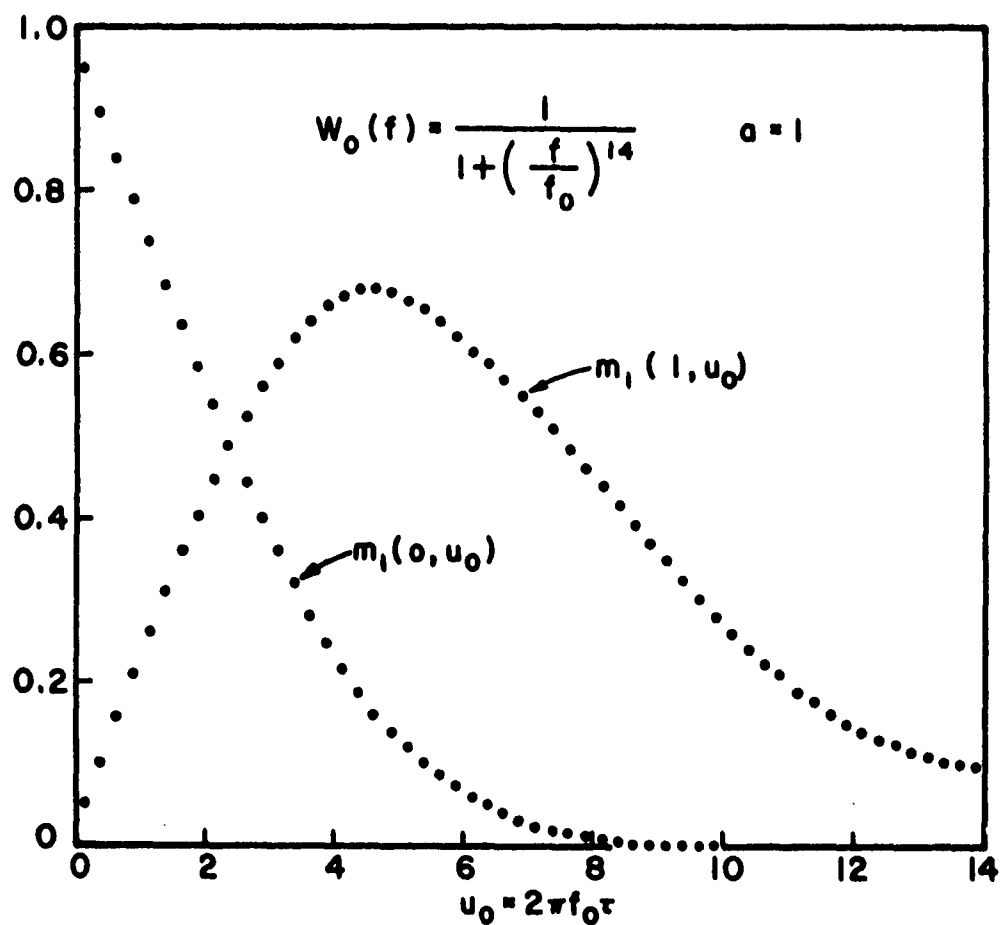


Figure 60  $m_n(n, u)$  is the Probability that a Given Interval  $u_0$  Contains Exactly  $n$  Stationary Points of a Random Process Consisting of a Sine Wave of Frequency  $f_0/2$  Plus Gaussian Noise Having the Power Spectral Density  $W_0(f)$ . The Ratio of the Average Sine Wave Power to the Average Noise Power is Denoted by the Parameter  $a$ .

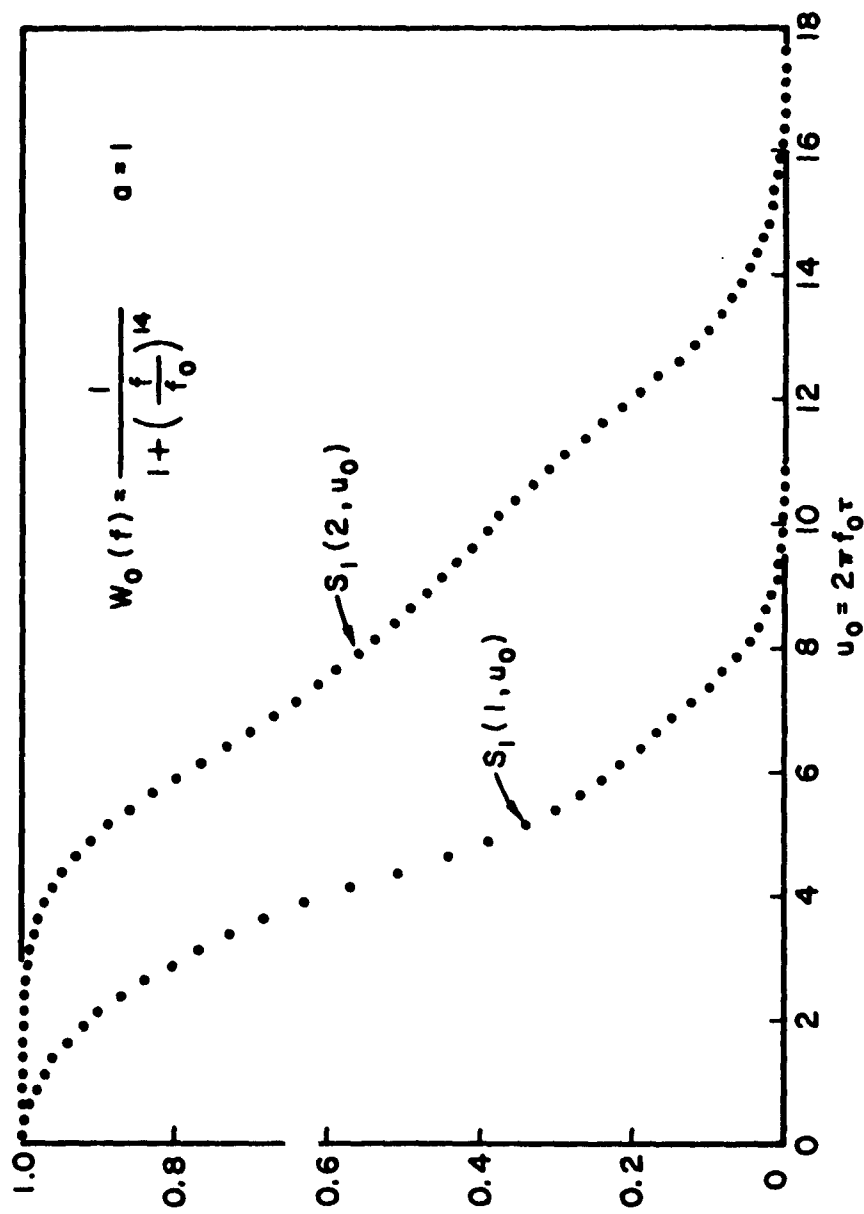


Figure 61 A Random Process Consisting of a Sine Wave of Frequency  $f_0/2$  Plus Gaussian Noise Having the Power Spectral Density  $W_0(f)$  Defines  $S_a(n, u_0)$ , the Conditional Probability that the  $n$ th Stationary Point from a Given Stationary Point in  $du_0$  Occurs After the Time  $du_0 + u_0$ . The Ratio of the Average Sine Wave Power to the Average Noise Power is Denoted by the Parameter  $a$ .

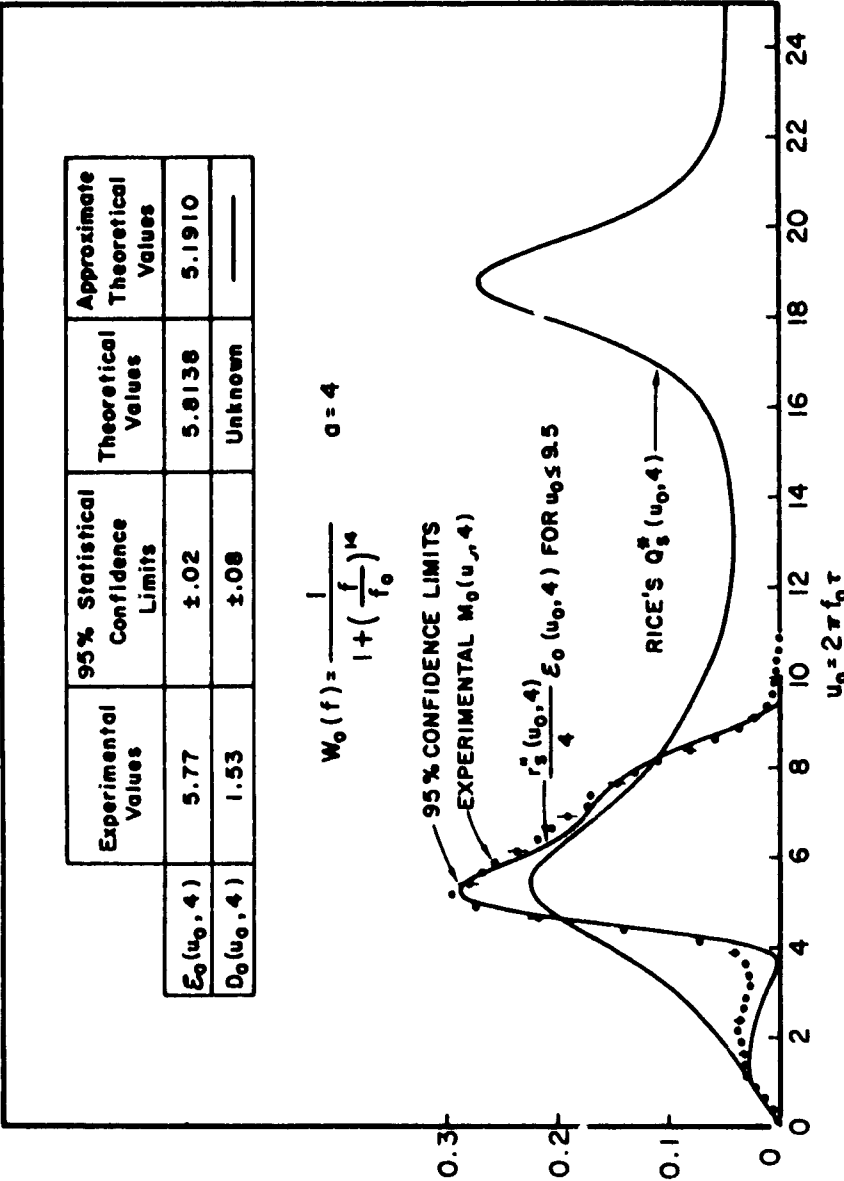


Figure 62:  $M_0(u_0, a)$  is the Probability Density Function for Successive Intervals Defined by Adjacent Stationary Points of a Random Process Consisting of a Sine Wave of Frequency  $f_0/2$  Plus Gaussian Noise Having the Power Spectral Density  $W_0(f)$ . The Ratio of the Average Sine Wave Power to the Average Noise Power is Denoted by the Parameter  $a$ . Theoretical Approximations are Compared with Experimental Results.

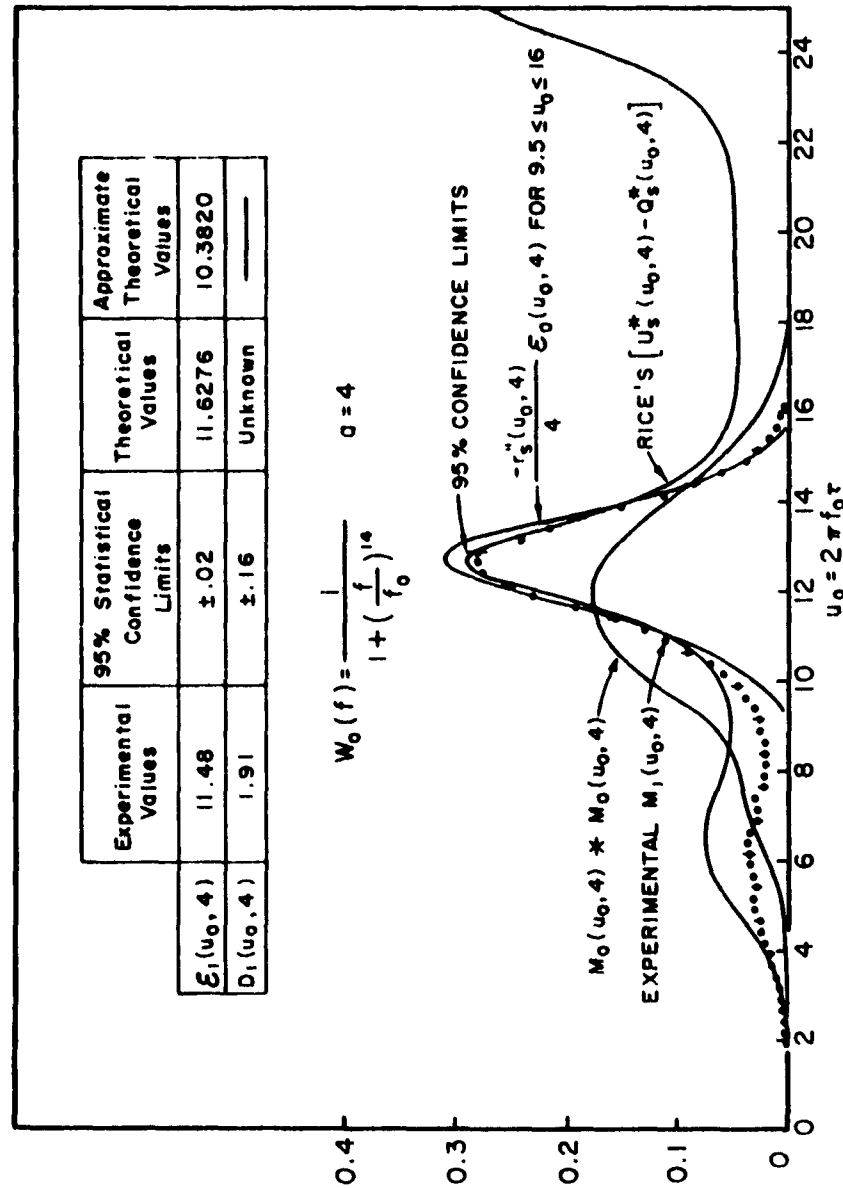


Figure 63  $M_1(u_0, a)$  is the Probability Density Function for the Sum of Two Successive Intervals Defined by Adjacent Stationary Points of a Random Process Consisting of a Sine Wave of Frequency  $f_0/2$  Plus Gaussian Noise Having the Power Spectral Density  $W_0(f)$ . The Ratio of the Average Sine Wave Power to the Average Noise Power is Denoted by the Parameter  $a$ .

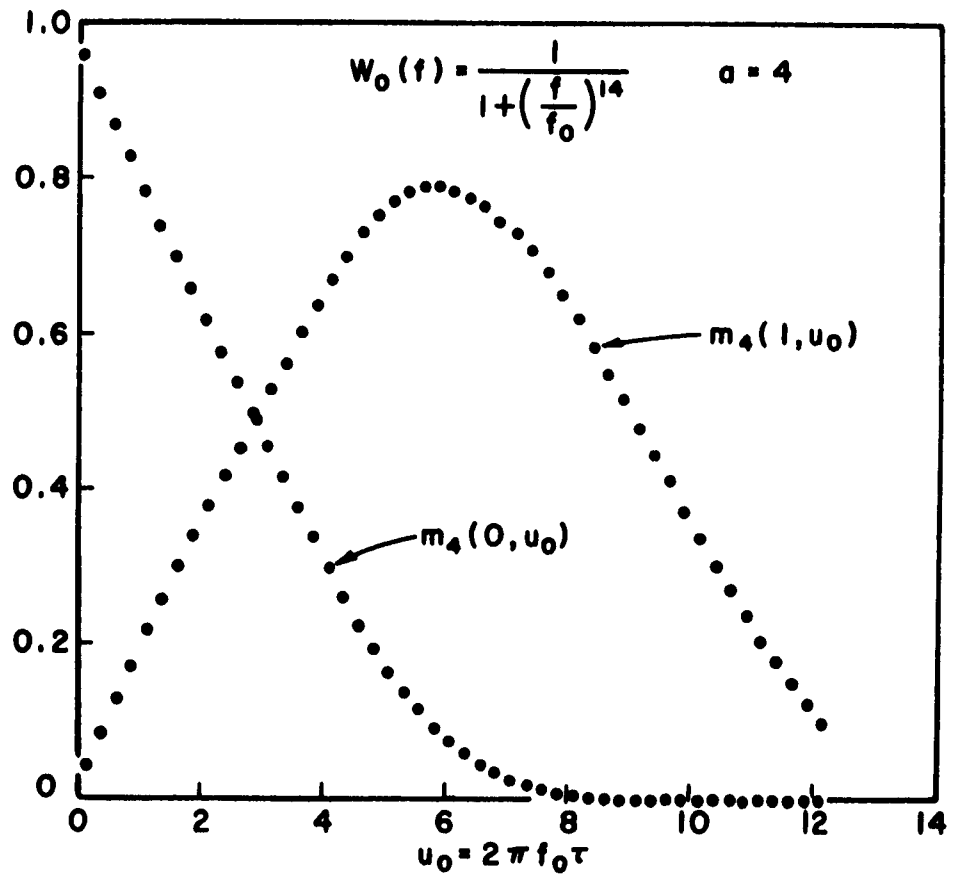


Figure 64  $m_p(n, u_0)$  is the Probability that a Given Interval  $u_0$  Contains Exactly  $n$  Stationary Points of a Random Process Consisting of a Sine Wave of Frequency  $f_0/2$  Plus Gaussian Noise Having the Power Spectral Density  $W_0(f)$ . The Ratio of the Average Sine Wave Power to the Average Noise Power is Denoted by the Parameter  $a$ .



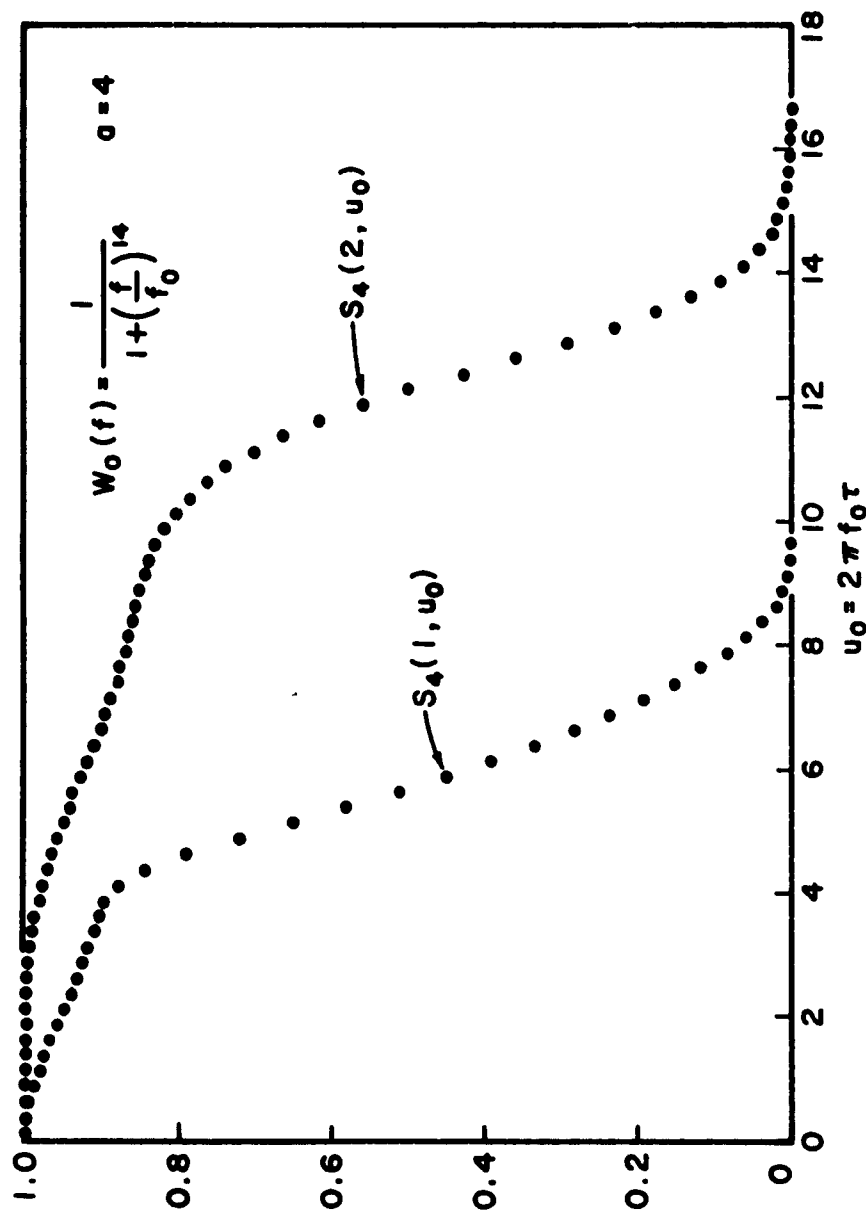


Figure 65 A Random Process Consisting of a Sine Wave of Frequency  $f_0/2$  Plus Gaussian Wave of Frequency  $f_0/2$  Plus Gaussian Noise Having the Power Spectral Density  $W_0(f)$  Defines  $S_4(n, u_0)$ . The Conditional Probability that the  $n$ th Stationary Point from a Given Stationary Point in  $du_0$  Occurs After the Time  $du_0$ . The Ratio of the Average Sine Wave Power to the Average Noise Power is Denoted by the Parameter  $a$ .

conditional probability that a stationary point of  $\xi(u, a)$  occurs between  $u + u_0$  and  $u + u_0 + du_0$  given a stationary point of  $\xi(u, a)$  at time  $u$ . In accordance with Equation (99),  $U_s^*(u_0, a) - Q_s^*(u_0, a)$  serve as approximations to the initial behavior of  $M_1(u_0, a)$  for small " $a$ " and are presented in Figures 51, 55, 59, and 63. Notice that  $U_s^*(u_0, a)du_0$  is the exact conditional probability that a stationary point of  $\xi^*(u, a)$  occurs between  $u + u_0$  and  $u + u_0 + du_0$  given a stationary point of  $\xi^*(u, a)$  at time  $u$ .

Figures 51, 55, 59, and 63 also compare the convolution of  $M_0(u_0, a)$  with itself,  $M_0(u_0, a) * M_0(u_0, a)$ , and  $M_1(u_0, a)$  for  $a = 0, .2, 1, 4$ . These comparisons serve to demonstrate that two successive intervals defined by the adjacent stationary points of  $\xi(u, a)$  are statistically dependent.

The normalized autocorrelation function  $r_s(u_0, a)$ , see Appendix, for the infinitely clipped process  $\eta(u, a)$  can be computed by applying the transformation associated with the ideal differentiator operator to the general result given by Davenport and Middleton.

Figure 62 compares the experimental  $M_0(u_0, 4)$  with a first portion of  $\frac{r_s''(u_0, a)}{4} \mathcal{E}_0(u_0, 4)$  in accordance with Equation (105). The comparison is satisfactory.

Figure 63 compares the experimental  $M_1(u_0, 4)$  with a second portion of  $\frac{r_s'''(u_0, a)}{4} \mathcal{E}_0(u_0, 4)$  in accordance with Equation (105). Again, the comparison is satisfactory.

# IX. STATISTICAL DEPENDENCE OF ZERO-CROSSING INTERVALS

The recent work of Longuet-Higgins (8) leads one to the following important theorem.

Theorem: If  $\xi(t)$  is a Gaussian process having a finite expected number of zeros per unit time, then the sum of  $(m+1)$  successive zero-crossing intervals of  $\xi(t)$  and the sum of the next  $(n+1)$  successive zero-crossing intervals  $\xi(t)$  are statistically dependent for all nonnegative integral  $m, n$ .

Proof:

For Gaussian processes having power spectral densities with asymptotic behavior  $f^{-4}$  (the singular case), Longuet-Higgins showed that  $P_l(\tau)$ , the probability density function for the sum of  $(l + 1)$  successive zero-crossing intervals, tends to a positive value as  $\tau \rightarrow 0$ . Accordingly,

$$\lim_{\tau \rightarrow 0} P_{m+n+1}(\tau) \neq \lim_{\tau \rightarrow 0} P_m(\tau) * P_n(\tau) \equiv \lim_{\tau \rightarrow 0} \int_0^\tau P_m(l) P_n(\tau-l) dl = 0 \quad (108)$$

This completes the proof of the theorem for the singular case.

For Gaussian processes having power spectral densities with asymptotic behavior other than  $f^{-4}$  (the regular case), Longuet-Higgins showed that

$$P_m(\tau) = O\left(\tau^{\frac{1}{2}(m+2)(m+3)-2}\right) \text{ as } \tau \rightarrow 0 \quad (109)$$

Hence, as  $\tau \rightarrow 0$

$$P_{m+n+1}(\tau) = O\left(\tau^{\frac{1}{2}(m+n+3)(m+n+4)-2}\right) \quad (110)$$

and

$$P_m(\tau) * P_n(\tau) = O\left(\tau^{\frac{1}{2}(n+2)(n+3) + \frac{1}{2}(m+2)(m+3)-3}\right) \quad (111)$$

Suppose Equations (110) and (111) were equal for some nonnegative integral  $m, n$ . Then,

$$\frac{1}{2}(m+n+3)(m+n+4)-2 = \frac{1}{2}(n+2)(n+3) + \frac{1}{2}(m+2)(m+3)-3 \quad (112)$$

and,

$$mn + m + n + 1 = 0 \quad (113)$$

Equation (113) is clearly false for all nonnegative integral  $m, n$ .

Accordingly, as  $\tau \rightarrow 0$

$$P_{m+n+1}(\tau) \neq P_m(\tau) * P_n(\tau) \quad (114)$$

This completes the proof of the theorem. For  $m = n = 0$ , the content of the theorem was given by Palmer (11) and McFadden (28).

For certain Gaussian processes, the convolutions shown in Figures 19, 27, 31, 35, and 51 verify the truth of the theorem for  $m = n = 0$ .

In order to observe the statistical dependence between the  $i$ th and  $(i+n)$ th zero-crossing intervals of a random process, two of the experimental systems described in Section IIA were used to display 5000 random samples of the  $i$ th and  $(i+n)$ th zero-crossing intervals on an oscilloscope. The skipping discussed in Section

IIA was set at 11 or 12 each with probability  $\frac{1}{2}$ . The resulting intensity pattern on the oscilloscope represents an approximation to the joint probability density of these intervals. If the intensity pattern corresponding to  $n \rightarrow \infty$  is similar to the intensity pattern corresponding to  $n = n_1$ , then one can conclude that the  $i$ th and  $(i+n_1)$ th zero-crossing intervals of a finite memory process are practically independent.

For a Gaussian process having power spectral density  $W_3(f)$ , Figure 66 illustrates the statistical dependence between the  $i$ th and  $(i+n)$ th zero-crossing intervals of the process for  $n = 1, 2, 3, 4$ , and  $\infty$ .  $n = \infty$  represents a condition such that the two zero-crossing intervals are separated by approximately 71 average zero-crossing intervals. This condition was convenient experimentally and corresponds to a one second time separation between the zero-crossing intervals. Notice the symmetry of the intensity patterns about the straight line passing through the origin with a slope of  $45^\circ$ . This symmetry results from the fact that the joint probability density of the intervals is invariant under a time reversal of the random process.

The conditional mean of the  $(i+n)$ th zero-crossing interval given the  $i$ th zero-crossing interval is found from Figure 66 by considering narrow vertical strips of the intensity patterns and

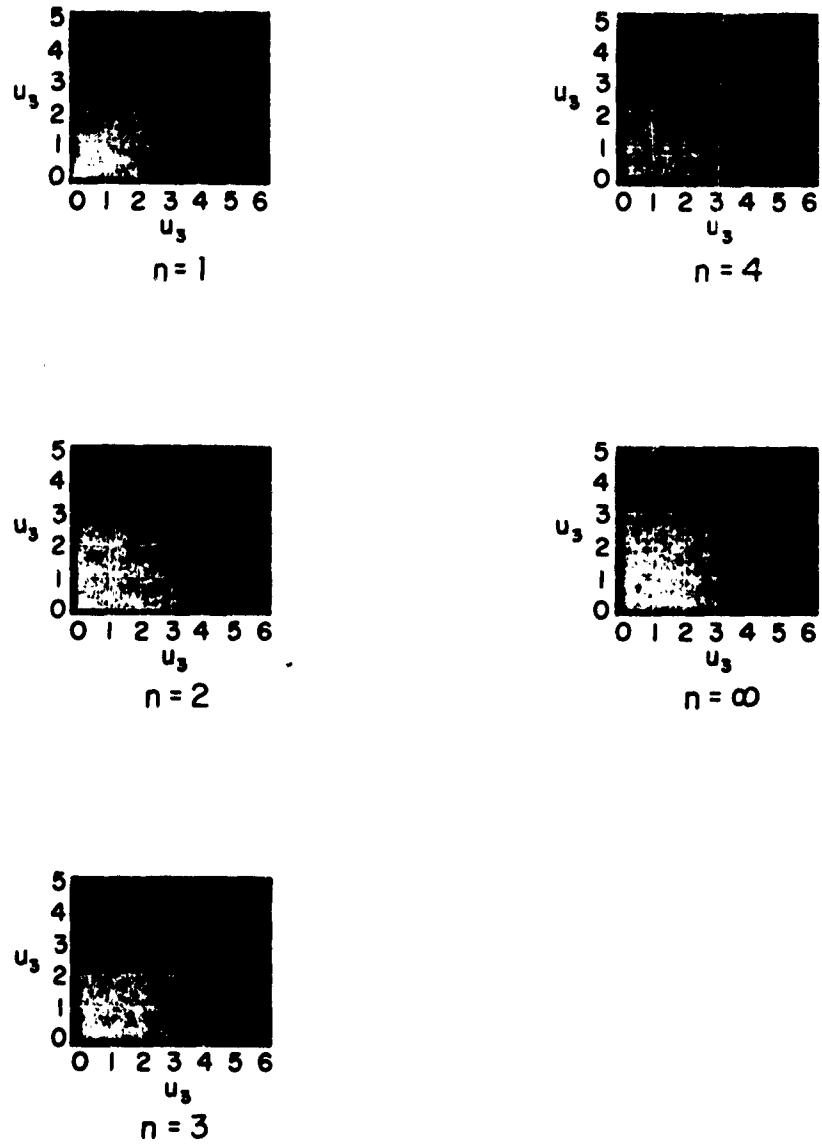


Figure 66: Each Intensity Pattern Represents an Approximation to the Joint Probability Density of the  $i$ th and  $(i+n)$ th Zero-Crossing Intervals of a Gaussian Process Having Power Spectral Density  $W_3(f)$ .

determining the center of gravity for each strip when unit intensity is assigned unit mass. A line joining these points is called a regression curve. By using the principle of least squares one can determine the best fitting straight line to the regression curve. The slope of this best fitting straight line represents the correlation coefficient  $\rho_n$ . From Figure 66 we see that when  $n \geq 3$  the regression curve is approximately a line parallel to the axis of abscissas, and the conditional mean value is approximately equal to the mean value of the zero-crossing intervals. Thus when  $n \geq 3$ ,  $\rho_n \doteq 0$  or the zero-crossing intervals are approximately uncorrelated.

By comparing the intensity pattern for  $n = \infty$  to the others we see that when  $n \geq 4$  the statistical dependence practically vanishes. However, when we compare the intensity pattern for  $n = \infty$  to that corresponding to  $n = 1$  we see significant dependence. This dependence is in agreement with the theorem of this section. These observations may be useful to guide the development of models aimed at developing a suitable theory of the zero-crossing intervals of Gaussian processes. For example, we see immediately that a theory based on the independence of successive zero-crossing intervals is destined to be inadequate.

Similar photographs were made for all of the other random processes considered in this report. For the Gaussian process having the power spectral density  $W_4(f)$ , the correlation coefficient  $\rho_n$  is non-zero when  $n \leq 4$ , and the  $i$ th and  $(i+n)$ th zero-crossing intervals are statistically dependent when  $n \leq 4$ . For all of the other random processes, the correlation coefficient  $\rho_n$  practically vanishes when  $n \geq 3$ , and the statistical dependence between the  $i$ th and  $(i+n)$ th zero-crossing intervals practically vanishes when  $n \geq 4$ .



## X. APPLICATIONS

The sampling technique for generating Gaussian noise which was described in Section IIIB is one application resulting from this study of the zero-crossing intervals. Another application concerns an integral technique for measuring pulse duration and has been reported in the literature (36).

In certain countermeasure applications of the zero-crossing phenomenon one requires a modulating noise waveform having an "optimum"  $P_o(\tau)$ , the probability density function for successive zero-crossing intervals. Usually one asks that a certain mean,  $E_o(\tau)$ , and a certain standard deviation,  $\sigma_o$ , be associated with the  $P_o(\tau)$ . The other required properties of  $P_o(\tau)$  for "optimum" conditions are somewhat vague. Here we shall give a few results concerning the "optimum"  $P_o(\tau)$ .

### A. THE MOST RANDOM DISTRIBUTION OF SUCCESSIVE ZERO-CROSSING INTERVALS

Consider a sequence of successive zero-crossing intervals  $\{\tau_i\}$  generated by a sample function of an ergodic random process having a finite expected number of zeros per unit time. Let each of the  $\tau_i$  have a common probability density  $P_o(\tau)$ , and let the  $n$  dimensional joint probability density for the sequence of intervals  $\{\tau_i\}$  be denoted by  $P(\tau_1, \tau_2, \tau, \dots, \tau_n)$ . In order to determine the most random distribution of successive

zero-crossing intervals, we adopt the criterion that the relative entropy per zero-crossing interval,  $H'$ , given by

$$H' = - \lim_{n \rightarrow \infty} \frac{1}{n} \int_0^{\infty} \dots \int_0^{\infty} P(\tau_1, \tau_2, \dots, \tau_n) \ln P(\tau_1, \tau_2, \dots, \tau_n) d\tau_1 \dots d\tau_n \quad (115)$$

is a measure of the randomness. By a well-known principle from information theory, the maximum of  $H'$  occurs when the sequence of successive zero-crossing intervals,  $\{\tau_i\}$ , are statistically independent. That is when

$$P(\tau_1, \tau_2, \dots, \tau_n) = P_0^n(\tau) \quad \text{for all } n \quad (116)$$

Accordingly, in order to maximize  $H'$  we need only maximize the relative entropy,  $H$ , given by

$$H = - \int_0^{\infty} P_0(\tau) \ln P_0(\tau) d\tau \quad (117)$$

Let the constraints be:

$$\int_0^{\infty} P_0(\tau) d\tau = 1 \quad (118)$$

$$\int_0^{\infty} \tau P_0(\tau) d\tau = E_0(\tau) \quad (119)$$

and

$$\int_0^{\infty} \tau^2 P_0(\tau) d\tau = E_0(\tau^2) \quad (120)$$

By applying the calculus of variations we find that the maximum relative entropy,  $H$ , results when:

$$P_o(\tau) = \frac{1}{D\sqrt{2\pi} \Phi(\frac{m}{D})} e^{-\frac{(\tau-m)^2}{2D^2}} \quad (121)$$

where

$$E_o(\tau) = m + \lambda D$$

$$E_o(\tau^2) = m^2 + \lambda Dm + D^2$$

$$\lambda = \frac{\phi(\frac{m}{D})}{\Phi(\frac{m}{D})}$$

$$\phi(x) = \frac{1}{\sqrt{2\pi}} e^{-x^2/2}$$

$$\Phi(x) = \frac{1}{\sqrt{2\pi}} \int_{-\infty}^x e^{-y^2/2} dy$$

Given  $E_o(\tau)$  and  $E_o(\tau^2)$  one can determine  $m$  and  $D$  and hence  $P_o(\tau)$  by using the tables reported by K. Pearson (37).

Accordingly, for a given mean,  $E_o(\tau)$ , and a given standard deviation,  $\sigma_o = [E_o(\tau^2) - E_o^2(\tau)]^{1/2}$ , the most random distribution of successive zero-crossing intervals is represented by the truncated Gaussian probability density function shown in Figure 67 and by Equation (116). Since successive zero-crossing intervals must be statistically independent in order to yield the maximum relative entropy per zero-crossing interval, the theorem of Section IX implies that a Gaussian process or an infinitely clipped Gaussian process can not generate the most random distribution of successive zero-crossing intervals. Moreover, for Gaussian

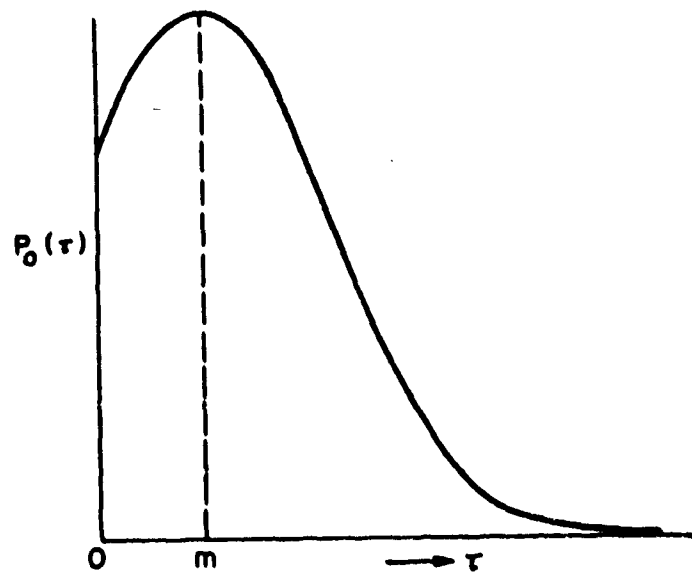


Figure 67 The Truncated Gaussian Probability Density,  $P_0(\tau)$ , Represents the Most Random Distribution of Successive Zero-Crossing Intervals Having a Given Mean and a Given Standard Deviation.

processes of finite memory,  $P_o(\tau)$  for large  $\tau$  must have an asymptotic exponential (5, 13, 38, 41) behavior such as:

$$P_o(\tau) \sim e^{-a\tau} \quad (122)$$

Physically, this means that the random process having a  $P_o(\tau)$  given by Equation (121) cannot be a Gaussian process or an infinitely clipped Gaussian process. That is, one cannot obtain a random process having a  $P_o(\tau)$  given by Equation (121) by the familiar technique of spectrally shaping "white" Gaussian noise with a linear filter.

It is interesting to note that if the constraints are given by Equations (118) and (119) only, then the maximum entropy  $H$  occurs when

$$P_o(\tau) = \frac{1}{E_o(\tau)} e^{-\frac{\tau}{E_o(\tau)}} \quad (123)$$

The Gaussian process having power spectral density  $W_1(f)$  generates a  $P_o(\tau)$  that approximates an exponential density of the form given by Equation (123) as is seen in Figure 18. Furthermore, successive zero-crossing intervals of this Gaussian process are approximately independent as is seen in Figure 19.

#### B. TECHNIQUE FOR ESTIMATING THE ASYMPTOTIC EXPONENTIAL BEHAVIOR OF $P_o(\tau)$

Here we describe a technique for estimating the  $a$  in Equation (122). Lewis (39) and McFadden (32) showed that:

$$E_o(\tau^2) = 2E_o(\tau) \int_0^{\infty} p(0, \tau) d\tau \quad (124)$$

If  $P_0(\tau)$  is asymptotically exponential then  $p(0, \tau)$  and  $Z(1, \tau)$  are also asymptotically exponential as is seen from Equations 39 and 41. Hence, in order to determine  $\alpha$  in Equation (122) we determine a "reasonable" exponential to tie on to the measured  $p(0, \tau)$  such that Equation (124) is satisfied for measured  $E_0(\tau^2)$  and theoretical  $E_0(\tau)$ . Semi-log plots of  $P_0(\tau)$ ,  $p(0, \tau)$  and  $Z(1, \tau)$  are useful for determining where to tie on the exponential. However, the point of "tie on" is still somewhat arbitrary. Accordingly, we end up with at most rough estimates of  $\alpha$ . Using normalized time, some rough estimates of  $\alpha_n$  associated with the asymptotic exponential behavior:

$$P_0(u_n) \sim e^{-\alpha_n u_n} \quad (125)$$

are given below.

For tie on point at  $u_1 = 8$ ,  $\alpha_1 = 0.28$

For tie on point at  $u_2 = 12$ ,  $\alpha_2 = 0.11$

For tie on point at  $u_3 = 4$ ,  $\alpha_3 = 0.47$

## XI. CONCLUSIONS

The results of this study of the zero-crossing intervals of random processes should prove useful for guiding the development of some new techniques which are useful in both science and technology.

The sampling technique for generating Gaussian noise is perhaps the simplest technique available for generating such noise.

The integral technique for measuring pulse duration should be especially useful for airborne or space instrumentation applications.

At present none of the probabilities or probability densities presented in this report can be derived explicitly by analytical methods.

The probability density  $P_0(\tau)$  for the case of Gaussian noise having a power spectral density  $W_1(f)$  is not exactly  $\frac{1}{\pi} e^{-\tau/\pi}$ .

The hypothesis that successive zero-crossing intervals of Gaussian processes form a wide sense Markov chain is false for some Gaussian processes.

The experimental initial values of  $P_0(u_n)$  and  $P_1(u_n)$  for  $n = 1, 3$  obtained by extrapolation agree satisfactorily with the approximate theoretical initial values.

The results of this study should prove useful for guiding the development of models aimed at developing a suitable theory for the zero-crossing intervals of certain random processes. In general the models must not assume that successive zero-crossing intervals of random processes are statistically independent.

For the Gaussian process having the power spectral density  $W_4(f)$ , the correlation coefficient  $\rho_n$  is nonzero when  $n \leq 4$ , and the  $i$ th and  $(i+n)$ th zero-crossing intervals are statistically dependent when  $n \leq 4$ . For all of the other random processes, the correlation coefficient  $\rho_n$  practically vanishes when  $n \geq 3$ , and the statistical dependence between the  $i$ th and  $(i+n)$ th zero-crossing intervals practically vanishes when  $n \geq 4$ .



## XII. APPENDIX

For a Gaussian process having a normalized autocorrelation function  $\rho(\tau)$ , the conditional probability,  $U(\tau) d\tau$ , that a zero occurs between  $t + \tau$ ,  $t + \tau + d\tau$  given a zero at  $t$  is given by:

$$U(\tau) d\tau = \frac{d\tau}{\pi} \left[ -\rho''(0) \right]^{-\frac{1}{2}} \left[ \frac{M_{23}}{H} \right] \left[ 1 - \rho^2(\tau) \right]^{-\frac{3}{2}} \left[ 1 + H \tan^{-1} H \right] \quad (126)$$

where

$$H = M_{23} \left[ M_{22}^2 - M_{23}^2 \right]^{-\frac{1}{2}}$$

$$-\frac{\pi}{2} \leq \tan^{-1} H \leq \frac{\pi}{2}$$

$$M_{22} = -\rho''(0) \left[ 1 - \rho^2(\tau) \right] - \left[ \rho'(\tau) \right]^2$$

$$M_{23} = \rho''(\tau) \left[ 1 - \rho^2(\tau) \right] + \rho(\tau) \left[ \rho'(\tau) \right]^2$$

For a Gaussian process having a normalized autocorrelation function  $\rho(\tau)$ , the conditional probability,  $Q(\tau) d\tau$ , that a downward zero-crossing occurs between  $t + \tau$ ,  $t + \tau + d\tau$  given an upward zero-crossing at time  $t$  is given by:

$$Q(\tau) d\tau = \frac{d\tau}{2\pi} \left[ -\rho''(0) \right]^{-\frac{1}{2}} \left[ \frac{M_{23}}{H} \right] \left[ 1 - \rho^2(\tau) \right]^{-\frac{3}{2}} \left[ 1 + H \cot^{-1} (-H) \right] \quad (127)$$

where

$$0 \leq \cot^{-1} (-H) \leq \pi$$

The normalized autocorrelation function,  $r(u_o, a)$ , for the infinitely clipped process  $\xi(u, a)$ , defined by Equation (82), is given by:

$$r(u_o, a) = -4 \sum_{\substack{n=1 \\ \text{odd } n}}^{\infty} \frac{h_{o,n}^2}{n!} \rho_o^n(u_o) - 8 \left[ \sum_{\substack{m=1 \\ \text{odd } m}}^{\infty} h_{m,0}^2 \cos \frac{mu_o}{2} + \sum_{\substack{n=1 \\ \text{odd } (m+n)}}^{\infty} \sum_{m=1}^{\infty} \frac{h_{m,n}^2}{n!} \rho_o^n(u_o) \cos \frac{mu_o}{2} \right] \quad (128)$$

where

$$h_{m,n}^2 = -\frac{1}{(2m!)^2} 2^{n_a m} \frac{{}_1F_1\left(\frac{m+n}{2}; m+1; -a\right)}{\Gamma\left[2 - \frac{(m+n)}{2}\right]}$$

${}_1F_1$  = confluent hypergeometric function

$\Gamma$  = gamma function

$a$  = signal-to-noise power ratio.

The normalized autocorrelation function,  $r_s(u_o, a)$ , for the infinitely clipped process  $\eta(u, a)$ , defined by Equation (106), is given by:

$$r_s(u_o, a) = -4 \sum_{\substack{n=1 \\ \text{odd } n}}^{\infty} \frac{h_{o,n}^2}{n!} \left[ \frac{\rho_o''(u_o)}{\rho_o''(0)} \right]^n - 8 \left\{ \sum_{\substack{m=1 \\ \text{odd } m}}^{\infty} h_{m,0}^2 \cos \frac{mu_o}{2} + \sum_{\substack{n=1 \\ \text{odd } (m+n)}}^{\infty} \sum_{m=1}^{\infty} \frac{h_{m,n}^2}{n!} \left[ \frac{\rho_o''(u_o)}{\rho_o''(0)} \right]^n \cos \frac{mu_o}{2} \right\} \quad (129)$$

where

$$h_{m,n}^2 = - \frac{1}{(2m!)^2} 2^n (ba)^m \frac{{}_1F_1^2\left(\frac{m+n}{2}; m+1; -ba\right)}{\Gamma^2\left[\frac{2-(m+n)}{2}\right]}$$

$$b = \frac{\sin \frac{3\pi}{14}}{4 \sin \frac{\pi}{14}}$$

#### REFERENCES

1. Rice, S. O., "Mathematical Analysis of Random Noise," Bell System Tech. J., Vol. 24, p. 58, (Equation 3.4-1), p. 60, (Equations 3.4-10), January 1945.
2. McFadden, J. A., "The Axis-Crossing Intervals of Random Functions-II," IRE Transactions on Information Theory IT-4, p. 18, (Equation 47), March 1958.
3. Middleton, D., "Spurious Signals Caused by Noise in Triggered Circuits," J. Appl. Phys., Vol. 19, pp. 817-830, September 1948.
- 3a. Middleton, D., Introduction to Statistical Communication Theory, McGraw-Hill Book Company, Inc., New York, Chapter 9, and Equations 4.52b, and 13.80, 1960.
4. Kohlenberg, A., "Notes on the Zero Distribution of Gaussian Noise," Tech. Memorandum No. 44, Lincoln Laboratory, MIT, Lexington, Mass., 1953.
5. Kuznetsov, P. I., Stratonovich, P. L., and Tikhonov, V. I., "On the Duration of the Exceedences of a Random Function," J. Tech. Phys., Moscow, Vol. 24, pp. 103-112, 1954.
6. Tikhonov, V. I., and Armiyanov, I. N., "Probability Density for the Duration of Fluctuations," Radiotekhnika, Vol. 15, No. 9, pp. 10-20, 1960.
7. Longuet-Higgins, M. S., "On the Intervals Between Successive Zeros of a Random Function," Proceedings of the Royal Society, Vol. 246, pp. 99-118, July 1959.

8. Longuet-Higgins, M. S., "The Distribution of Intervals Between Zeros of a Stationary Random Function," Phil. Trans. Royal Society (A), Vol. 254, pp. 557-599, May 1962.
9. Helstrom, C. W., "The Distribution of the Number of Crossings of a Gaussian Stochastic Process," IRE Transactions on Information Theory, pp. 232-237, December 1957.
10. Steinberg, H., Schultheiss, P. M., Wogrin, C. A., and Zweig, F., "Short-Time Frequency Measurement of Narrow-Band Random Signals by Means of a Zero Counting Process," J. Appl. Phys., Vol. 26, pp. 195-201, February 1955.
11. Palmer, D. S., "Properties of Random Functions," Proc. Cambridge Phil Soc., Vol. 52, pp. 672-686, October 1956.
12. Debart, H., "Zeros of a Random Stationary Signal," Cables and Transmissions, Vol. 14, pp. 191-199, July 1960.
13. Slepian, D., "The One-Sided Barrier Problem for Gaussian Noise," Bell System Tech. J., Vol. 41, No. 2, pp. 463-501, March 1962.
14. Brown, W. M., "Some Results on Noise Through Circuits," IRE Transactions on Information Theory, IT-5, Special Supplement, pp. 217-227, May 1959.
15. Bendat, J. S., Principles and Applications of Random Noise Theory, John Wiley and Sons, New York, Chapter 10, Equation 10-63, 1958.

16. Kac, M., "Some Remarks on Oscillators Driven by a Random Force," IRE Transactions on Circuit Theory, CT-7, pp. 476-479, 1960.
17. Miller, I., and Freund, J. E., "Some Results on the Analysis of Random Signals by Means of a Cut-Counting Process," J. Appl. Phys., Vol. 27, pp. 1290-1293, 1956.
18. White, G. M., "Experimental System for Studying the Zeros of Noise," Cruft Laboratory Technical Report No. 261, Harvard University, May 1957, and "Experimental Determination of the Zero-Crossing Distributions  $W(N, T)$ ," Cruft Laboratory, Technical Report No. 265, Harvard University, June 1957.
19. Favreau, R. R., Low, H., and Pfeffer, I., "Evaluation of Complex Statistical Functions by an Analog Computer," IRE Convention Record, Part 4, pp. 31-37, 1956.
20. Gates, C. R., "Probability Distribution of the Zeros of Random Noise," Doctoral Thesis, California Institute of Technology, 1951.
21. Blötekjaer, Kjell, "An Experimental Investigation of Some Properties of Band-Pass Limited Gaussian Noise," IRE Transactions on Information Theory, IT-4, pp. 100-102, September 1958.
22. Velichkin, A. I., and Ponomareva, V. D., "Experimental Investigation of the Duration of Noise Peaks," Radiotekhnika, Vol. 15, No. 10, pp. 21-26, 1960.
23. Grenander, Ulf, "Stochastic Processes and Statistical Inference," Arkiv för Matematik, Vol. 1, No. 17, see Theorem on page 257, 1950.

24. Rainal, A. J., "Digital Measurement of Axis-Crossing Intervals," Electronics, Vol. 33, No. 23, pp. 88-91, June 1960.
25. Rainal, A. J., "Sampling Technique for Generating Gaussian Noise," Rev. of Scientific Insts., Vol. 32, No. 3, pp. 327-331, March 1961.
26. McFadden, J. A., op. cit., p. 23, Equation 80.
27. Rice, S. O., op. cit., p. 54, Equation 3.3-11, p. 73, Equation 3.6-6.
28. McFadden, J. A., op. cit., p. 22, Table I., p. 15, Equation 6, p. 17.
29. Zuhrt, H., "The Distribution Curves of the Times during which an Arbitrarily Specified Value is Exceeded in the Case of White Noise," Archiv Der Elektrischen Übertragung, Vol. 15, Number 9, pp. 415-422, September 1961.
30. Ehrenfest, P. et al., "Theoretical and Observed Results for the Zero and Ordinate Crossing Problems of Stationary Gaussian Noise with Application to Pressure Records of Ocean Waves," Tech. Report. No. 1, Research Division, College of Engineering New York University, New York, December 1958.
31. Bialyi, L. I., "Density of Distribution of Intervals Between Zeros of a Narrow-band Normal Stationary Random Process," Radiotekhnika i Elektronika, Vol. 4, No. 3, pp. 266-269, 1959.

32. McFadden, J. A., "On the Lengths of Intervals in a Stationary Point Process," Journal of the Royal Statistical Society, Series B, Vol. 24, No. 2, pp. 364-383, 1962.
33. Dishal, Milton, "Gaussian-Response Filter Design," Electrical Communication, Vol. 36, No. 1, 1959.
34. Rice, S. O., "Statistical Properties of a Sine Wave Plus Random Noise," Bell System. Tech. J., Vol. 27, p. 119, (Equation 2.7), January 1948.
35. Rainal, A. J., "Zero-Crossing Intervals of Gaussian Processes," IRE Transactions on Information Theory, Vol. IT-8, No. 6, pp. 372,- 378, October 1962.
36. Rainal, A. J., "Integral Technique for Measuring Pulse Duration," IRE Transactions on Instrumentation, Vol. I-11, No. 1, pp. 11-14, June 1962.
37. Pearson, K., Tables for Statisticians and Biometricians, I., Second Edition, 1924, II, 1931.
38. Rice, S. O., "Distribution of the Duration of Fades in Radio Transmission," Bell System Tech. J., Vol. 37, pp. 581-635, May 1958.
39. Lewis T., "The Intervals Between Regular Events Displaced in Time by Independent Random Deviations of Large Dispersion," Journal of the Royal Statistical Society, B, Vol. 23, No. 2, pp. 476-483, 1961.
40. Davenport, Jr., W. B., "Signal-to-Noise Ratios in Bandpass Limiters," Journal Applied Physics, Vol. 24, p. 721, Equation 13, 1953.
41. Newell, G. F., and M. Rosenblatt, "Zero-Crossing Probabilities for Gaussian Stationary Processes," The Annals of Mathematical Statistics, Vol. 33, No. 4, pp. 1306-1313, December 1962.



## ELECTRONICS DISTRIBUTION

10	ASTIA Arlington Hall Station Arlington 12, Virginia	1	AFMDC (MDRRF-1) Holloman AFB, N.M.
	ASD Wright-Patterson AFB, Ohio	1	Air University Library (AUI-6234) Maxwell AFB, Ala.
1	Attn: ASAPRL	2	9AF (DOTR-FR (Capt. O.E. McCain) Shaw AFB, S.C.
1	ASAPT	1	ADC (ADDOA) Ent AFB, Colorado
1	ASNC	1	Director Weapons Systems Evaluation Group Room 1E-875, The Pentagon Washington 25, D.C.
1	ASND	10	Scientific and Technical Information Facility Attn: NASA Representative (Code: S-AK/DL) P.O. Box 5700 Bethesda, Maryland
1	ASNG	1	Commanding Officer U.S. Army Signal Research and Development Lab. Attn: SIGRA/SL-SE, Mr. I.O. Myers Fort Monmouth, N.J.
1	ASNPVD-1	1	Chief Signal Officer Research and Development Division Avionics and Surveillance Branch Washington 25, D.C.
1	ASNPVD-2	1	Assistant Secretary of Defense Research and Development Board Attn: Technical Library Department of Defense Washington 25, D.C.
1	ASNR	1	Director National Security Agency Attn: C3/TDL Fort George G. Meade, Md.
1	ASNS	1	Army Ordnance Missile Command Attn: ORDXM-RR, Holloway, Jr. Redstone Arsenal, Alabama
1	ASNSD	2	Commanding General Army Ordnance Missile Command Attn: ORDXM-RFE/Re-Entry Physics Section Redstone Arsenal, Alabama
1	ASNV	1	Commanding Officer U.S. Army Signal Research and Development Lab. Attn: SIGRA/SL-N-5, Dr. H. Bennett Fort Monmouth, N.J.
1	ASNXX	1	Commanding General White Sands Missile Range Attn: ORDBS-OM-TL New Mexico
1	ASNY	2	Commanding Officer Picatinny Arsenal Attn: Tech. Information Section-ORDBB-VA6 Dover, New Jersey
1	ASDRG(Mr. Catansarite)	1	USA Signal Electronic Research Unit P.O. Box 205 Mountain View, Calif.
1	ASRC	1	US Army Signal Corps School Attn: DST, USASCS (Mr. Henry Allem) Fort Monmouth, New Jersey
1	ASRE	1	Chief of Naval Research Attn: Code 427 Department of the Navy Washington 25, D.C.
1	ASRNET-3	1	Commander U.S. Naval Ordnance Laboratory Attn: Eva Liberman, Librarian White Oak, Silver Spring, Maryland
1	ASRNGE	1	Director Material Laboratory New York Naval Shipyard Brooklyn 1, N.Y.
1	ASRNOO	1	Commander U.S. Naval Missile Center Attn: Technical Library, Code NO 9022 Point Mugu, California
1	ASRNC (Mr. Stimmel)		
1	ASRNC (Major Novak)		
2	ASRNCC-1		
1	ASRNCC-2		
1	ASRNET-1		
2	ASRNCF-1		
2	ASRNGW-2		
1	ASRNRS		
1	ASRNRS-3		
1	ASROO		
1	ASRSSE-2		
1	ASTFPE (Captain Gregory)		
1	ASOQ (Gp Captain Fletcher)		
	RADC Griffiss AFB, New York		
1	Attn: RAD, Dr. Irving J. Gabelman		
1	RALC (J.E. Cruickshank)		
1	RALS8 (M. A. Diabi)		
1	RAUAA (John P. Huss)		
1	RAUAT		
1	RAUMA (C.R. Miller)		
1	RAUMM		
2	RAWE		
1	RAWEC		
1	RAWES		
2	RAWI		
	AFSC Andrews AFB Washington 25, D.C.		
1	Attn: SCTAN		
1	SCRC (Lt. Col. Thompson)		
	HQ. USAF Washington 25, D.C.		
1	Attn: AFRDR-IN (Lt. Col. Pinson)		
1	AFOOR-SV-ES (Lt. Col. Smith)		
1	AFORQ-SA (Lt. Col. Ragsdale)		
1	AFMPP-EQ (Lt. Col. Manbeck)		
1	AFORQ-AD		
1	USAFSS (ODC-R) San Antonio, Texas		
2	PACAF (PFSE-E) APO 953 San Francisco, California		
2	USAFE (DCS/Ops) APO 633 New York, New York		
1	3535th NTW Attn: Electronic Warfare Familiarisation Course Mather AFB, Calif.		
1	TAC (OA) Langley AFB, Virginia		
1	DCAS (DCLMT/TDC) AF Unit Post Office Los Angeles 45, Calif.		
	SAC Offutt AFB, Nebr.		
1	Attn: DORQP		
1	DOPLT		

## ELECTRONICS DISTRIBUTION CONTD

- 1 Commanding Officer  
U.S. Naval Air Development Center  
Engineering Development Laboratory  
Attn: J. M. McGlone  
Johnsville, Pa.
- 1 Commanding Officer  
U.S. Naval Ordnance Laboratory  
Attn: Code 74  
Corona, California
- 1 Chief  
Bureau of Naval Weapons  
Department of the Navy  
Attn: RRRE-2  
Washington 25, D. C.
- 2 Director  
U.S. Naval Research Laboratory  
Attn: Code 2027  
Washington 25, D. C.
- 1 Chief, Bureau of Ships  
Attn: Code 335  
Room 1532 Main Navy Building  
Washington 25, D. C.
- 1 Airborne Instruments Laboratory  
A Division of Cutler-Hammer Inc  
Attn: Library  
Walt Whitman Road  
Melville, Long Island, New York
- 1 Analytic Services Inc  
Attn: Library  
1150 Leesburg Pike  
Bailey's Crossroads, Virginia
- 2 The Johns Hopkins University  
Applied Physics Laboratory  
Attn: Mr. George L. Seelstad  
8621 Georgia Avenue  
Silver Spring, Maryland
- 1 Bjorksten Research Laboratories, Inc.  
P. O. Box 265  
Madison 1, Wisconsin
- 1 Cook Electric Company  
Cook Technological Center Division  
6401 W. Oakton Street  
Morton Grove, Ill.
- 1 Electronic Communications, Inc.  
Research Division  
1830 York Road  
Timonium, Maryland
- 1 General Dynamics/Fort Worth  
A Division of General Dynamics Corporation  
Attn: Chief Librarian  
P. O. Box 748  
Fort Worth 1, Texas
- 1 General Electric Company  
Advanced Electronics Center  
Attn: Library  
Cornell University Industrial Research Park  
Ithaca, New York
- 1 Grumman Aircraft Engineering Corp.  
Engineering Library, Plant 5  
Attn: M. O. Friedlander, Head Librarian  
Bethpage, Long Island, New York
- 2 The Hallcrafters Company  
Attn: Library  
4401 West Fifth Avenue  
Chicago 24, Illinois
- 1 HRB-Singer, Inc.  
Attn: Library  
Science Park Box 60  
State College, Pa.
- 1 The University of Michigan  
Institute of Science and Technology  
Attn: IRLA  
P. O. Box 618  
Ann Arbor, Michigan
- 2 ITT Federal Laboratories  
Div. International Telephone and Telegraph Corp.  
500 Washington Avenue  
Nutley, New Jersey
- 1 Jansky and Bailey  
A Division of Atlantic Research Corp.  
1339 Wisconsin Ave., N. W.
- 1 Massachusetts Institute of Technology  
Lincoln Laboratory  
Attn: Library  
P. O. Box 73  
Lexington 73, Massachusetts
- 1 Massachusetts Institute of Technology  
Electronic Systems Laboratory  
Attn: John E. Ward, RM 34-101  
Cambridge, Massachusetts
- 1 Lockheed Georgia Company  
Attn: Department 72-15  
Marietta, Georgia
- 1 Martin Marietta Corporation  
Martin Company Division  
Attn: Science-Technology Library  
Baltimore 3, Maryland
- Mitre Corporation  
Attn: Library  
Bedford, Massachusetts
- 1 Motorola Inc.  
Systems Research Laboratory  
8330 Indiana Avenue  
Riverside, California
- 2 North American Aviation, Inc.  
Attn: Technical Library  
International Airport  
Los Angeles 9, California
- 1 Northrop Corporation  
Norair Division  
Attn: Technical Information, 3924-11  
1001 E. Broadway  
Hawthorne, Calif.
- 2 Radio Corporation of America  
Defense Electronic Products, DSD  
Attn: L. R. Hund, Librarian  
8500 Balboa Blvd.  
Van Nuys, Calif.
- 2 Raytheon Company  
Attn: Librarian  
P. O. Box 636  
Santa Barbara, Calif.
- 1 Revere Copper and Brass Incorporated  
Foil Division  
Attn: Mr. Arthur Ferretti  
196 Diamond Street  
Brooklyn 22, New York
- 1 Stanford University  
Stanford Electronics Laboratories  
Attn: Security Officer  
Stanford, California
- 1 Sylvania Electric Products Inc.  
Technical Information Section  
P. O. Box 188  
Mountain View, California
- 1 The Ohio State University  
Research Foundation  
Attn: Dr. Curt A. Lewis  
1314 Kinnear Road  
Columbus 12, Ohio
- 1 The Rand Corporation  
Attn: Library  
1700 Main Street  
Santa Monica, California
- 1 The University of Michigan  
University Research Security Office  
Attn: Dr. R. F. Barton, Director CEL  
P. O. Box 622  
Ann Arbor, Michigan
- 2 Thompson Ramo Wooldridge Inc.  
Ramo Wooldridge Division  
Attn: Technical Library  
8433 Fallbrook Avenue  
Canoga Park, California
- 1 Space Technology Laboratories, Inc.  
STL Technical Library  
Attn: Document Acquisitions Group  
One Space Park  
Redondo Beach, California
- 1 Undynamics  
Div. of Universal Match Corporation  
Attn: Technical Library  
4407 Cook Avenue  
St. Louis 13, Missouri
- 1 Westinghouse Electric Corporation  
Defense Center - Baltimore  
Attn: Technical Information Center  
P. O. Box 1694  
Baltimore 3, Maryland